Particle Energization in Magnetic Reconnection Jets

L. Richard[1]

[1]*Swedish Institute of Space Physics, Uppsala, Sweden*

Acknowledgments: Yu. V. Khotyaintsev, D. B. Graham, A. Vaivads, L. Sorriso-Valvo, E. Yordanova, K. Steinvall, C. Norgren, J. Egedal, R. Nakamura, and the MMS team

louis.richard@irf.se

Workshop on Kinetic Physics of Astrophysical Plasmas, June 18-20, 2025

Introduction

Motivation

How do magnetic reconnection and turbulence heat the collisionless plasma and accelerate particles?

[Oka+2015, ApJ]

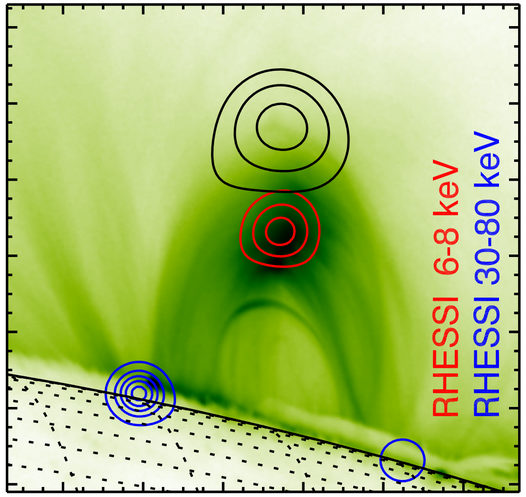

Solar Flares

[source : National Radio Astronomy Observatory/NSF]

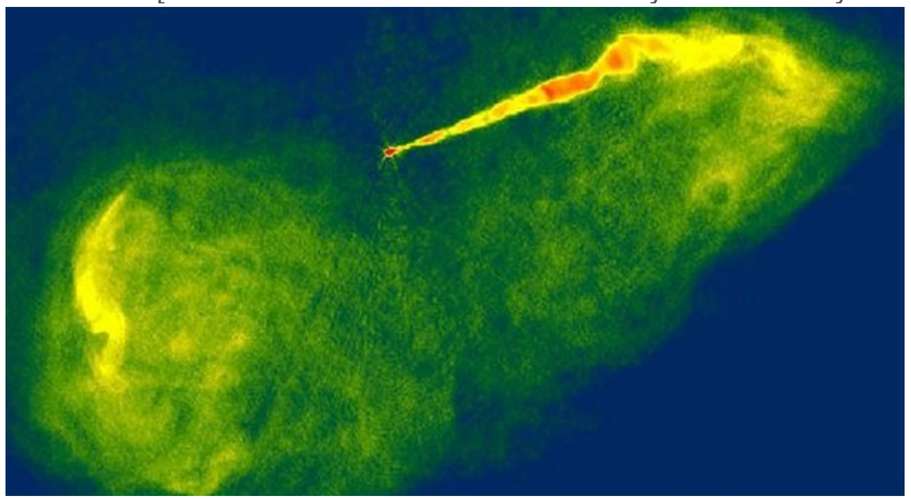

Active Galactic Nuclei (AGN) Jets

Reconnection Jets in the Magnetotail

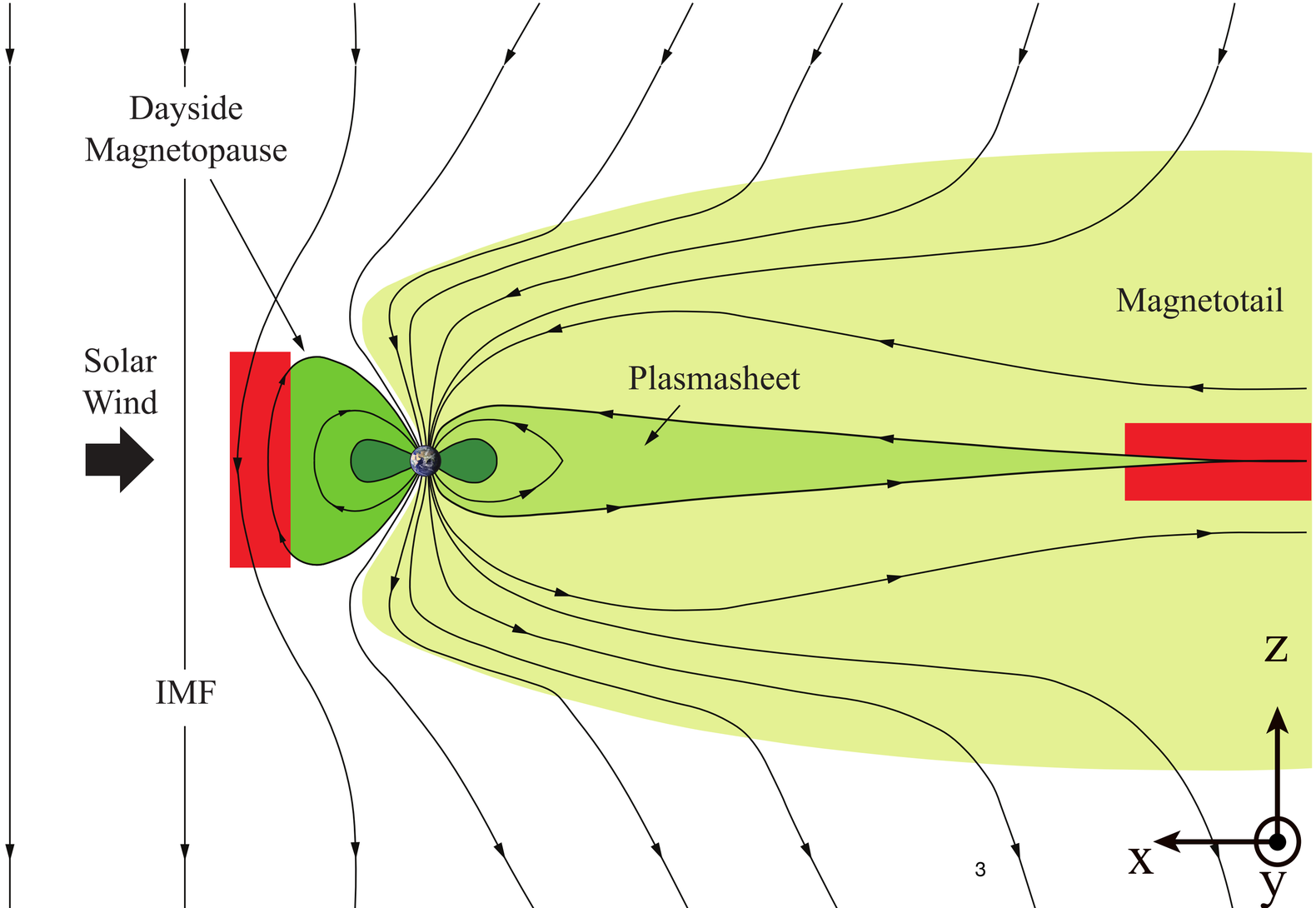

Reconnection Jets in the Magnetotail

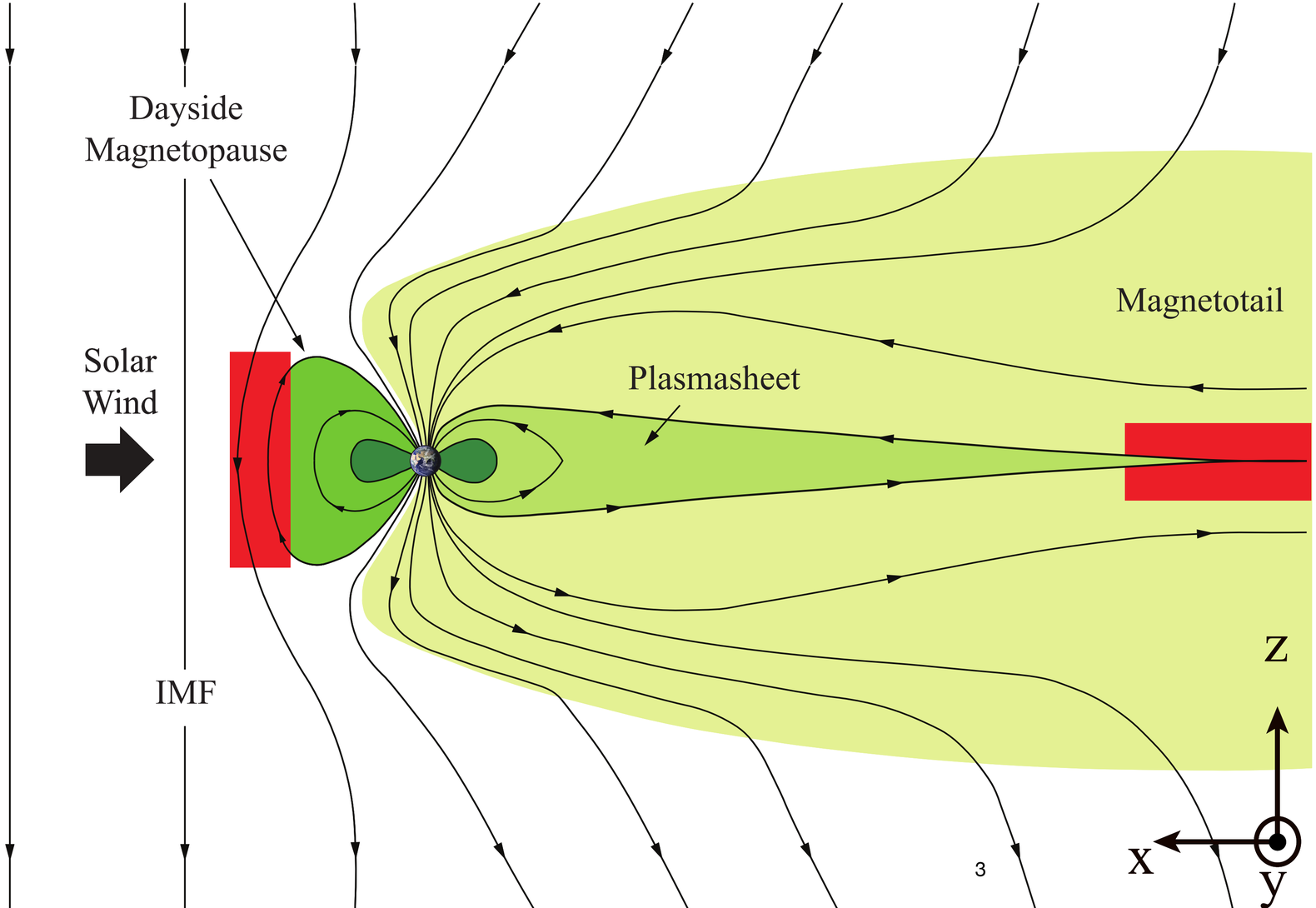

Reconnection Jets in the Magnetotail

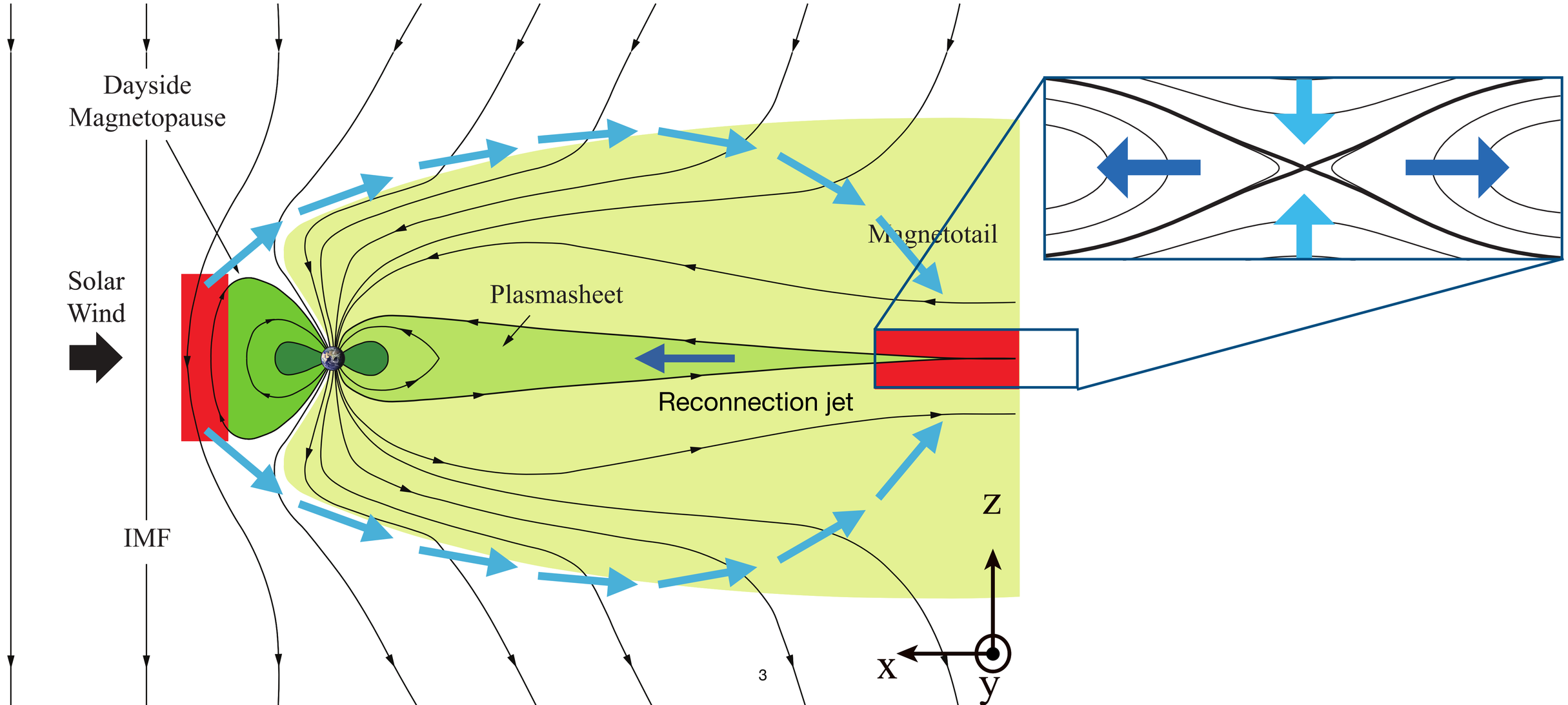

Reconnection Jets in the Magnetotail

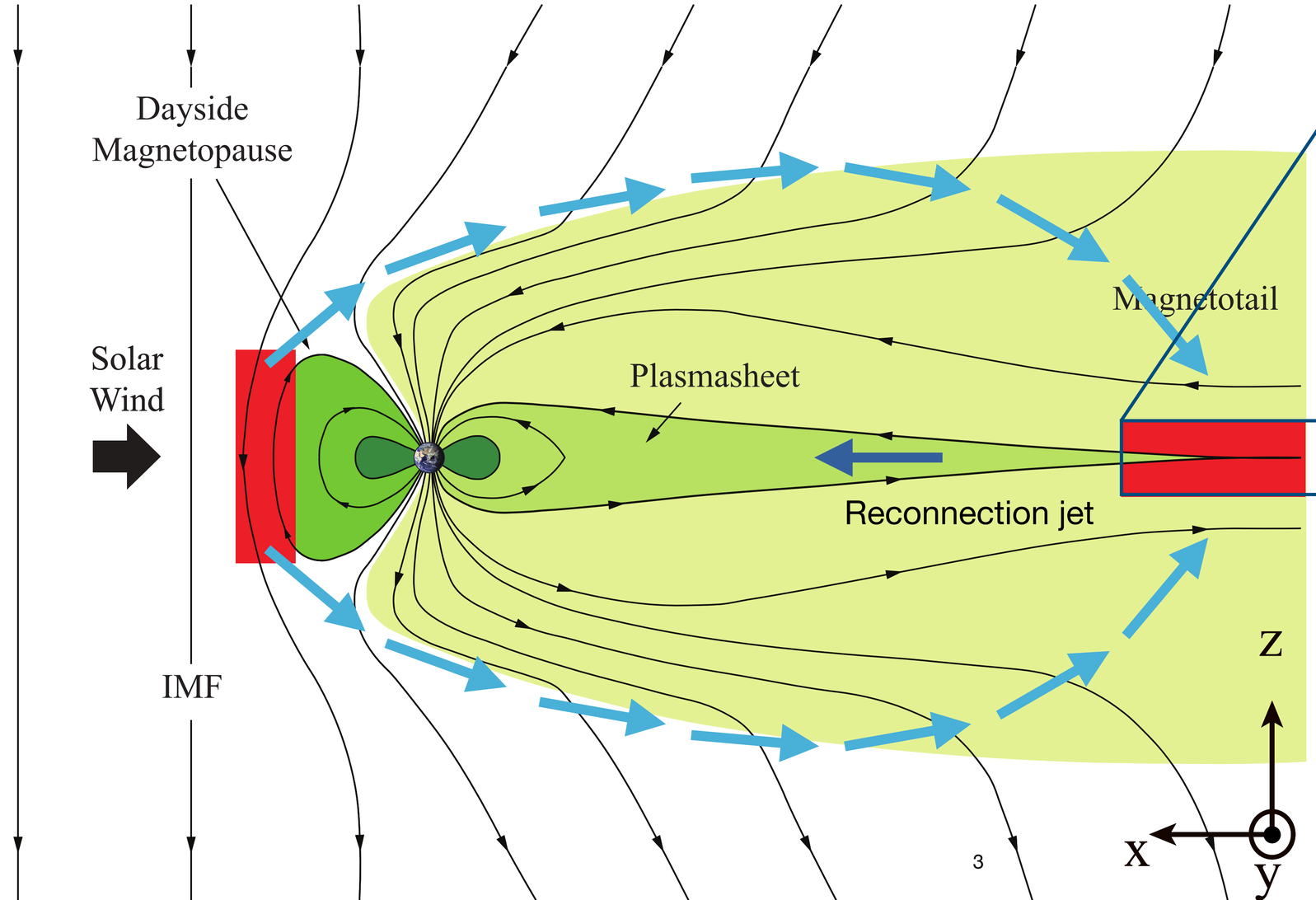

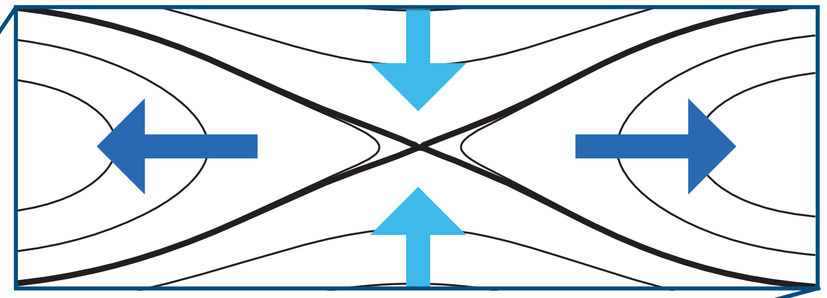

[Oka+2018, SSR]

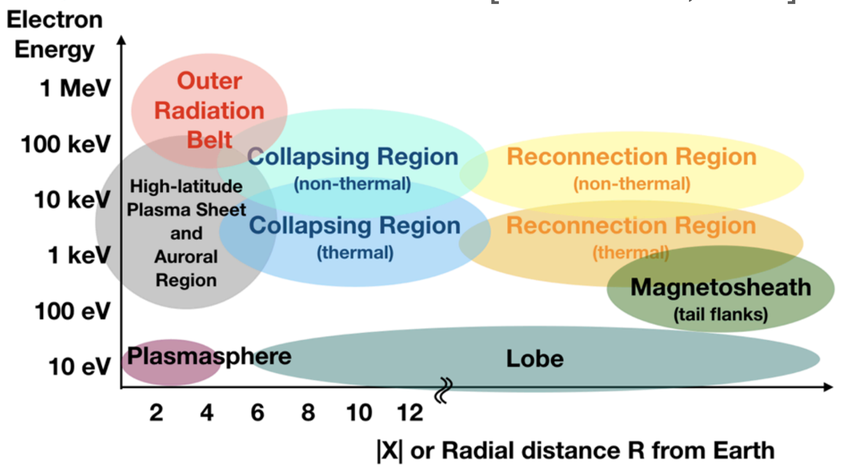

Reconnection Jets in the Magnetotail

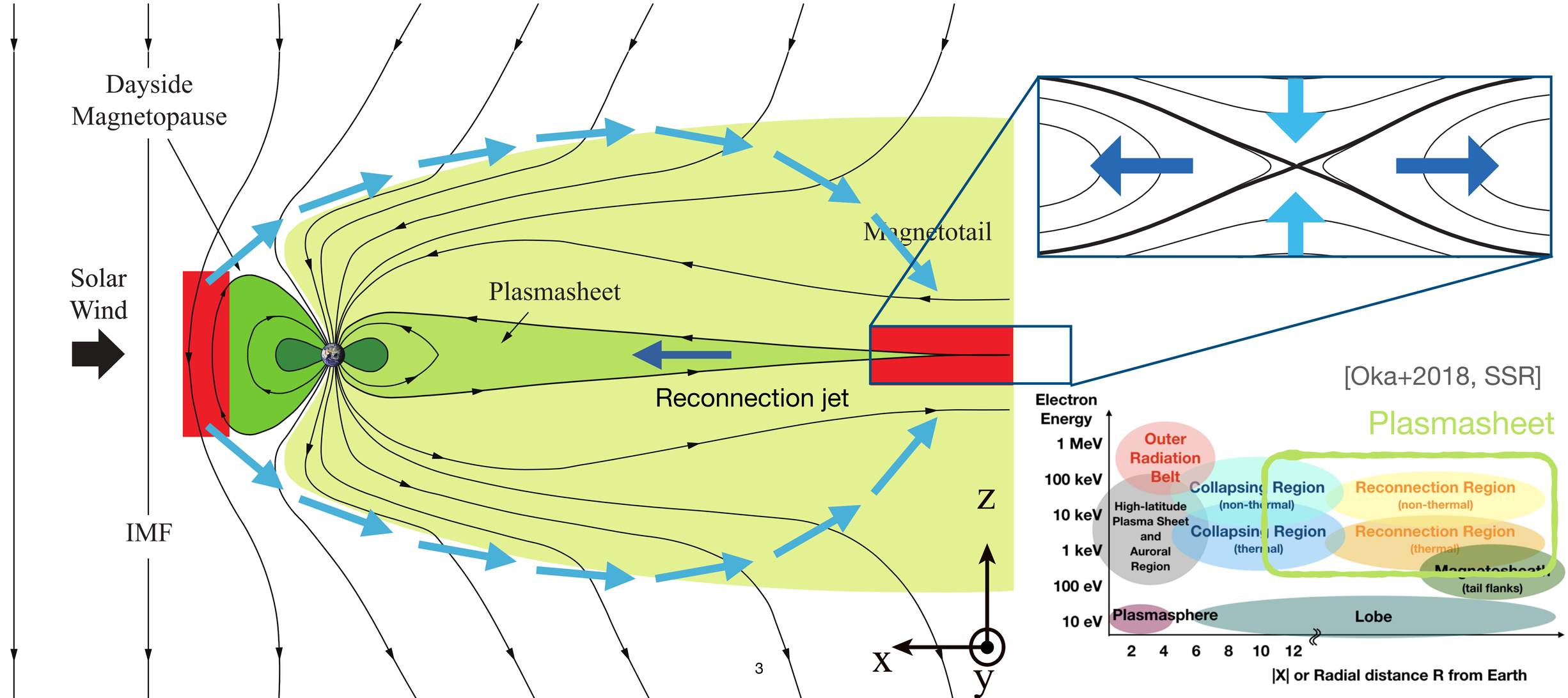

[Oka+2018, SSR]

Introduction

Outline

- The MMS mission & in situ observation of reconnection jets
- Turbulence
- Ion heating
- Electron heating
- Conclusions

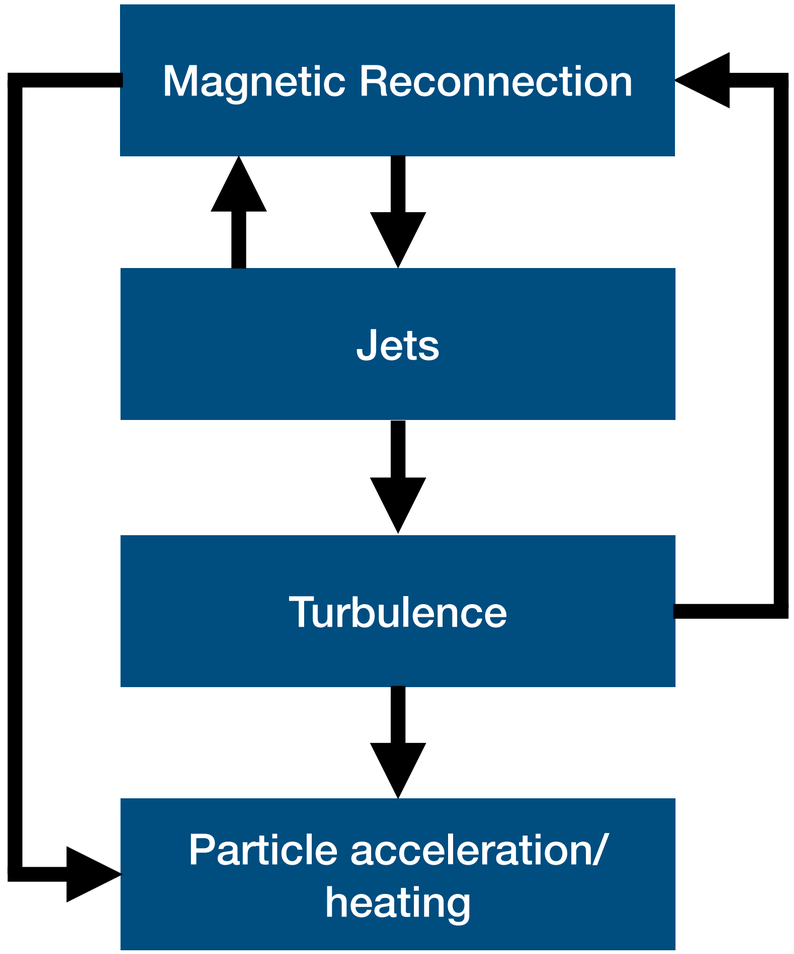

Introduction

Outline

- The MMS mission & in situ observation of reconnection jets
- Turbulence
- Ion heating
- Electron heating
- Conclusions

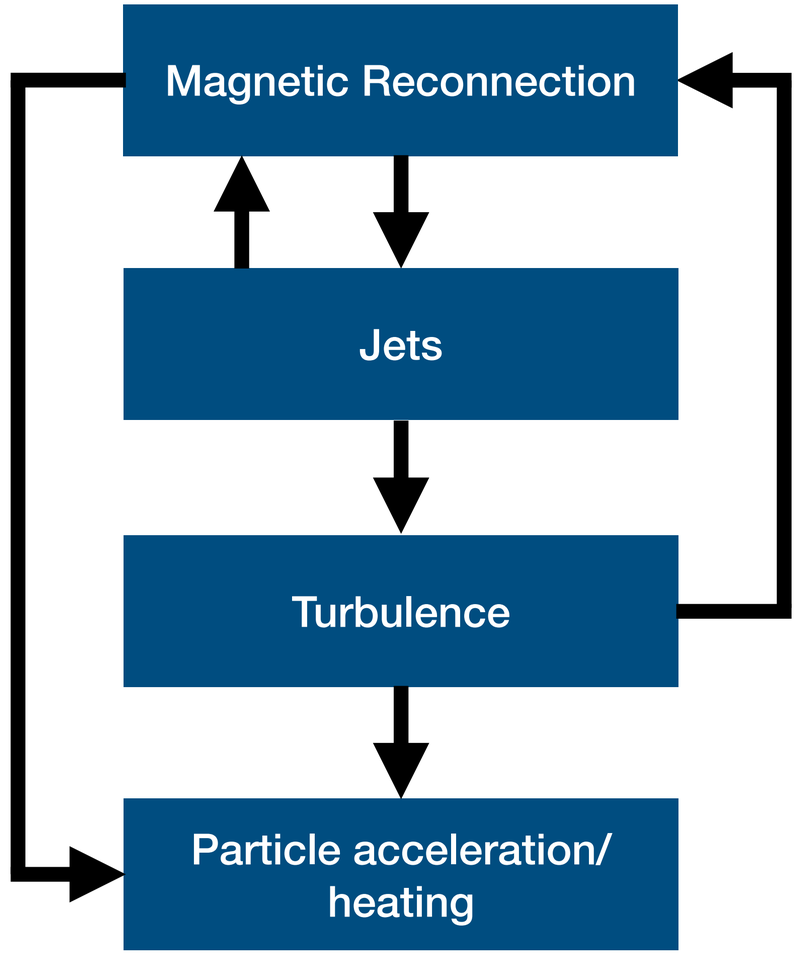

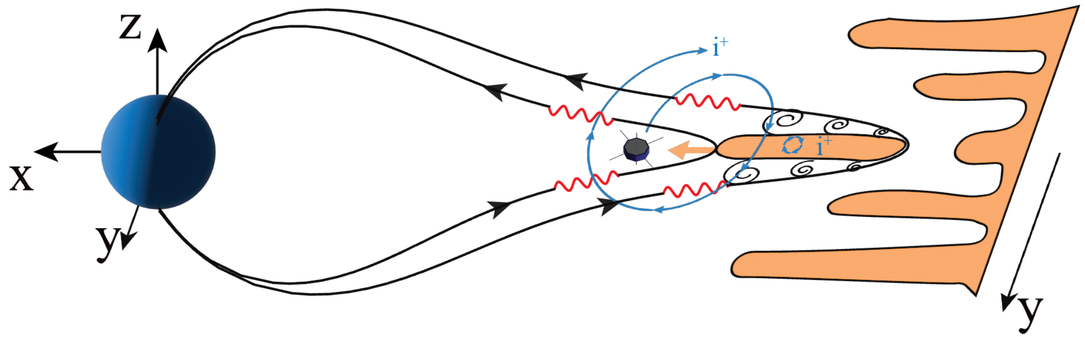

The Magnetospheric Multiscale (MMS) mission†

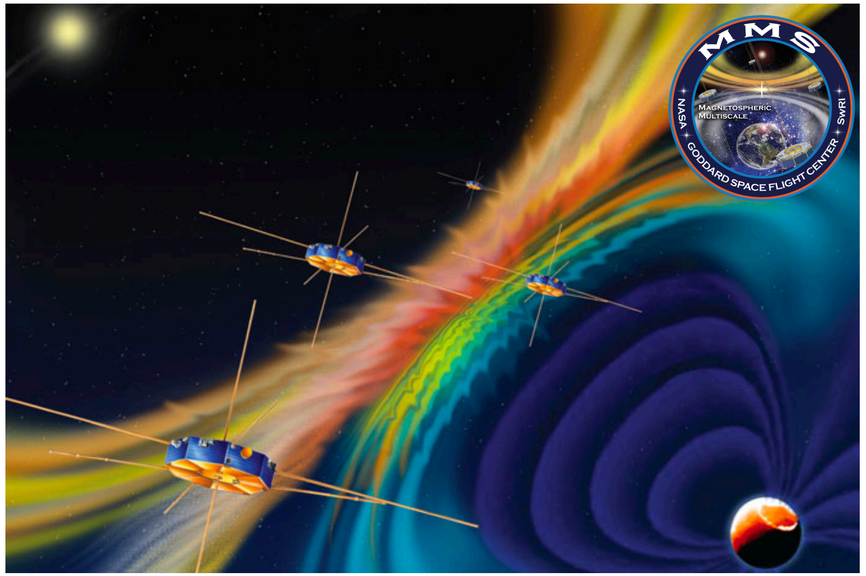

†https://www.nasa.gov/fy-2026-budget-request/

The Magnetospheric Multiscale (MMS) mission†

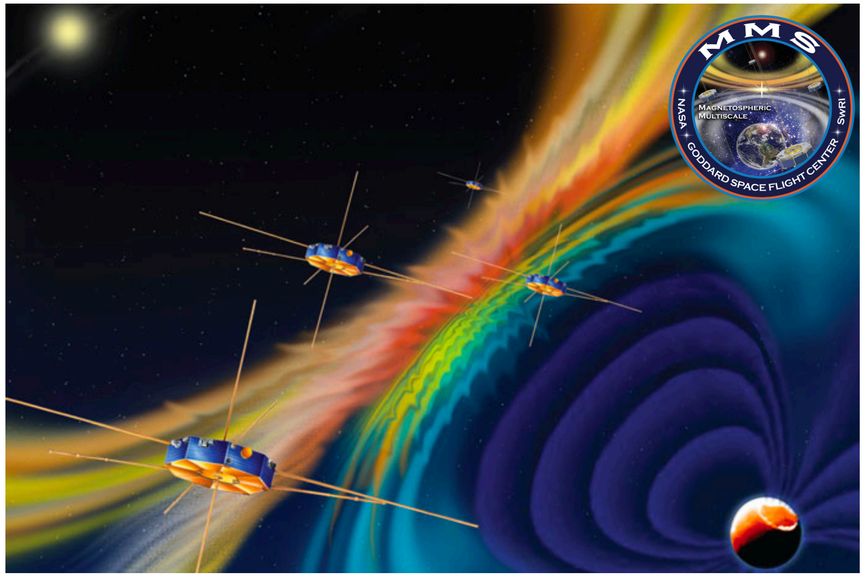

- NASA mission launched in 2015, designed to study magnetic reconnection in Earth's magnetosphere.
- Four spacecraft flying in a **tetrahedral formation with ~10 km separation**, enabling 3D measurements.
- Fields instruments provide **high-cadence measurements of electromagnetic fields**:
  - Electric and magnetic field data at up to 64 kHz (electric) and 8 kHz (magnetic).
- Particle instruments deliver **high-resolution plasma measurements**:
  - Thermal protons sampled every 150 ms and electrons every 30 ms.
  - Spin-resolution measurements (20 s cadence) of mass-resolved ions.
  - Suprathermal particles: ions at 10 s / 30 s and electrons at 30 s cadence.

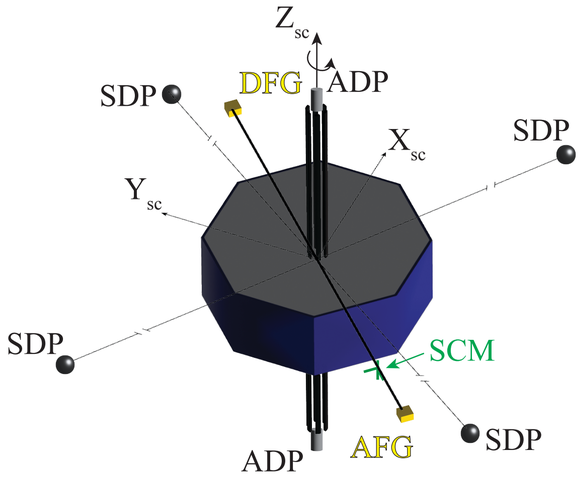

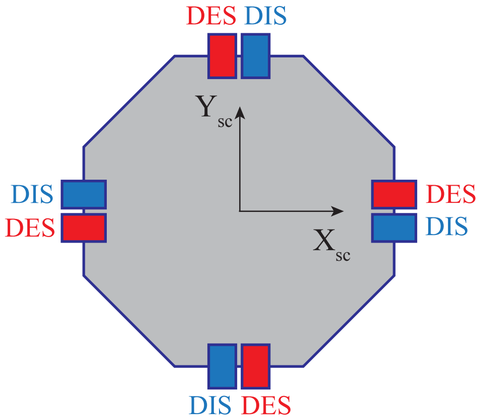

†https://www.nasa.gov/fy-2026-budget-request/

Magnetic Reconnection Jets

How do they look like?

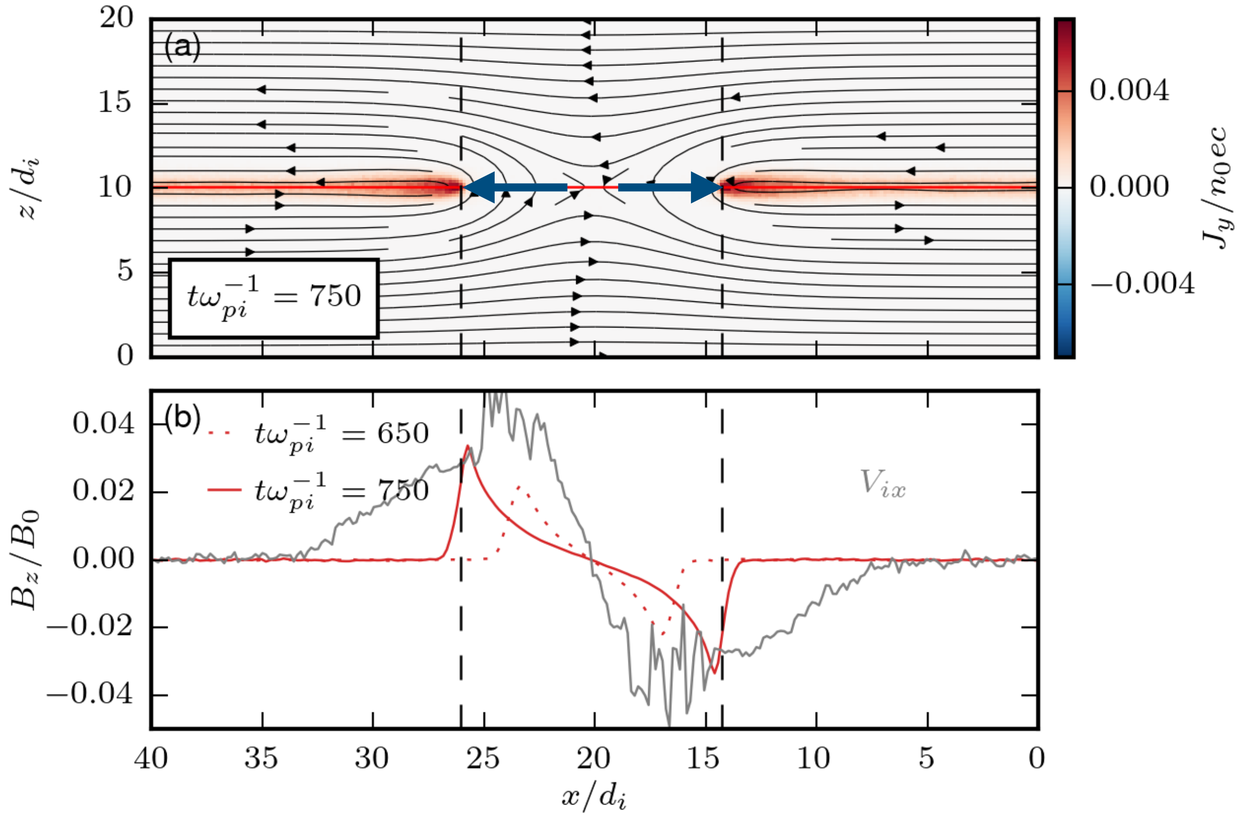

Magnetic Reconnection Jets

How do they look like?

- Reconnection jets are **short** (~1 min) and **fast** ($|\mathbf{V}_i| \geq 300\ \mathrm{km\ s^{-1}}$) **ion flows.**

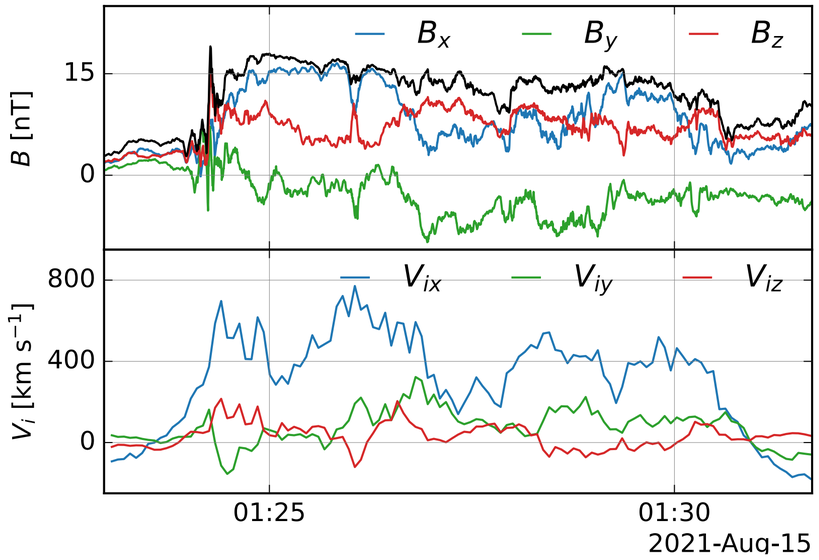

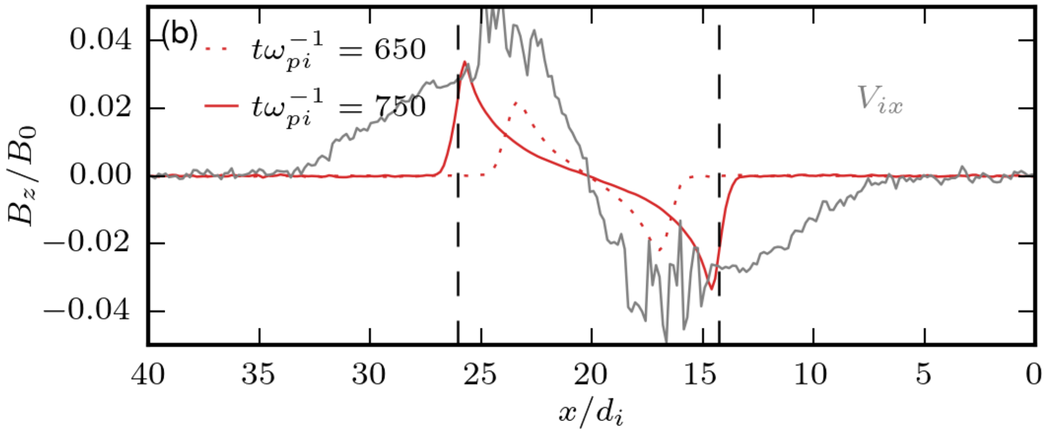

Magnetic Reconnection Jets

How do they look like?

- Reconnection jets are **short** (~1 min) and **fast** ($|\mathbf{V}_i| \geq 300$ km s^{-1}) **ion flows.**

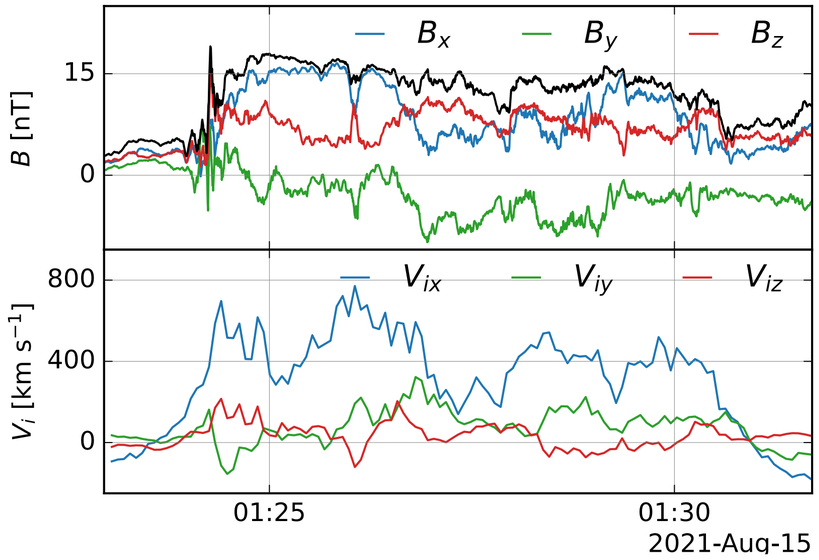

- Database of **2394 reconnection jets** in the Earth's plasma sheet compiled from MMS orbits 2017-2021.

[Richard+2022, GRL]

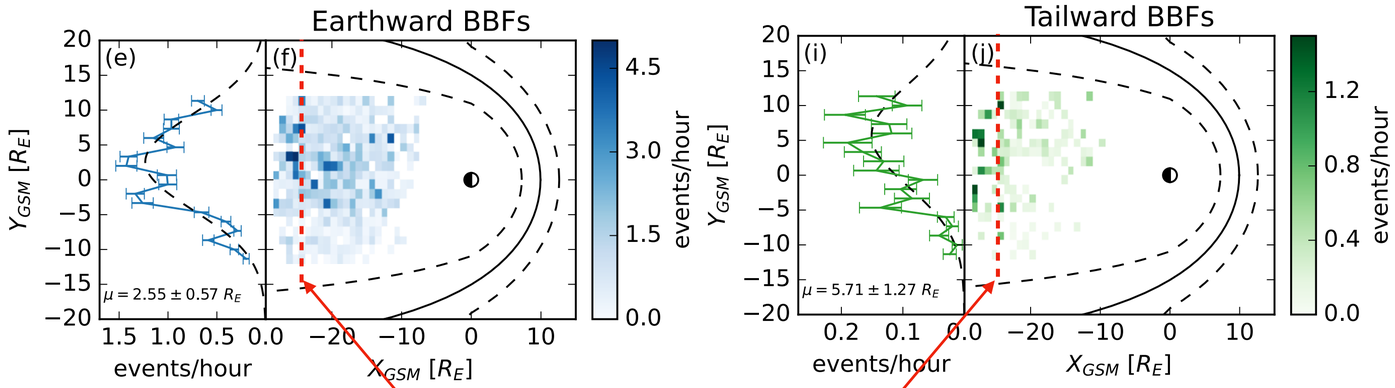

X-line at $\sim -25\ R_E$

Turbulence in Reconnection Jets

Why do we care?

Turbulence in Reconnection Jets

Why do we care?

- Turbulence-driven magnetic reconnection.

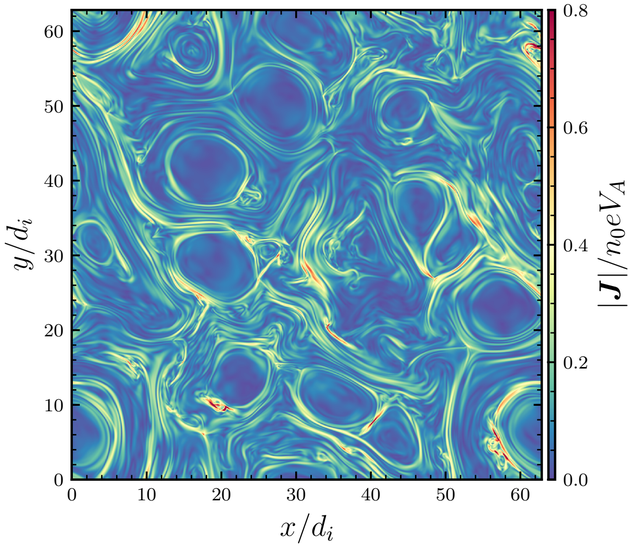

Turbulence in Reconnection Jets

Why do we care?

- Turbulence-driven magnetic reconnection.
- Turbulent magnetic reconnection.

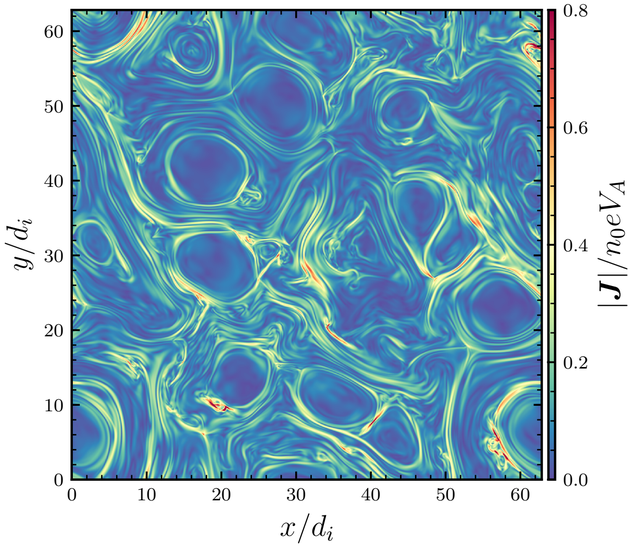

[Daughton+2011, Nat. Phys.]

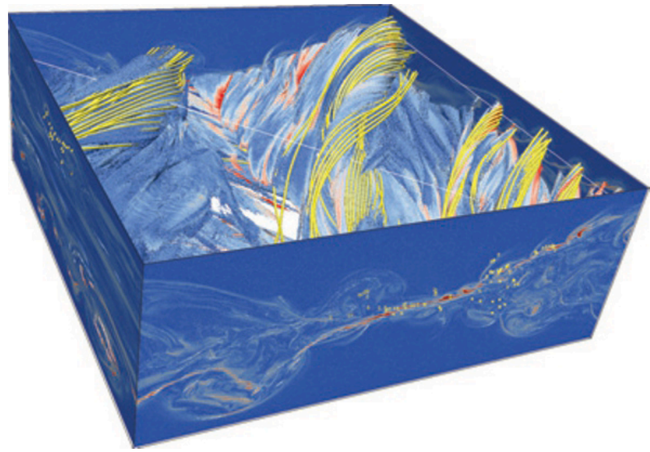

Turbulence in Reconnection Jets

Why do we care?

- Turbulence-driven magnetic reconnection.
- Turbulent magnetic reconnection.
- Secondary reconnection sites in turbulent outflows.

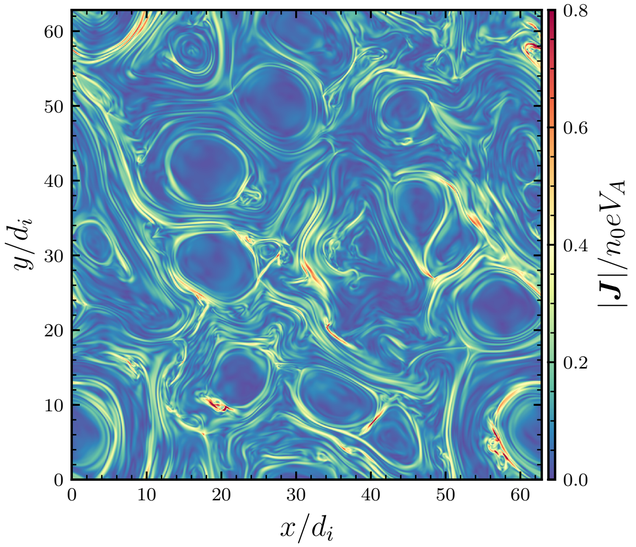

[Lapenta+2015, Nat. Phys.]

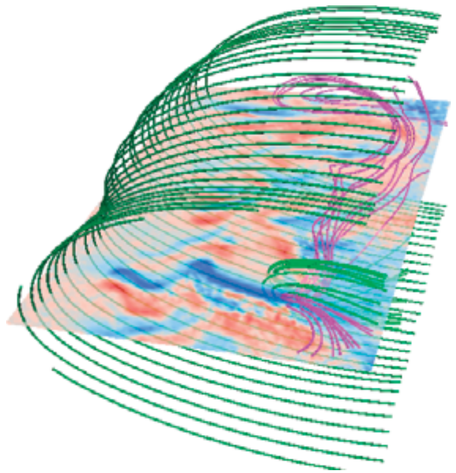

[Daughton+2011, Nat. Phys.]

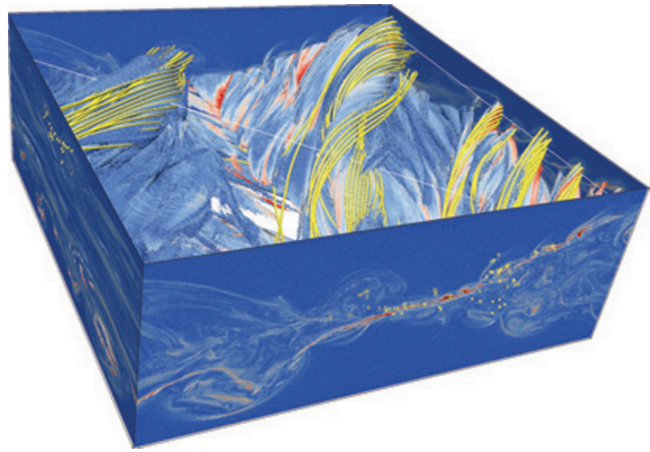

Turbulence in Reconnection Jets

Why do we care?

- Turbulence-driven magnetic reconnection.
- Turbulent magnetic reconnection.
- Secondary reconnection sites in turbulent outflows.
- Non-thermal particle acceleration in turbulent electromagnetic fields

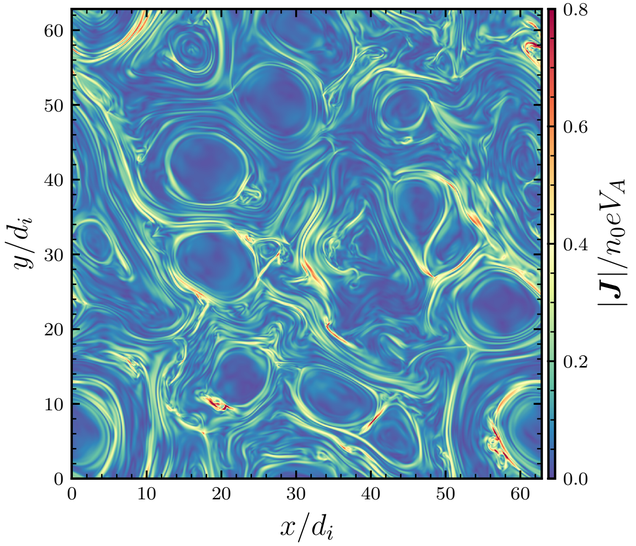

[Lapenta+2015, Nat. Phys.]

[Daughton+2011, Nat. Phys.]

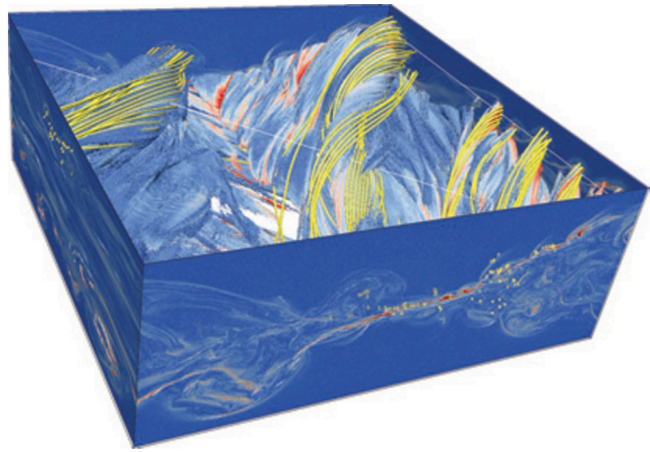

[Lapenta+2020, PRL]

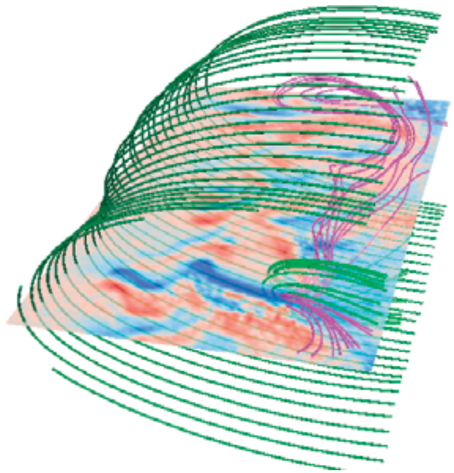

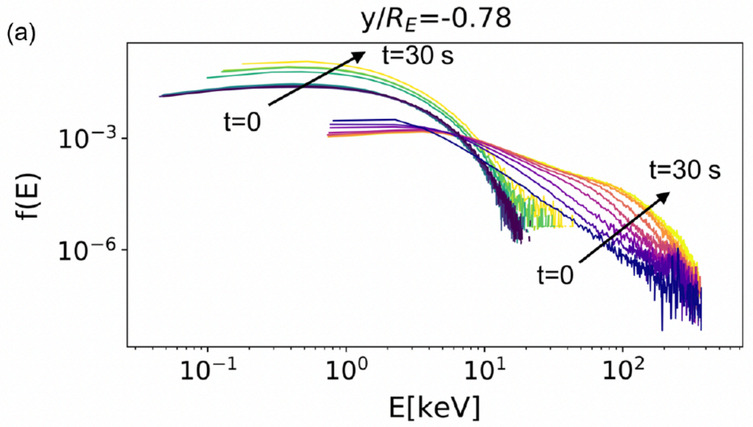

Turbulence in Reconnection Jets

Why do we care?

- Turbulence-driven magnetic reconnection.
- Turbulent magnetic reconnection.
- Secondary reconnection sites in turbulent outflows.
- Non-thermal particle acceleration in turbulent electromagnetic fields

How much does turbulence contribute to energy conversion in reconnection jets?

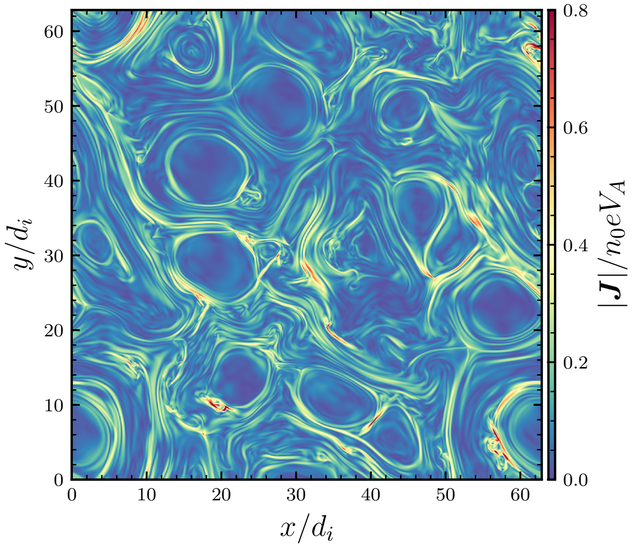

[Daughton+2011, Nat. Phys.]

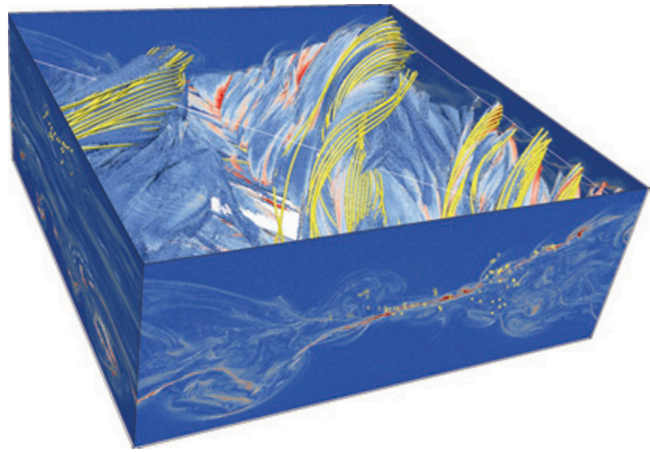

[Lapenta+2015, Nat. Phys.]

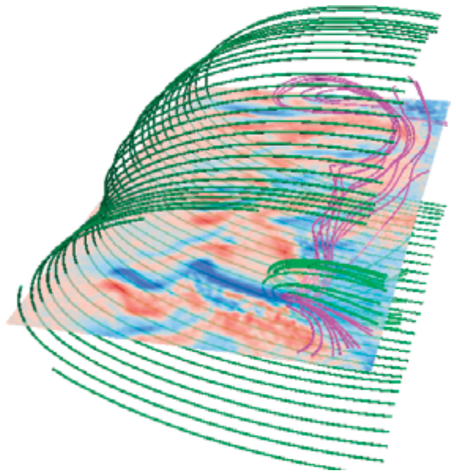

[Lapenta+2020, PRL]

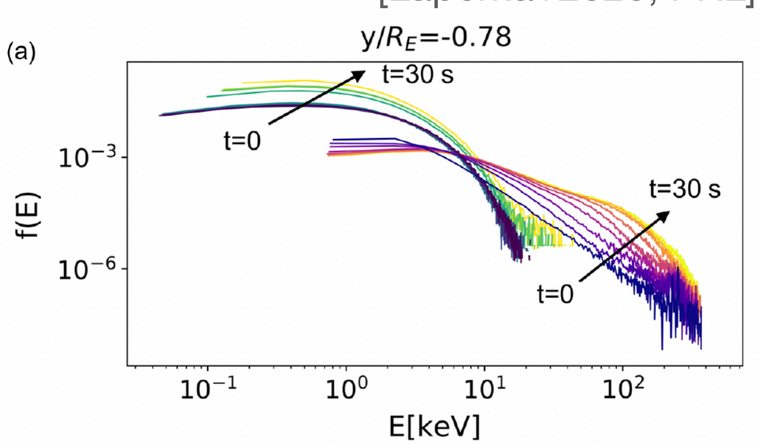

Turbulence in Reconnection Jets

Example

[Richard+2024, PRL]

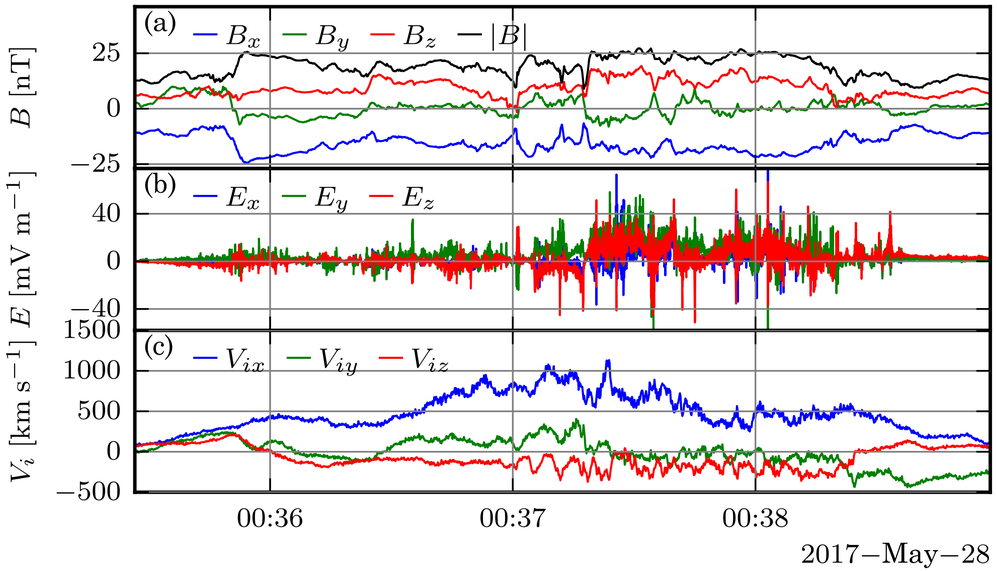

Turbulence in Reconnection Jets

Example

- Kolmogorov-like scaling at large (fluid) scales

[Richard+2024, PRL]

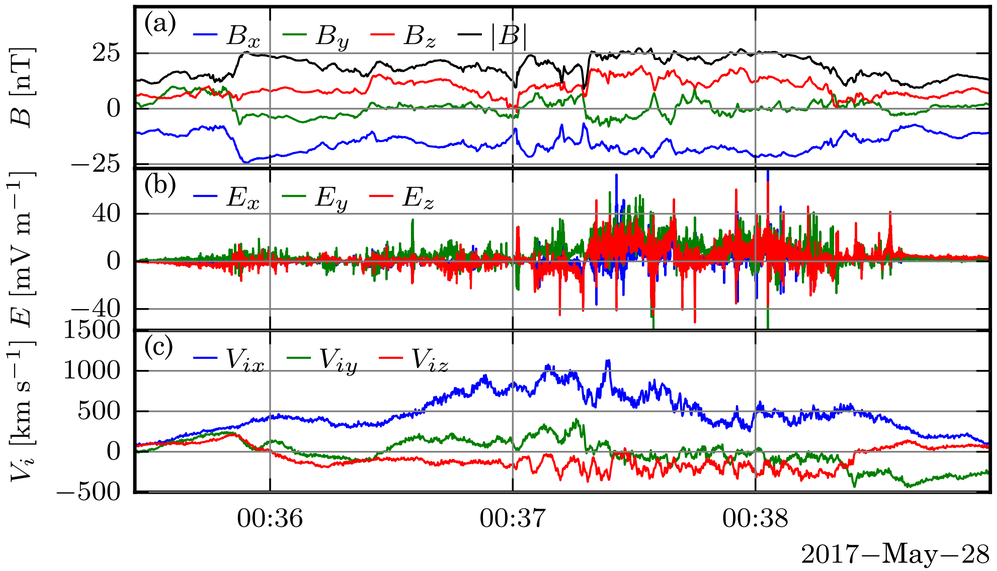

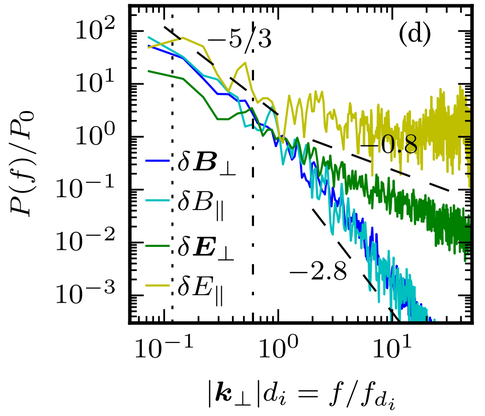

Turbulence in Reconnection Jets

Example

- Kolmogorov-like scaling at large (fluid) scales
- Third-order energy transfer for MHD turbulence [e.g., Politano & Pouquet, 1993, PRE]

$$-2\varepsilon = \frac{1}{2}\nabla_l \cdot \mathbf{Y} + S,$$

with ε the energy "cascade" rate, $\mathbf{Y}$ the total energy flux, S, the total energy source

[Richard+2024, PRL]

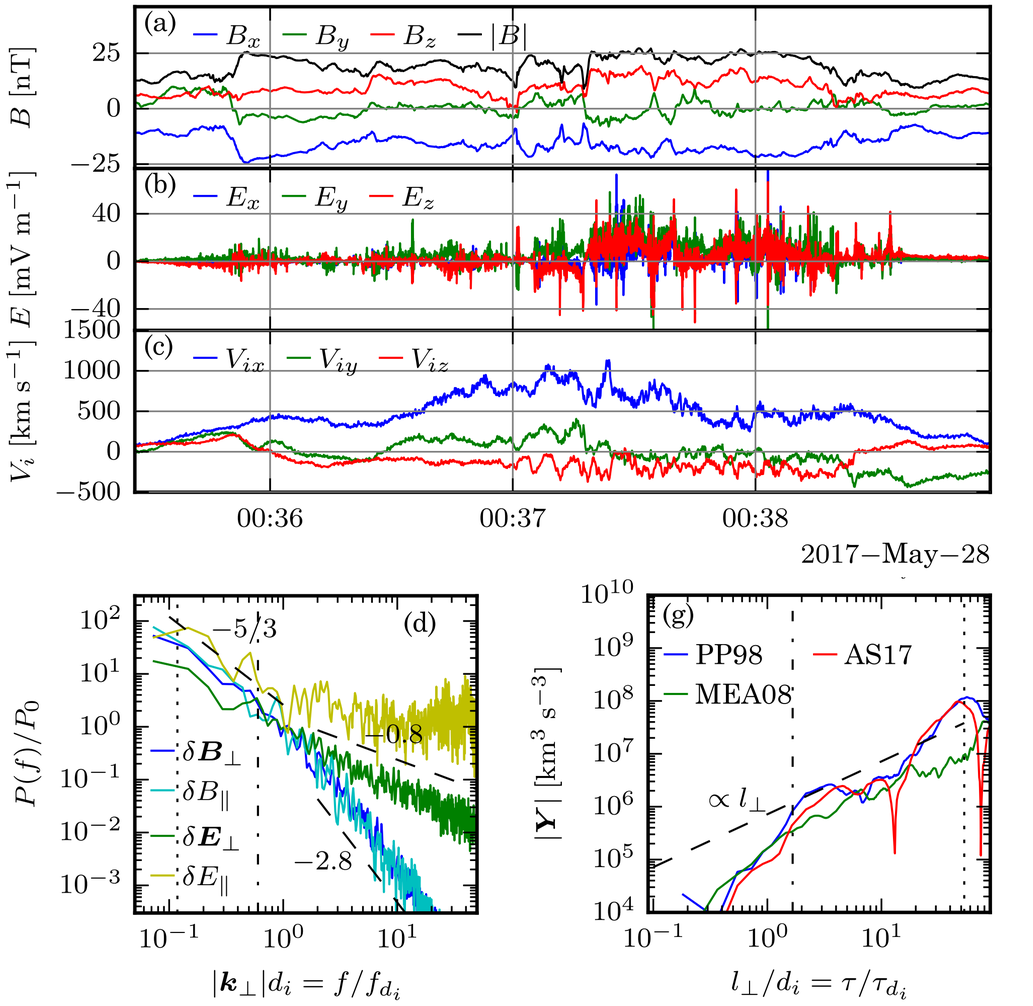

Turbulence in Reconnection Jets

Example

- Kolmogorov-like scaling at large (fluid) scales
- Third-order energy transfer for MHD turbulence [e.g., Politano & Pouquet, 1993, PRE]

$$-2\varepsilon = \frac{1}{2}\nabla_l \cdot \mathbf{Y} + S,$$

with ε the energy "cascade" rate, $\mathbf{Y}$ the total energy flux, S, the total energy source

The reconnection outflow shows signs of fully developed turbulence

[Richard+2024, PRL]

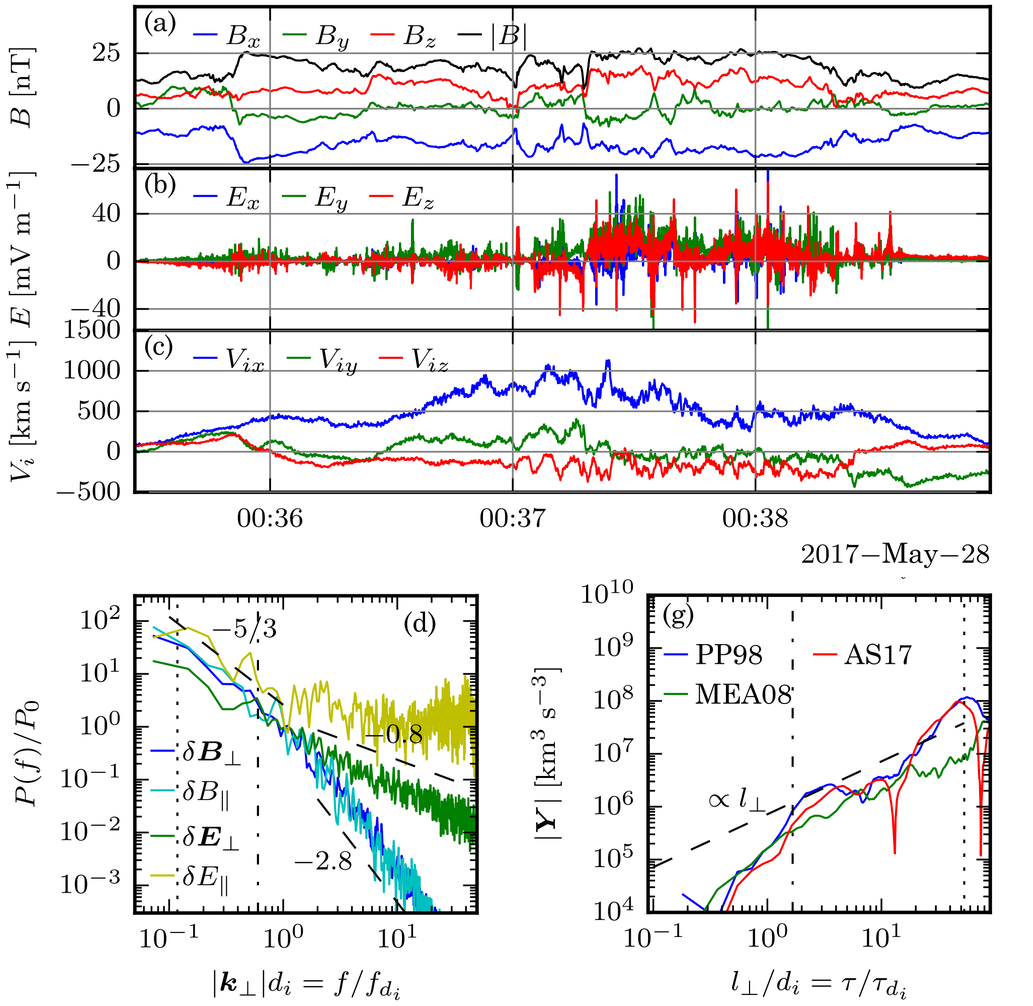

Turbulence in Reconnection Jets

Statistics

Turbulence in Reconnection Jets

Statistics

[Richard+2024, PRL]

- Kolmogorov-like scaling at large (fluid) scales.

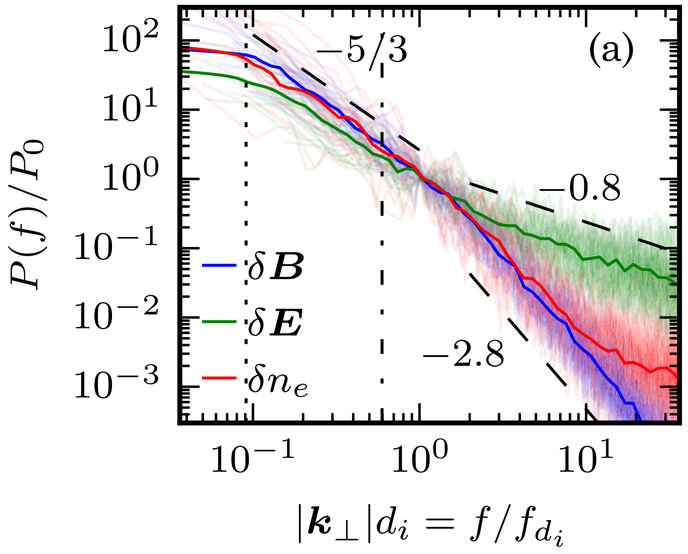

Turbulence in Reconnection Jets

Statistics

[Richard+2024, PRL]

- Kolmogorov-like scaling at large (fluid) scales.
- Breakdown of Kolmogorov's self-similarity assumption, i.e., intermittency
- Degree of intermittency estimated using the p-model [Meneveau and Sreenivasan, 1987, PRL]

$$\frac{\zeta(m)}{\zeta(3)} = 1 - log_2(p^{mh} + (1-p)^{mh})$$

The large-scale fluctuations indicate fully developed turbulence.

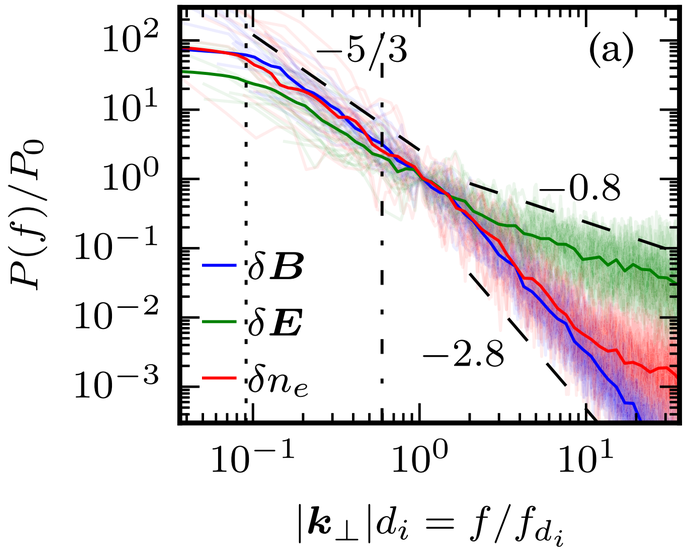

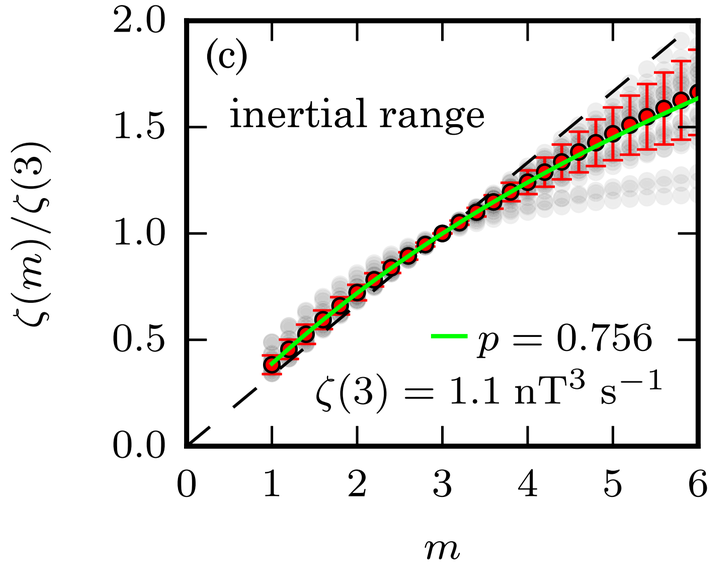

Turbulence in Reconnection Jets

Energy cascade rate

Turbulence in Reconnection Jets

Energy cascade rate

- Energy cascade rate $\varepsilon \sim 10^8$ J kg^{-1} s^{-1}

[Richard+2024, PRL]

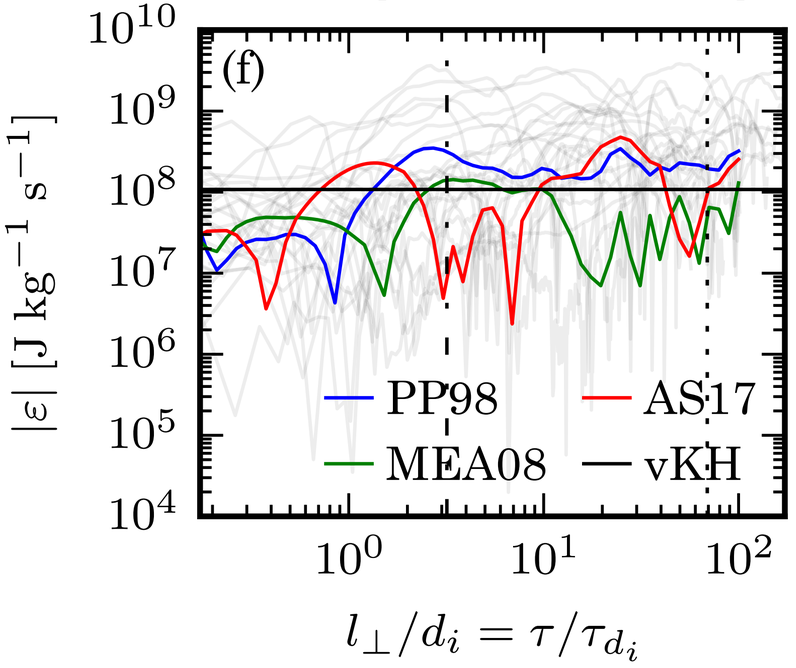

Turbulence in Reconnection Jets

Energy cascade rate

- Energy cascade rate $\varepsilon \sim 10^8$ J kg^{-1} s^{-1}

	SW	CME sheath	MSH	PSBL	KH
$\varepsilon_{jet}/\varepsilon$	10^5	10^3	10^2	10	4

[Richard+2024, PRL]

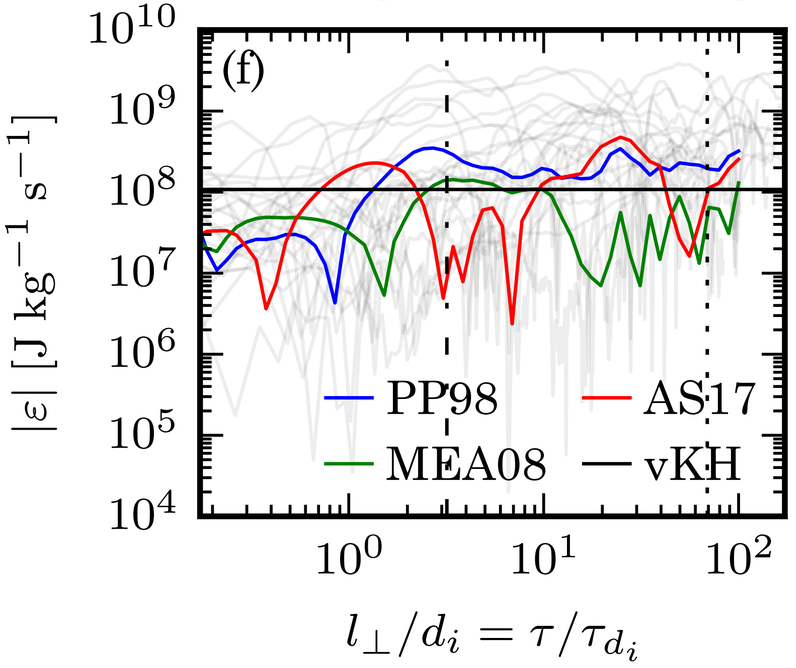

Turbulence in Reconnection Jets

Energy cascade rate

- Energy cascade rate $\varepsilon \sim 10^8$ J kg^{-1} s^{-1}

	SW	CME sheath	MSH	PSBL	KH
$\varepsilon_{jet}/\varepsilon$	10^5	10^3	10^2	10	4

- Energy injection (Von-Kármán-Howarth energy decay rate) is **balanced** by energy transfer across large scales.

[Richard+2024, PRL]

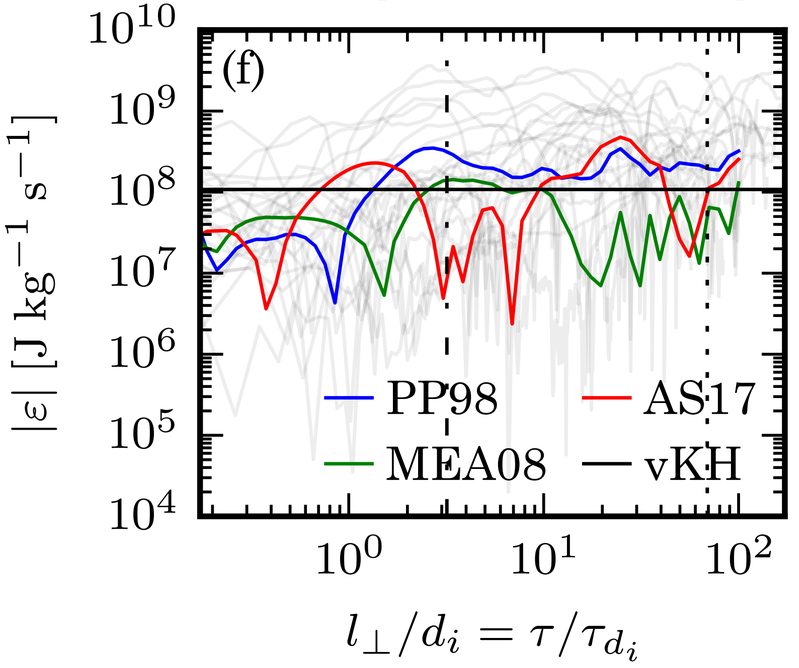

Turbulence in Reconnection Jets

Energy cascade rate

- Energy cascade rate $\varepsilon \sim 10^8$ J kg^{-1} s^{-1}

	SW	CME sheath	MSH	PSBL	KH
$\varepsilon_{jet}/\varepsilon$	10^5	10^3	10^2	10	4

- Energy injection (Von-Kármán-Howarth energy decay rate) is **balanced** by energy transfer across large scales.
- Rate of decrease of magnetic energy in the reconnection inflow

$$\dot{\mathscr{E}}_b = (B_r^2/2\mu_0)/\Delta t \sim 10^9 \text{ J kg}^{-1} \text{ s}^{-1}$$

Turbulent energy transfer rate is ~10% of the reconnection energy input rate.

[Richard+2024, PRL]

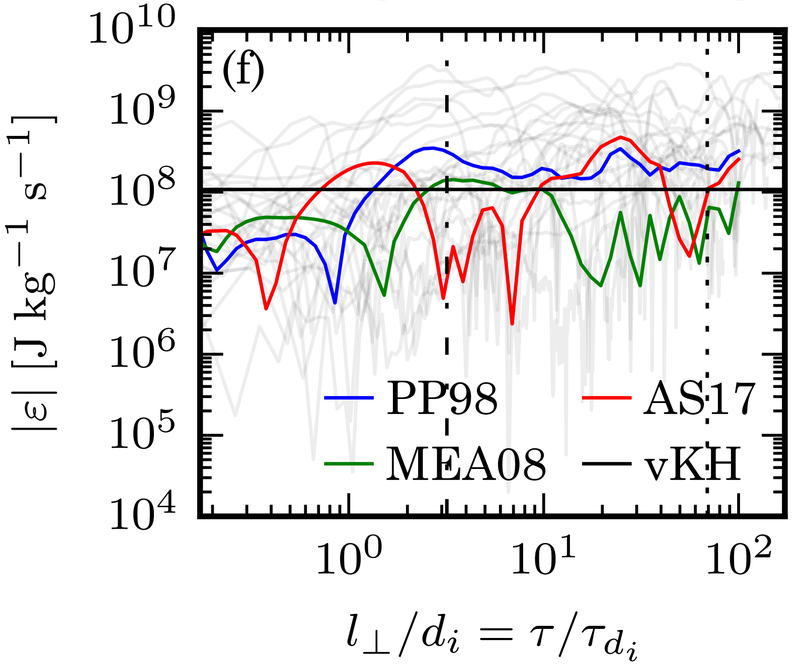

Ion Heating in Reconnection Jets

Why do we care?

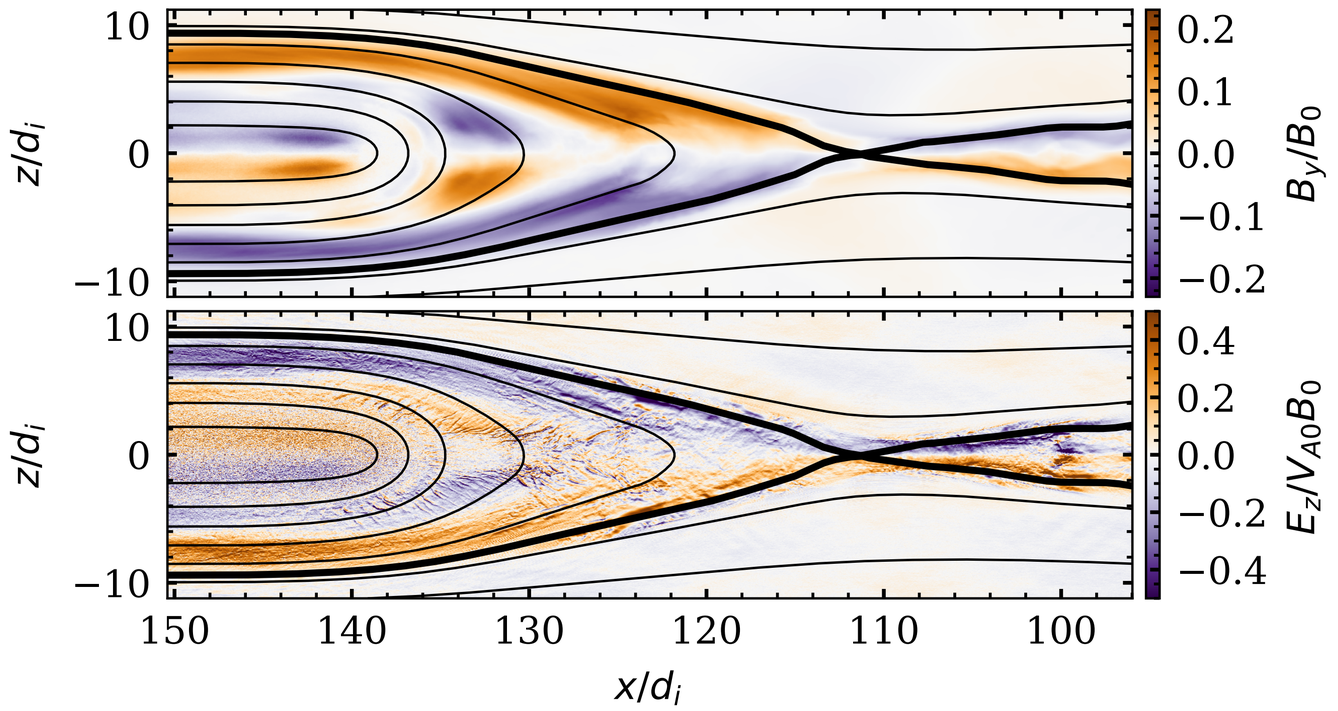

Ion Heating in Reconnection Jets

Why do we care?

- Ions in the reconnection jet are accelerated by the Hall electric field, forming counter-streaming beams [e.g., Wygant+2005, JGR].

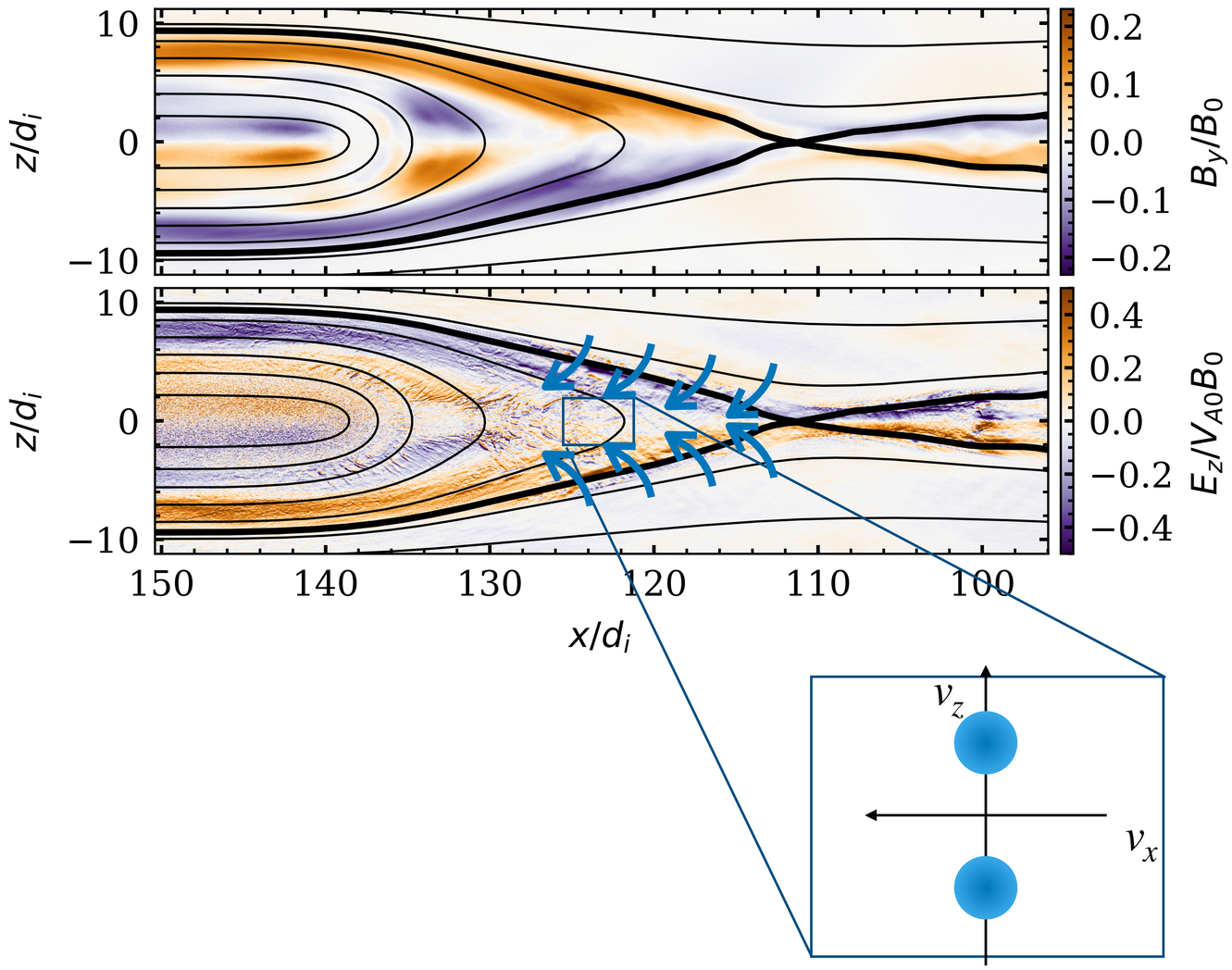

Ion Heating in Reconnection Jets

Why do we care?

- Ions in the reconnection jet are accelerated by the Hall electric field, forming counter-streaming beams [e.g., Wygant+2005, JGR].
- Temperature anisotropy decreases with distance from the reconnection region [Wu+2013, JGR].

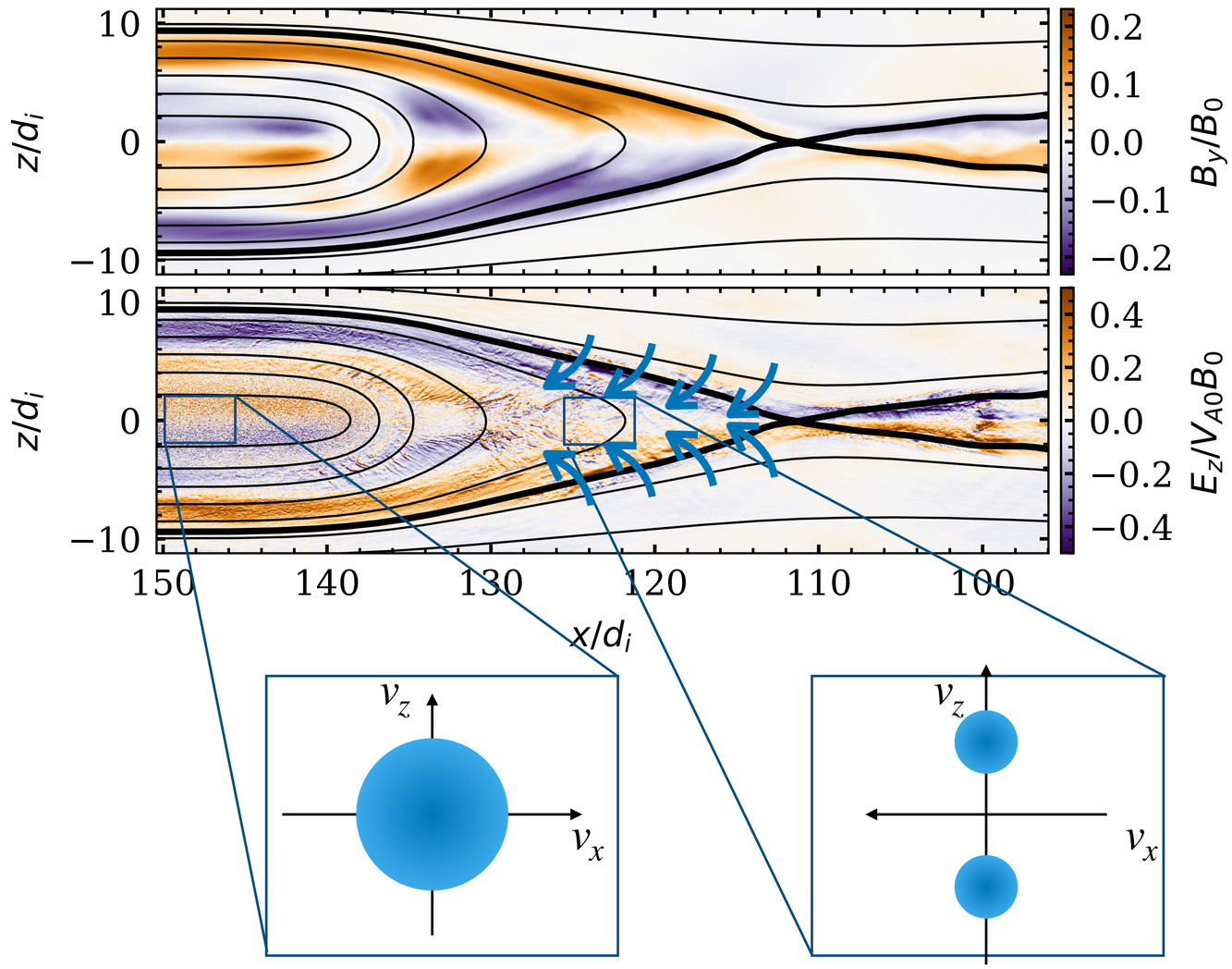

Ion Heating in Reconnection Jets

Why do we care?

- Ions in the reconnection jet are accelerated by the Hall electric field, forming counter-streaming beams [e.g., Wygant+2005, JGR].
- Temperature anisotropy decreases with distance from the reconnection region [Wu+2013, JGR].
- Wave-particle interactions are inefficient at scattering ions due to slow instability growth [Hietala+2015, GRL].

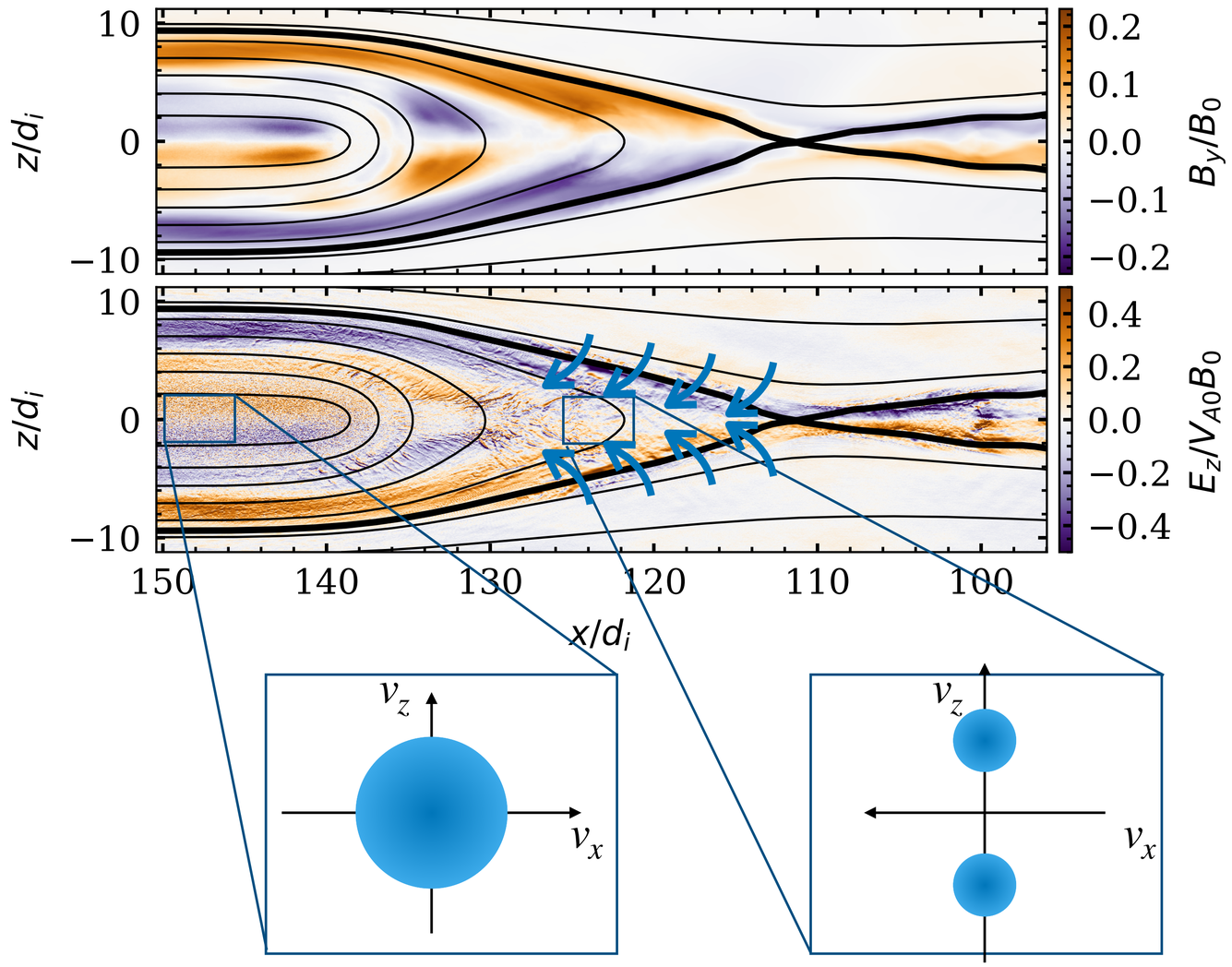

Ion Heating in Reconnection Jets

Why do we care?

- Ions in the reconnection jet are accelerated by the Hall electric field, forming counter-streaming beams [e.g., Wygant+2005, JGR].
- Temperature anisotropy decreases with distance from the reconnection region [Wu+2013, JGR].
- Wave-particle interactions are inefficient at scattering ions due to slow instability growth [Hietala+2015, GRL].

How are ion VDFs isotropized in the reconnection jet?

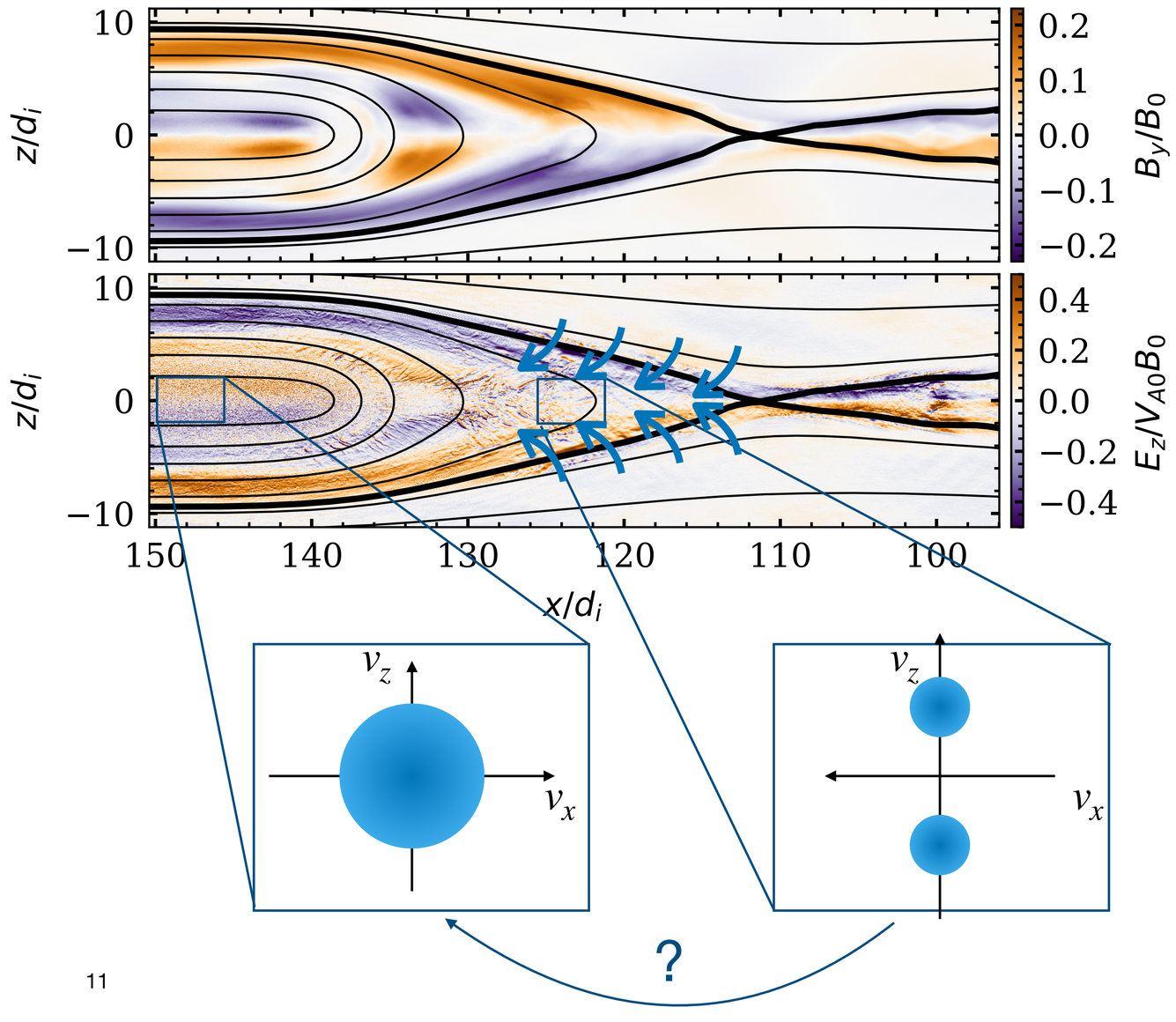

Ion Heating in Reconnection Jets

Data Distribution

Ion Heating in Reconnection Jets

[Richard+2023, PRL]

Data Distribution

- >70% of the measurements are within the instability thresholds, indicating that the plasma conditions are efficiently regulated.

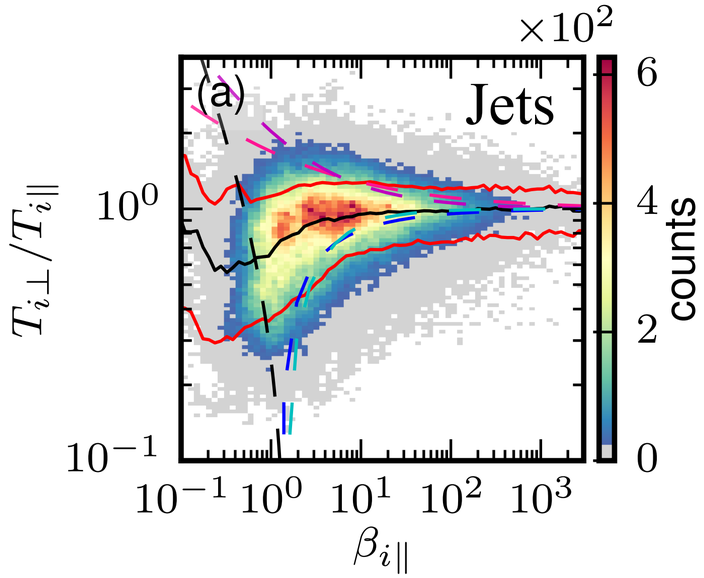

Ion Heating in Reconnection Jets

Data Distribution

- >70% of the measurements are within the instability thresholds, indicating that the plasma conditions are efficiently regulated.

- Magnetic reconnection drives ion VDFs out of LTE.

[Richard+2023, PRL]

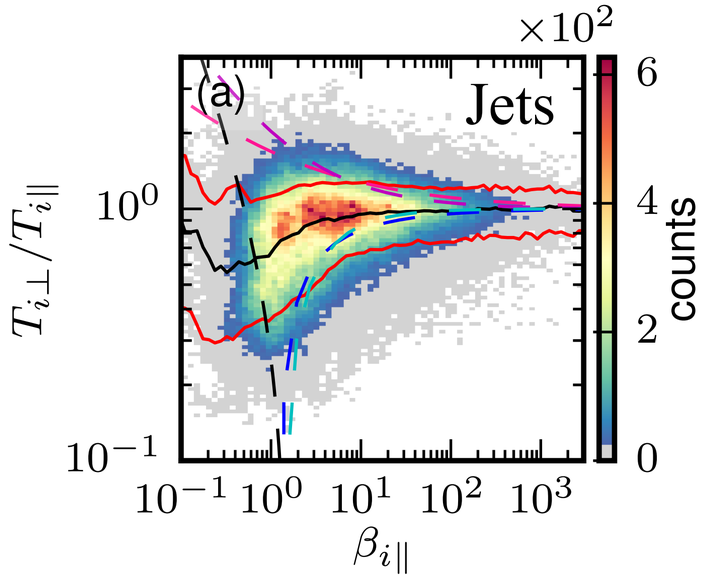

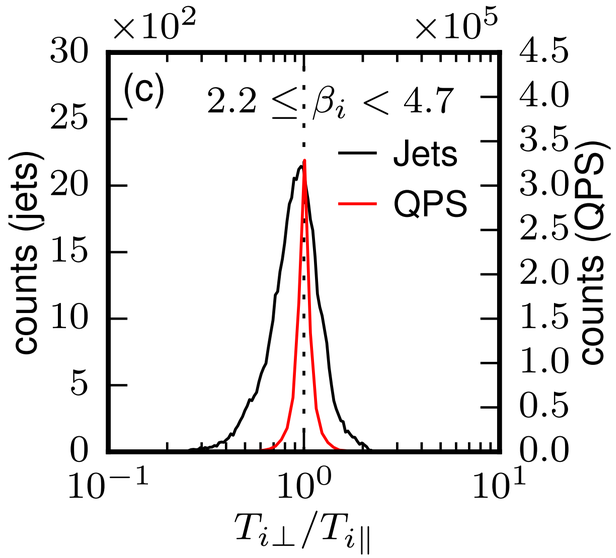

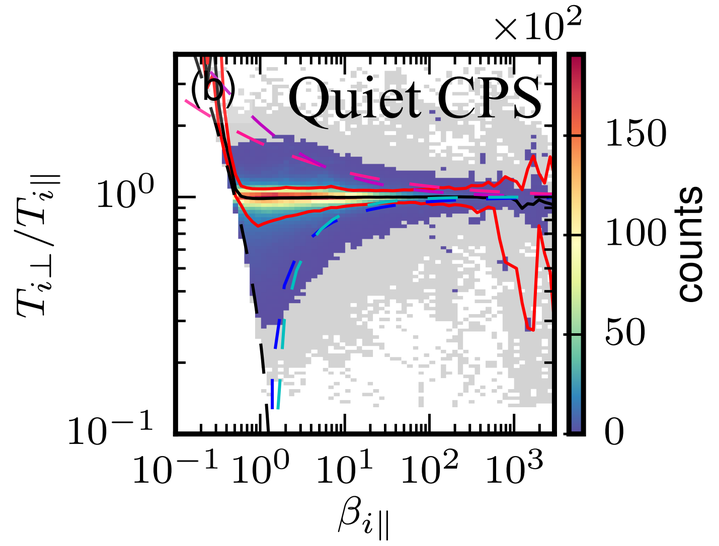

Ion Heating in Reconnection Jets

Data Distribution

[Richard+2023, PRL]

- >70% of the measurements are within the instability thresholds, indicating that the plasma conditions are efficiently regulated.

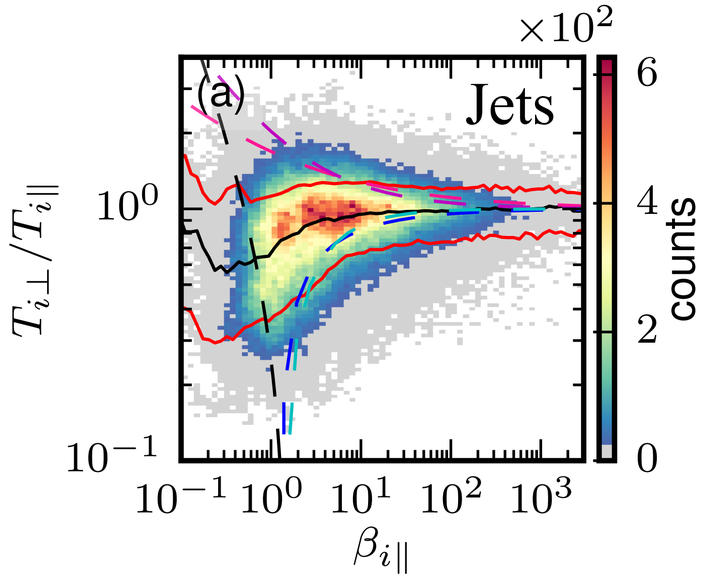

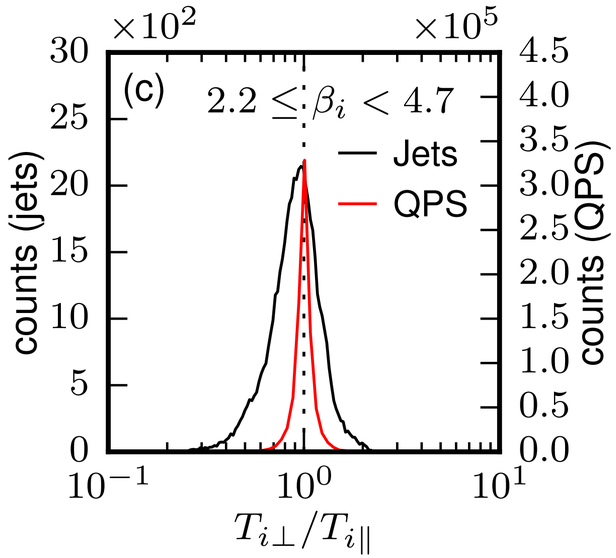

- Magnetic reconnection drives ion VDFs out of LTE.

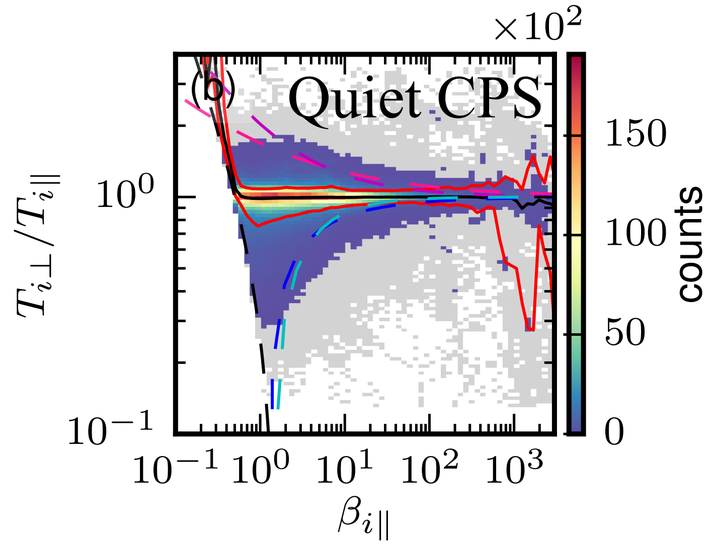

Ion VDFs are nearly isotropic in the quiet plasma sheet and in the reconnection jets.

Ion Heating in Reconnection Jets

Relaxation time

Ion Heating in Reconnection Jets

Relaxation time

- How long does it take to isotropize the ion VDFs?
  - At most, the travel time from the X-line to the spacecraft.

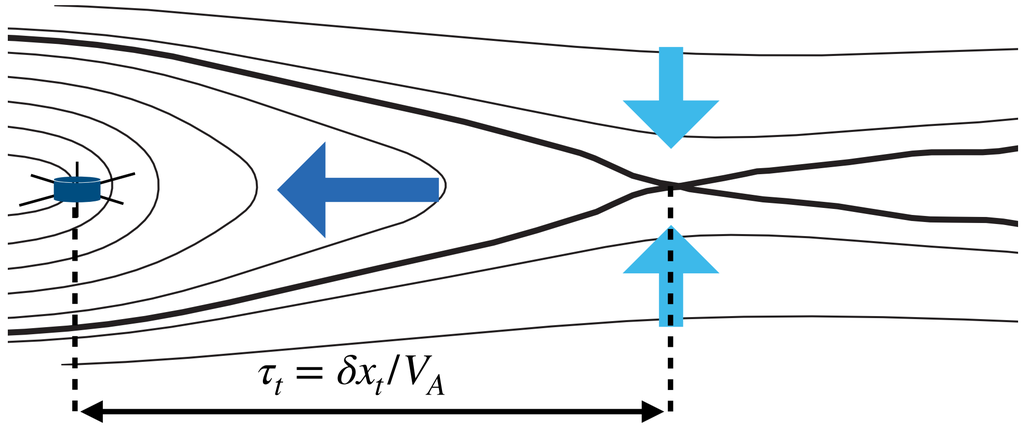

Ion Heating in Reconnection Jets

Relaxation time

- How long does it take to isotropize the ion VDFs?
  - At most, the travel time from the X-line to the spacecraft.

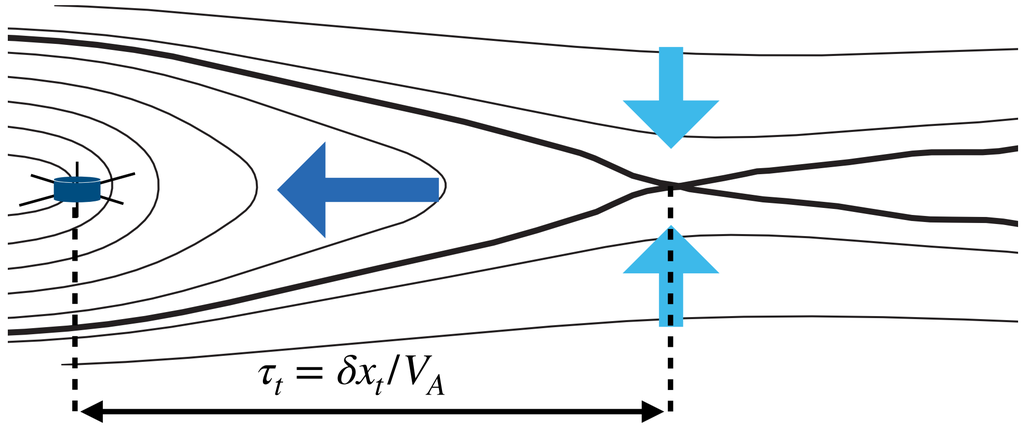

[Richard+2023, PRL]

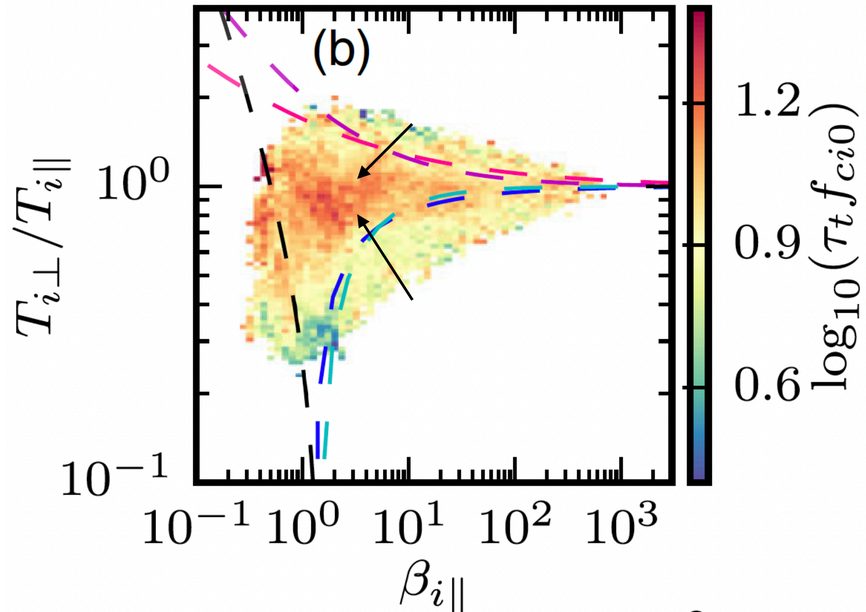

Non-LTE Ion VDFs are relaxed after
$\tau_t f_{ci0} \sim 10$**, i.e.,** $\delta x \sim 60 d_i$**.**

Ion Heating in Reconnection Jets

Current sheet scattering

Ion Heating in Reconnection Jets

Current sheet scattering

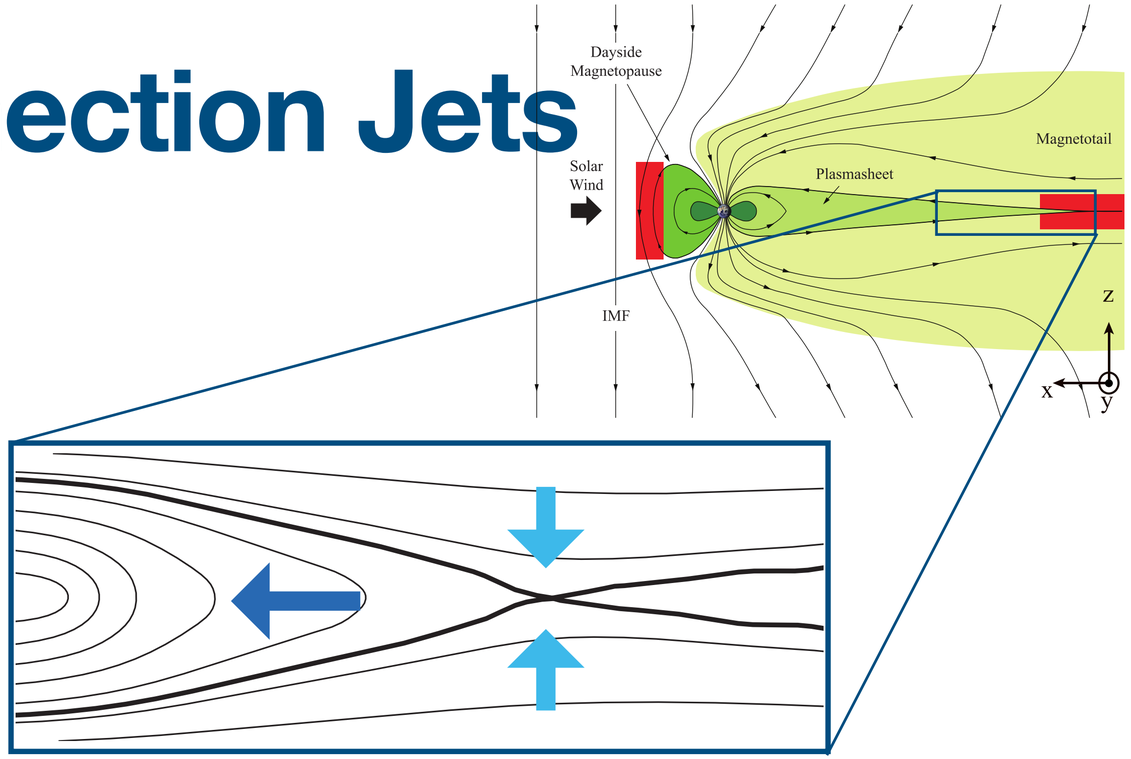

Ion Heating in Reconnection Jets

Current sheet scattering

- Ion motion in current sheets are identified based on $\kappa = \sqrt{r_c/\rho_i}$ [Büchner and Zelenyi, 1989, JGR]:
  - Adiabatic motion $\kappa \gg 1$
  - Chaotic motion $\kappa \approx 1$ -> strong scattering
  - Quasi-adiabatic motion $\kappa \ll 1$-> weak scattering

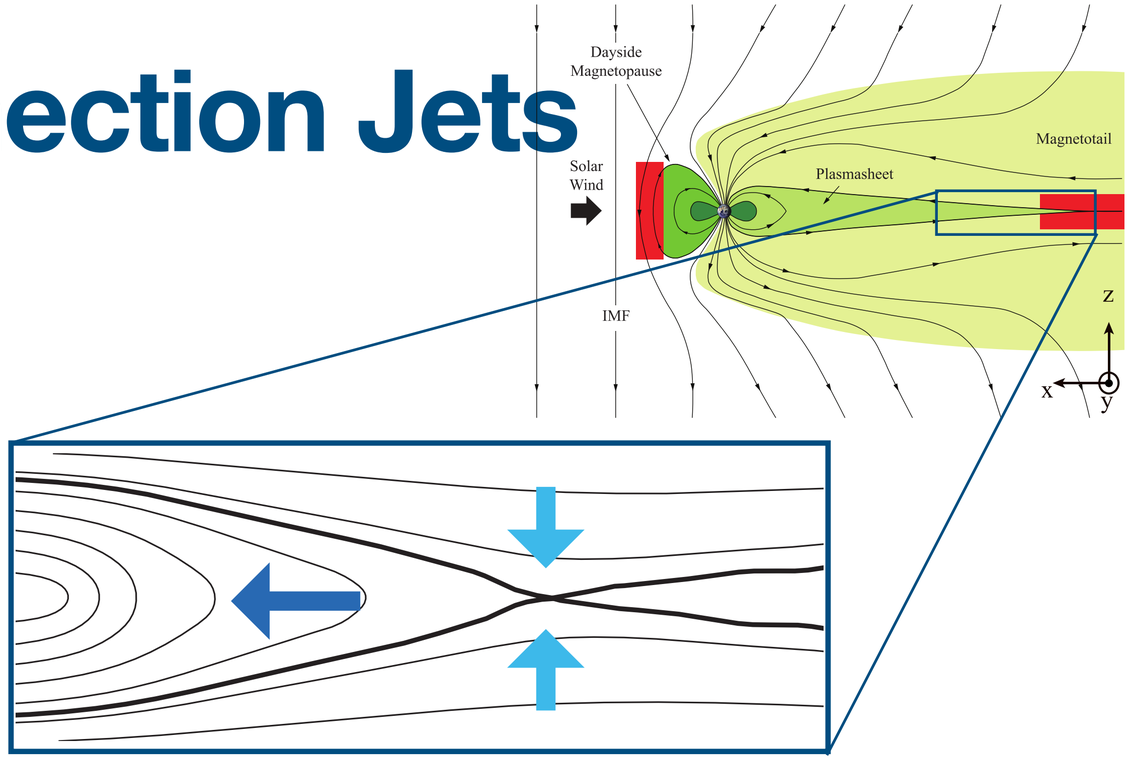

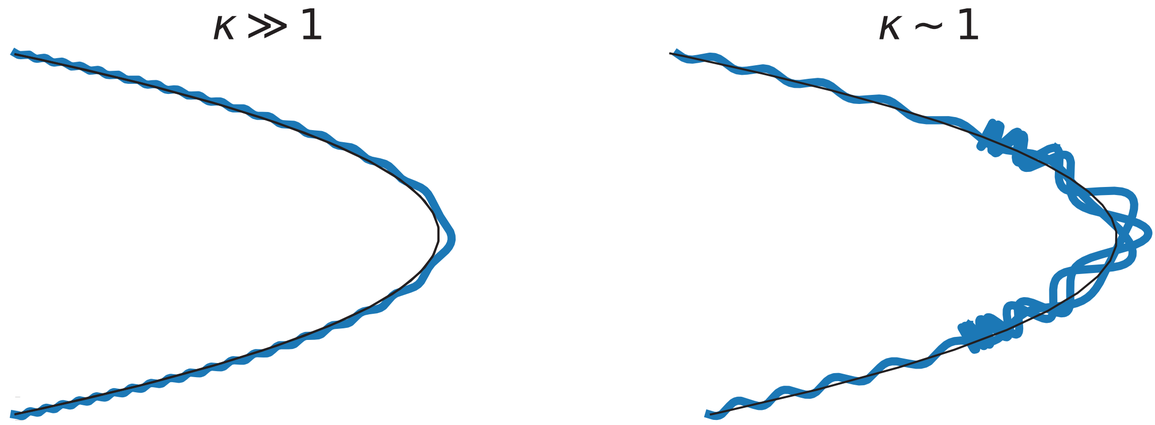

Ion Heating in Reconnection Jets

Current sheet scattering

- Ion motion in current sheets are identified based on $\kappa = \sqrt{r_c/\rho_i}$ [Büchner and Zelenyi, 1989, JGR]:
  - Adiabatic motion $\kappa \gg 1$
  - Chaotic motion $\kappa \approx 1$ -> strong scattering
  - Quasi-adiabatic motion $\kappa \ll 1$-> weak scattering
- 73% of ion VDFs in reconnection jets show chaotic or quasi-adiabatic motion.

Chaotic ion motion in the CS results in fast pitch-angle scattering

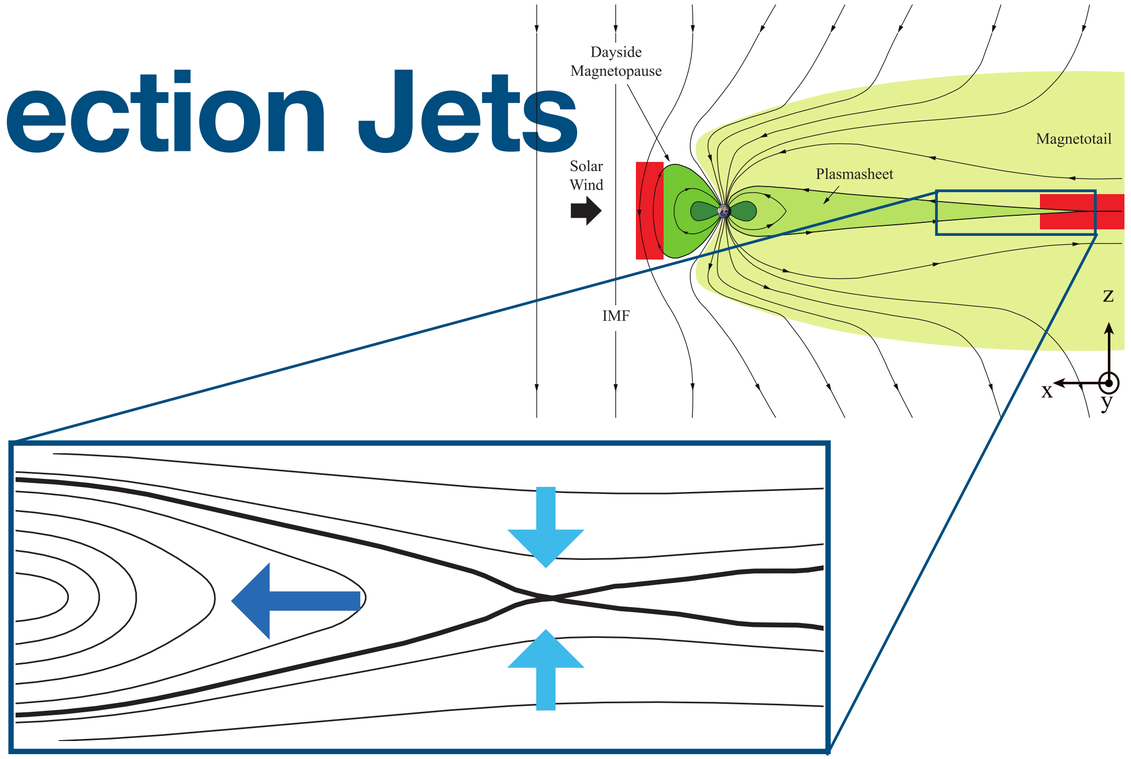

[Richard+2023, PRL]

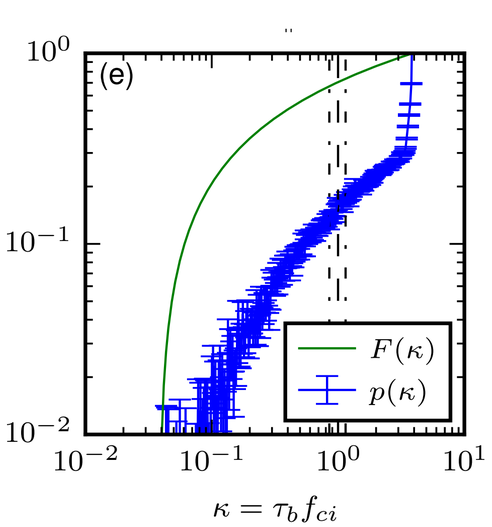

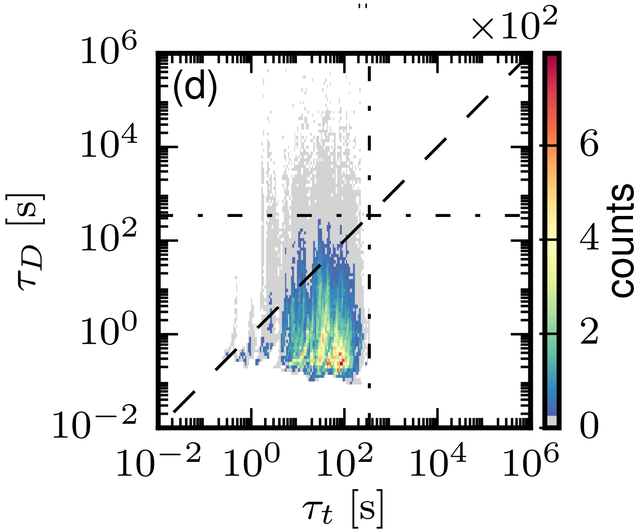

Parallel Electric Fields in Reconnection

Theory

Parallel Electric Fields in Reconnection

Theory

- As **magnetic flux tubes expand**, electron density should drops, while density of demagnetized ions stays constant **resulting in positive charge density.**

[Egedal+2015, PoP]

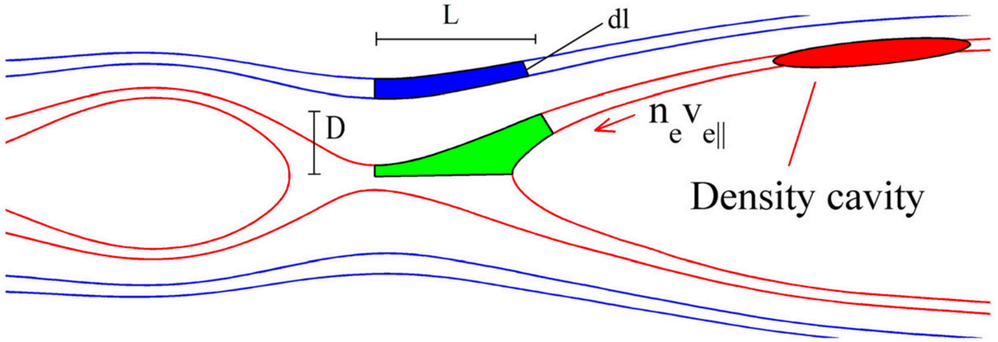

Parallel Electric Fields in Reconnection

Theory

- As **magnetic flux tubes expand**, electron density should drops, while density of demagnetized ions stays constant **resulting in positive charge density.**
- **Parallel electric fields** $E_{\parallel}$ form in the reconnection region to **maintain quasi-neutrality**.

[Egedal+2015, PoP]

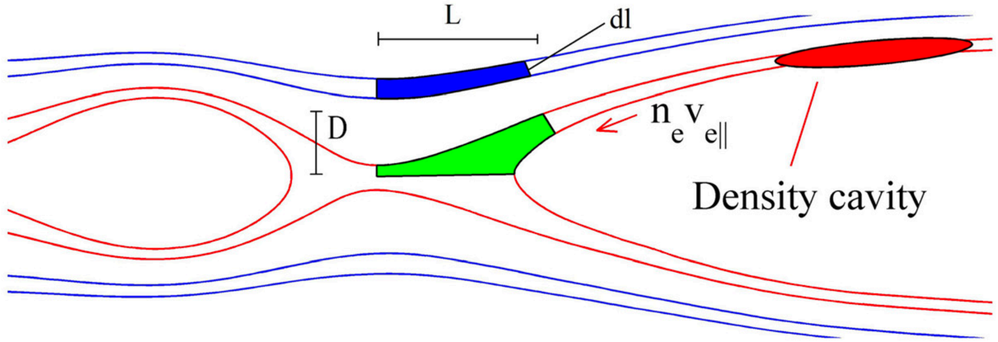

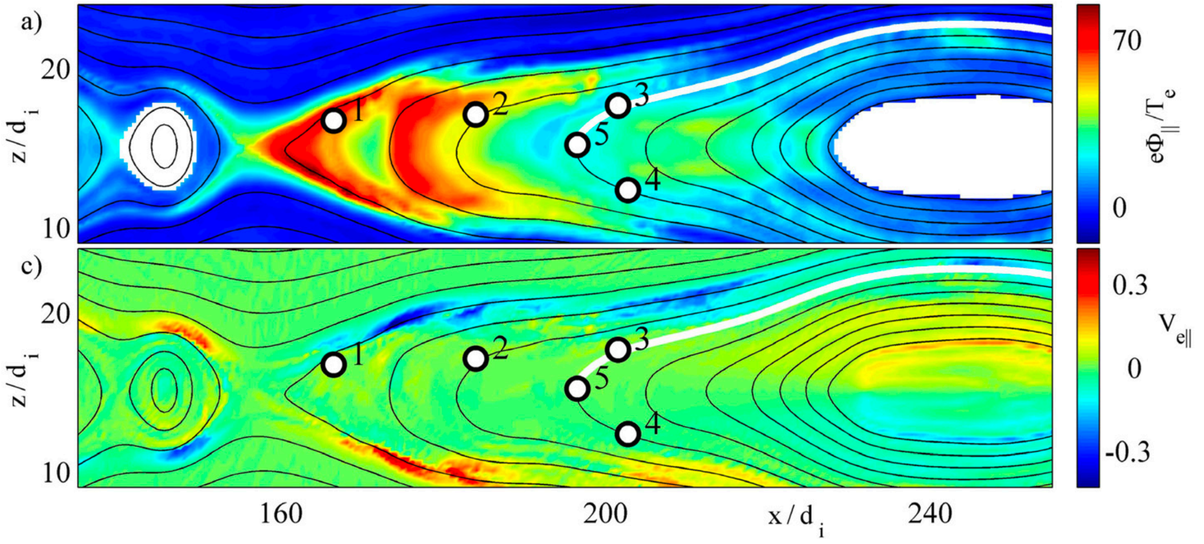

Parallel Electric Fields in Reconnection

Theory

- As **magnetic flux tubes expand**, electron density should drops, while density of demagnetized ions stays constant **resulting in positive charge density.**
- **Parallel electric fields** $E_{||}$ form in the reconnection region to **maintain quasi-neutrality**.
- $E_{||}$ **trap electrons** locally to balance charge and maintain quasi-neutrality.

[Egedal+2015, PoP]

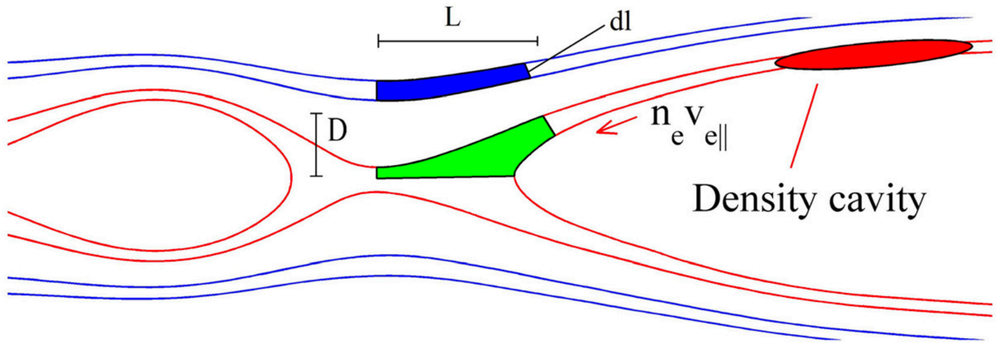

[Egedal+2005, PRL]

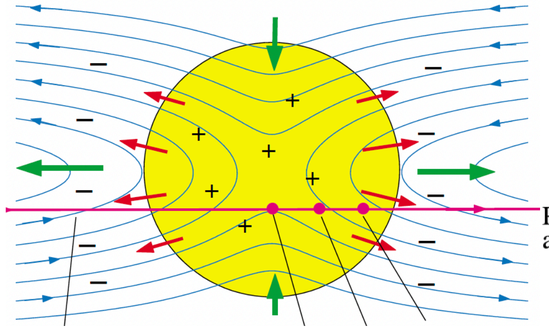

[Egedal+2015, PoP]

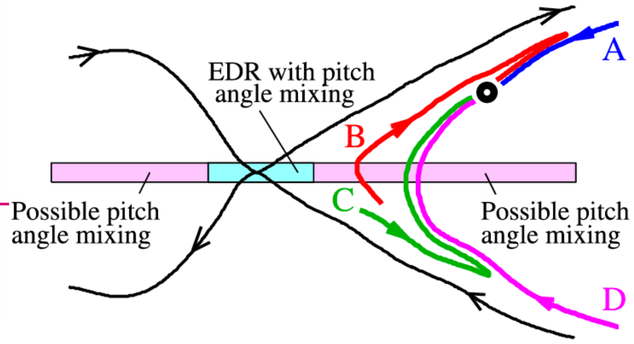

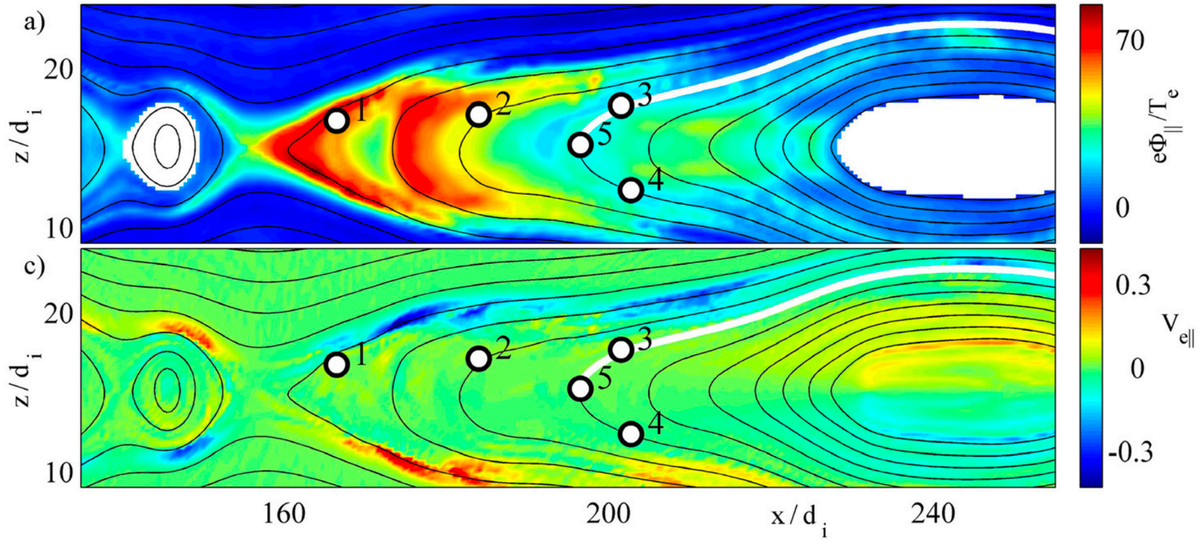

Electron Heating by Parallel Electric Fields

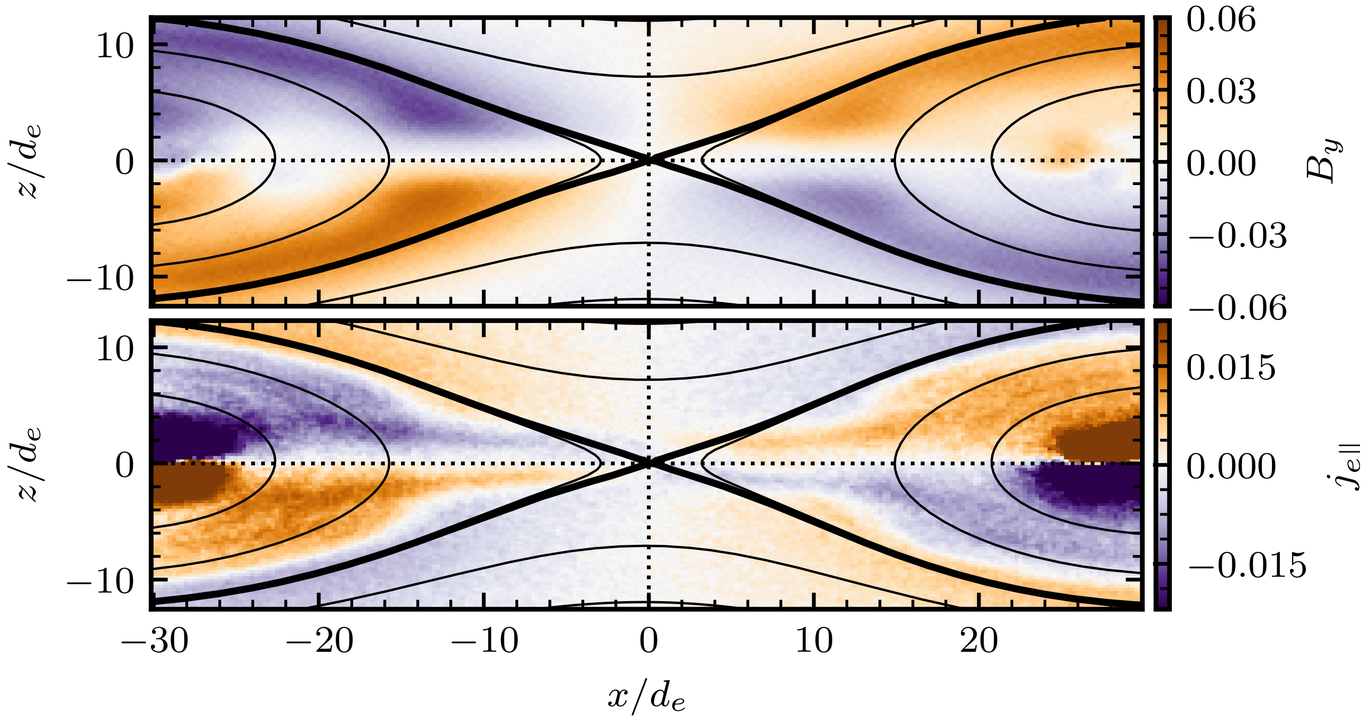

Electron Heating by Parallel Electric Fields

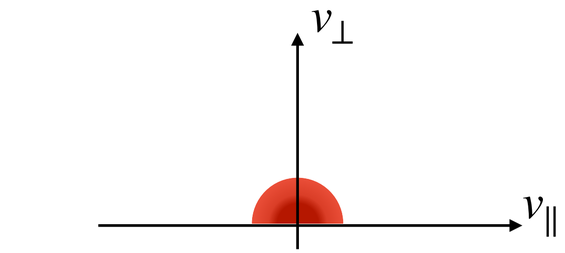

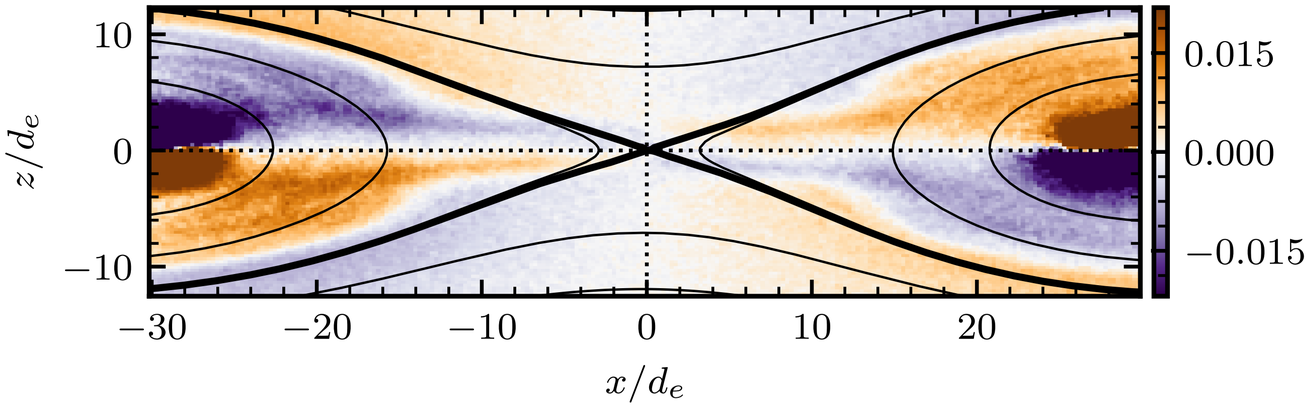

Electron Heating by Parallel Electric Fields

- Parallel electric fields accelerate electrons toward the X-line, forming **beam-type electron VDFs**.

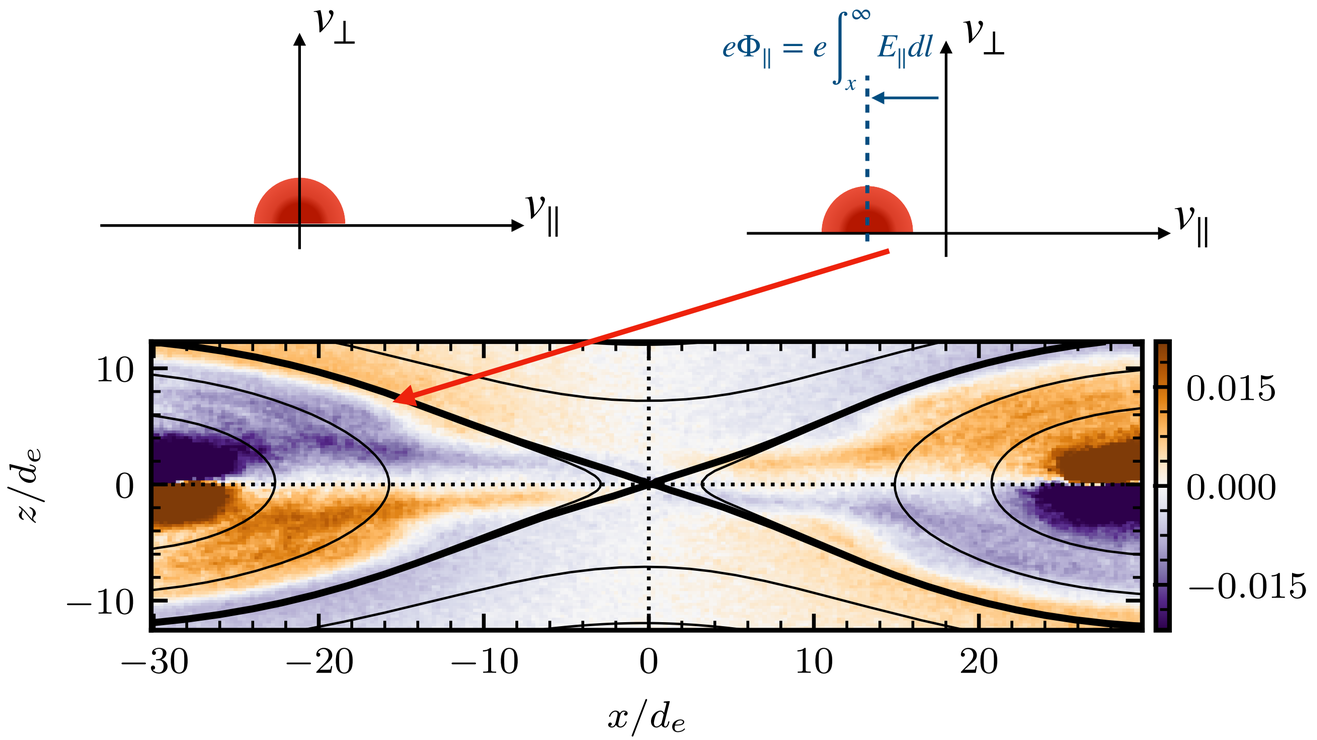

Electron Heating by Parallel Electric Fields

- Parallel electric fields accelerate electrons toward the X-line, forming **beam-type electron VDFs**.
- Trapped electrons form a **thermalized hot population**.

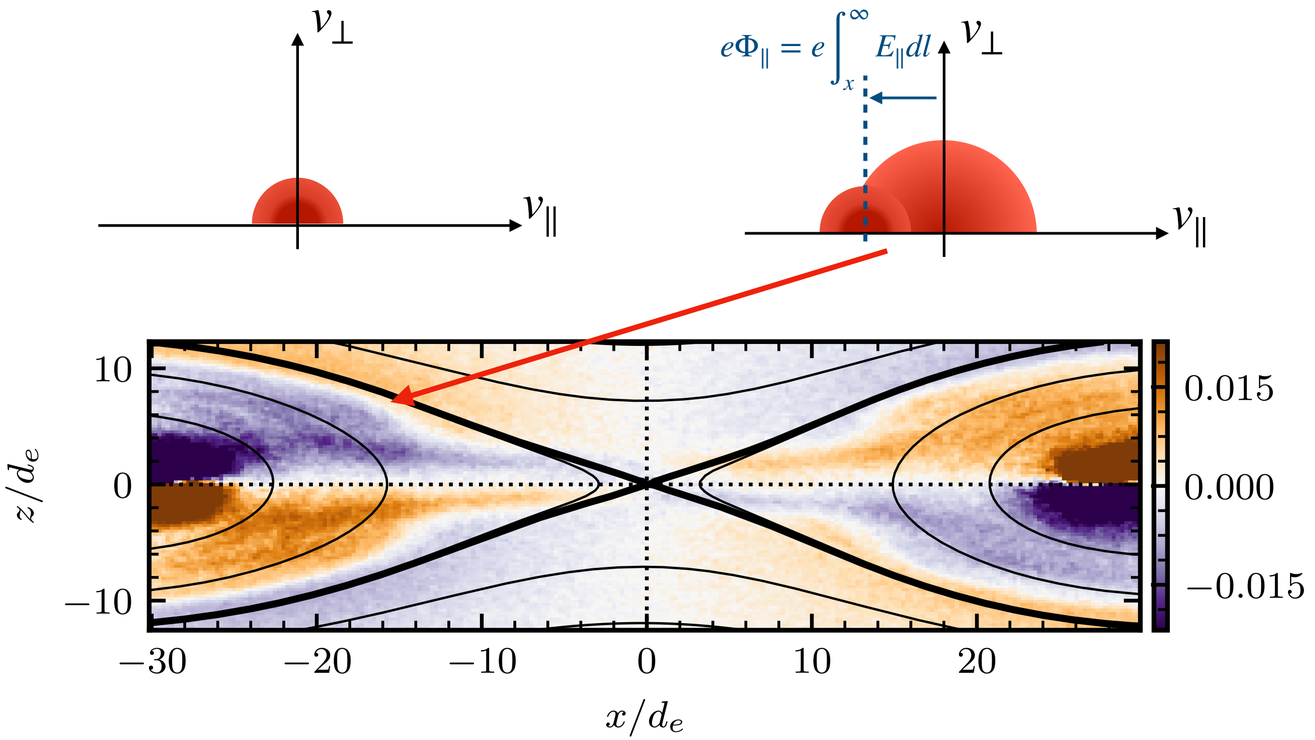

Electron Heating by Parallel Electric Fields

- Parallel electric fields accelerate electrons toward the X-line, forming **beam-type electron VDFs**.
- Trapped electrons form a **thermalized hot population**.
- Unstable beam + thermalized hot electron excites **electrostatic waves** and forming **flat-top VDFs** [Fujimoto, 2014, GRL].

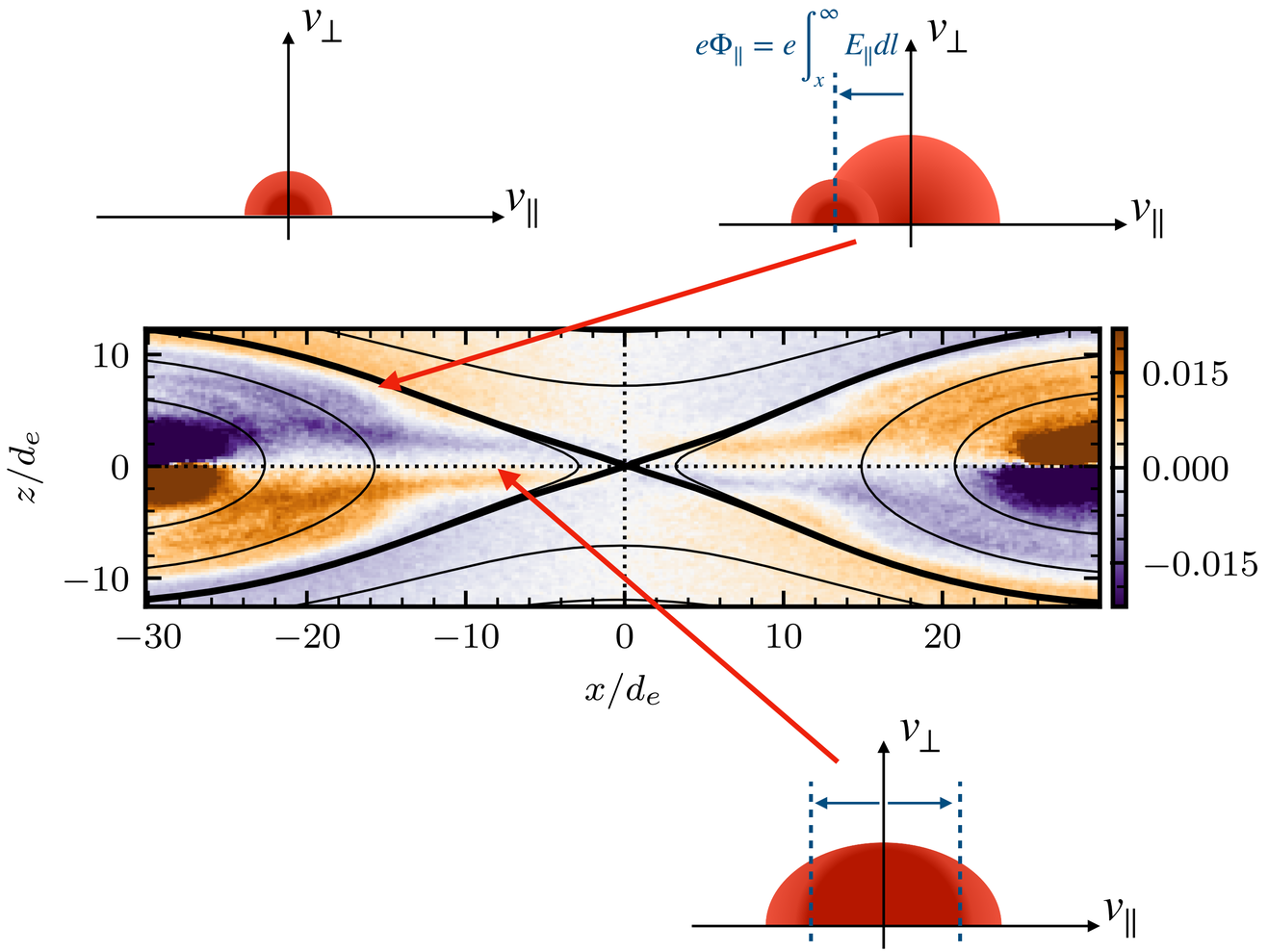

Electron Heating by Parallel Electric Fields

- Parallel electric fields accelerate electrons toward the X-line, forming **beam-type electron VDFs**.
- Trapped electrons form a **thermalized hot population**.
- Unstable beam + thermalized hot electron excites **electrostatic waves** and forming **flat-top VDFs** [Fujimoto, 2014, GRL].
- **Curvature scattering** of electrons isotropizes the flat-top VDFs.

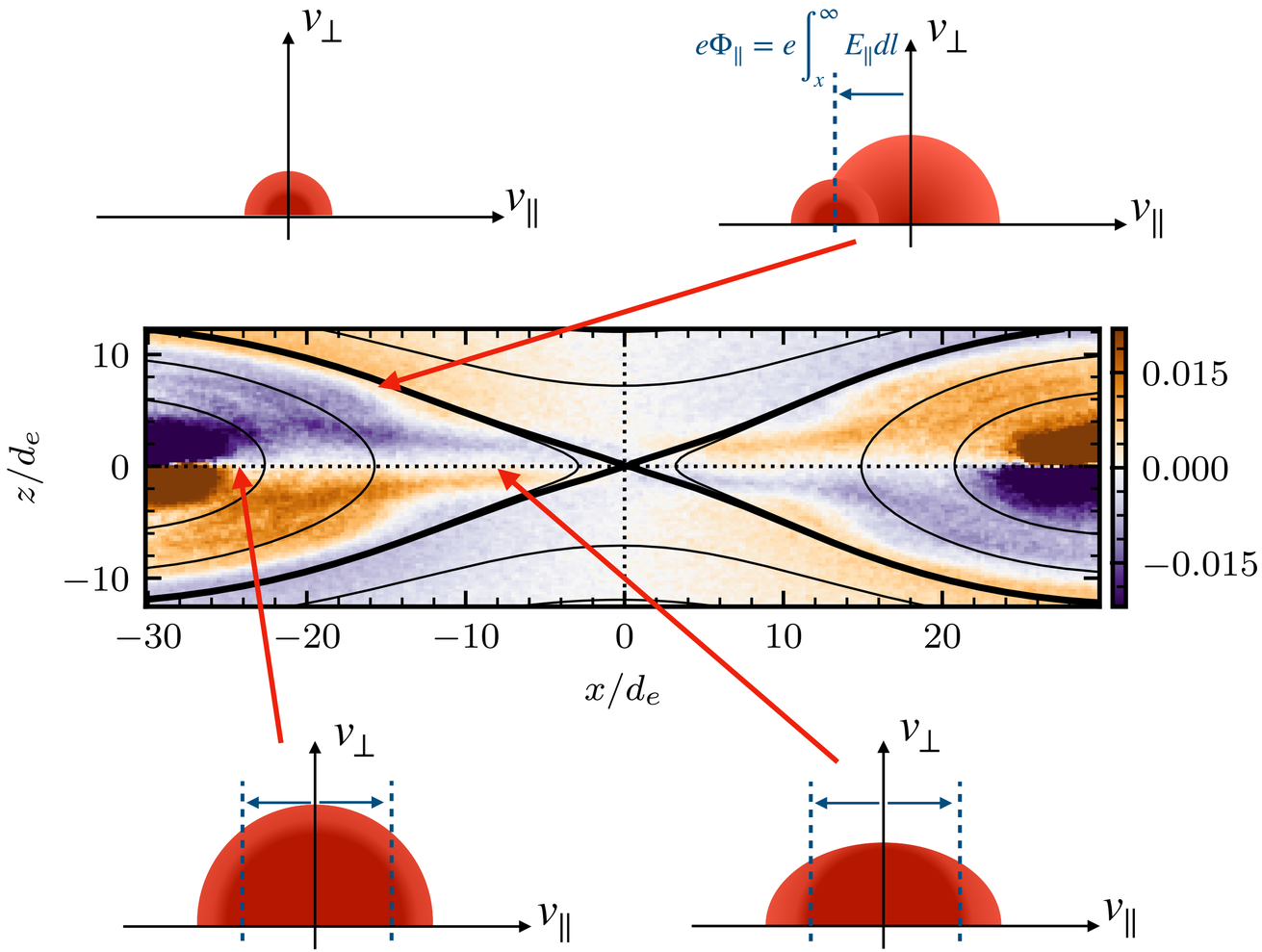

Electron Heating by Parallel Electric Fields

- Parallel electric fields accelerate electrons toward the X-line, forming **beam-type electron VDFs**.
- Trapped electrons form a **thermalized hot population**.
- Unstable beam + thermalized hot electron excites **electrostatic waves** and forming **flat-top VDFs** [Fujimoto, 2014, GRL].
- **Curvature scattering** of electrons isotropizes the flat-top VDFs.

What is the nature and the role of parallel electric fields in magnetic reconnection?

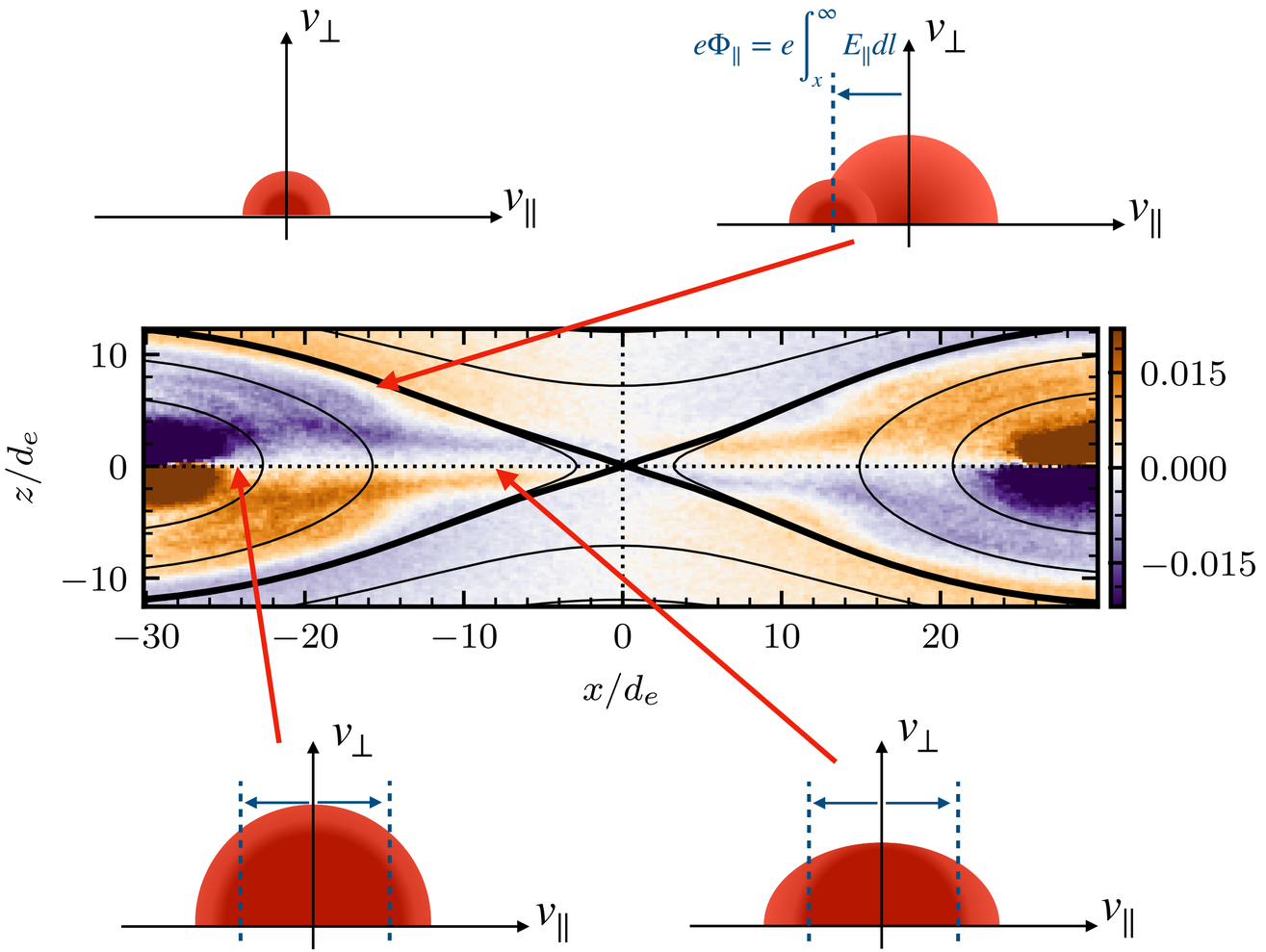

Electron VDFs in the Outflow

[Richard+2025, PRL]

Example

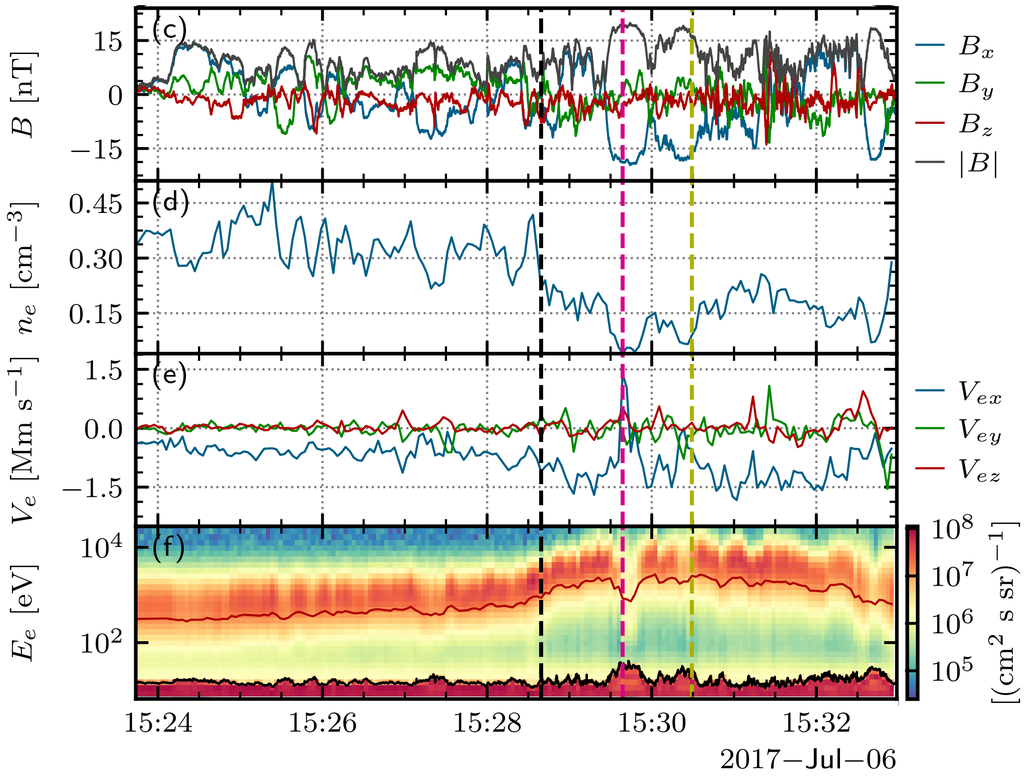

Electron VDFs in the Outflow

[Richard+2025, PRL]

Example

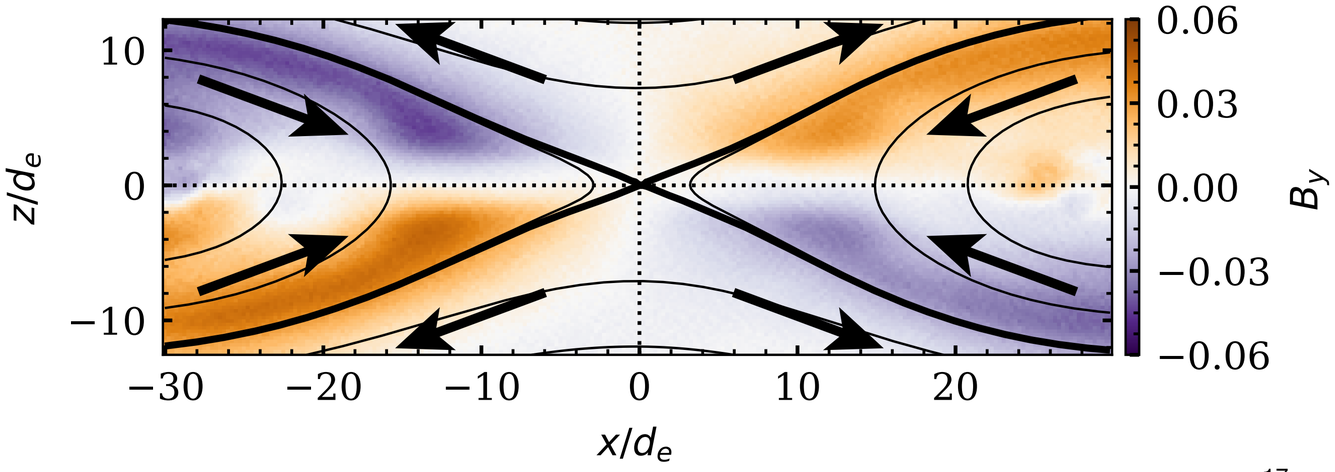

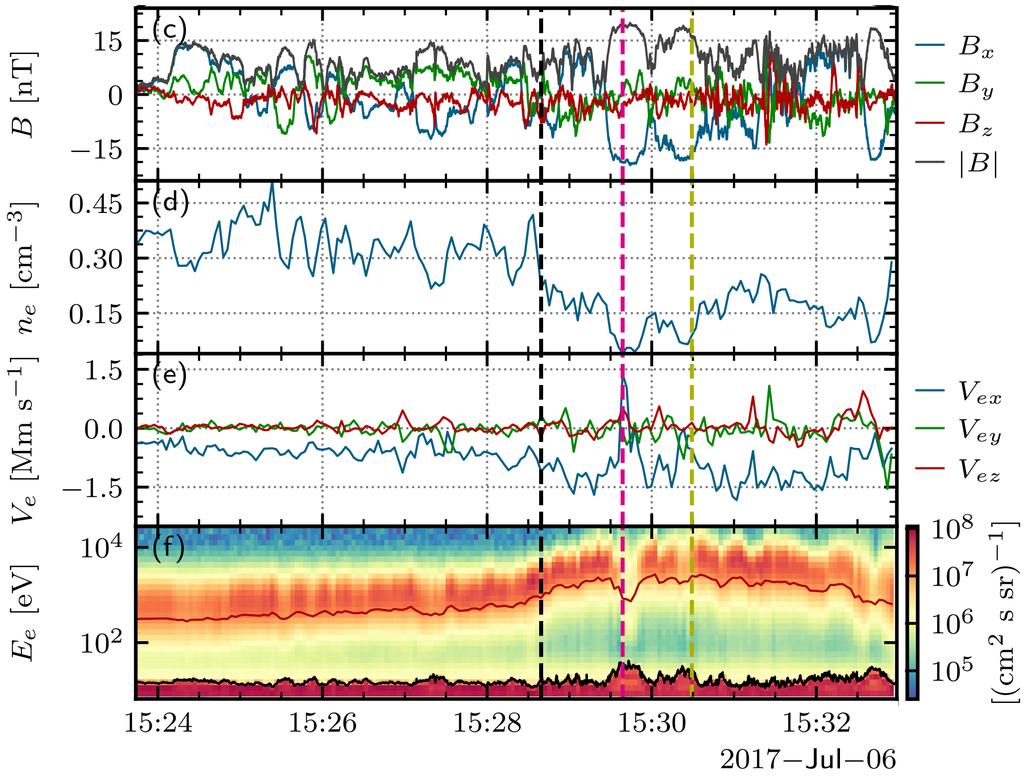

Electron VDFs in the Outflow

[Richard+2025, PRL]

Example

- Flat-top eVDF in the reconnection jet

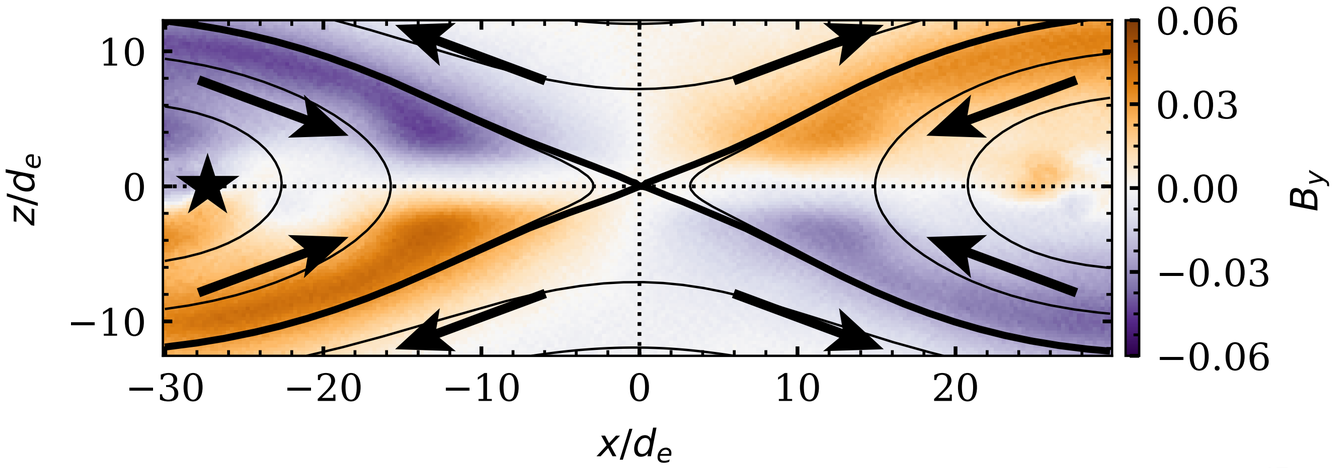

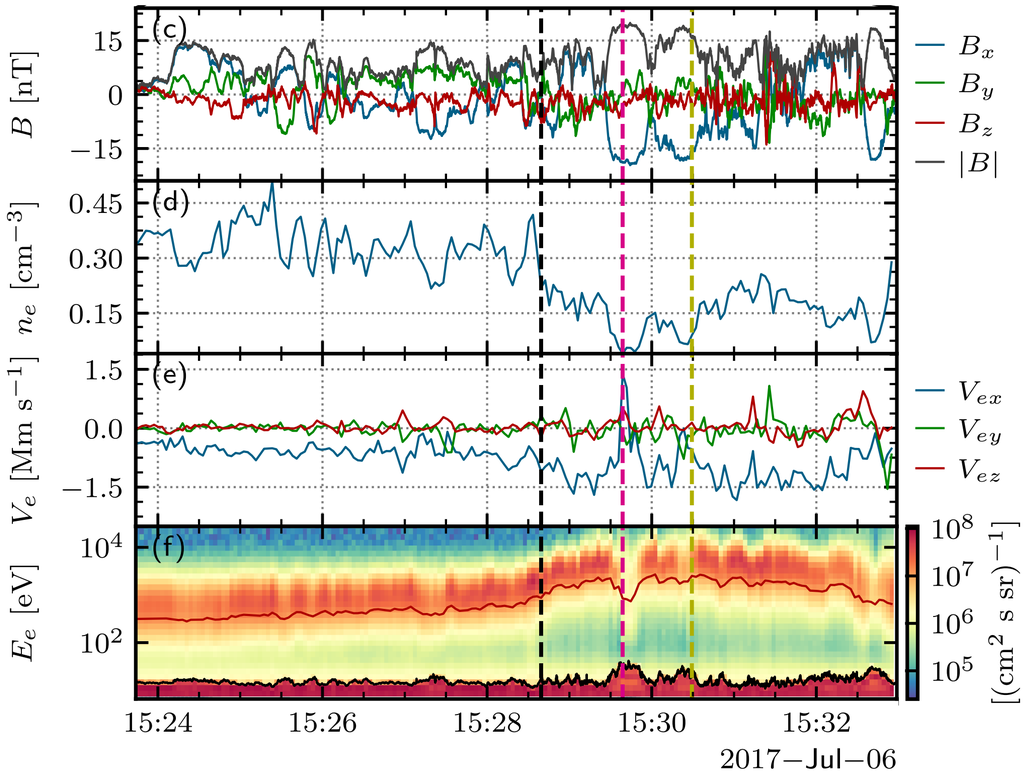

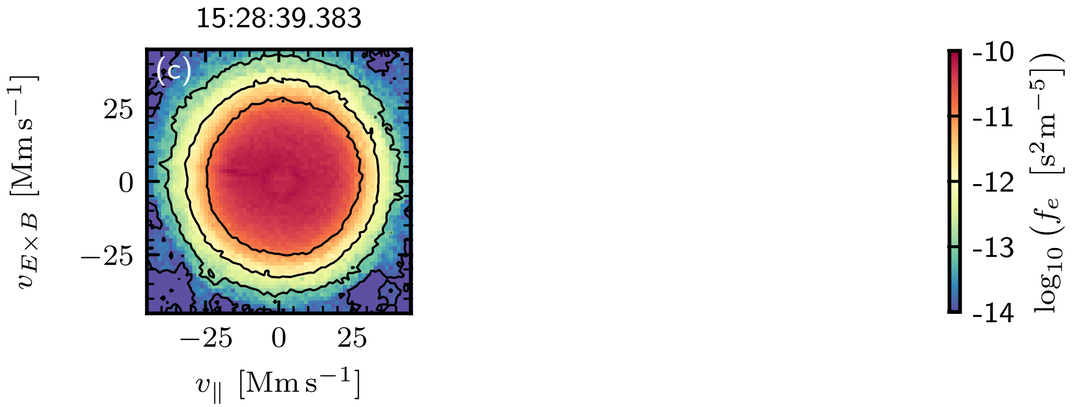

Electron VDFs in the Outflow

[Richard+2025, PRL]

Example

- Flat-top eVDF in the reconnection jet
- Beam + thermalized core at the separatrix flow (producing the Hall current)

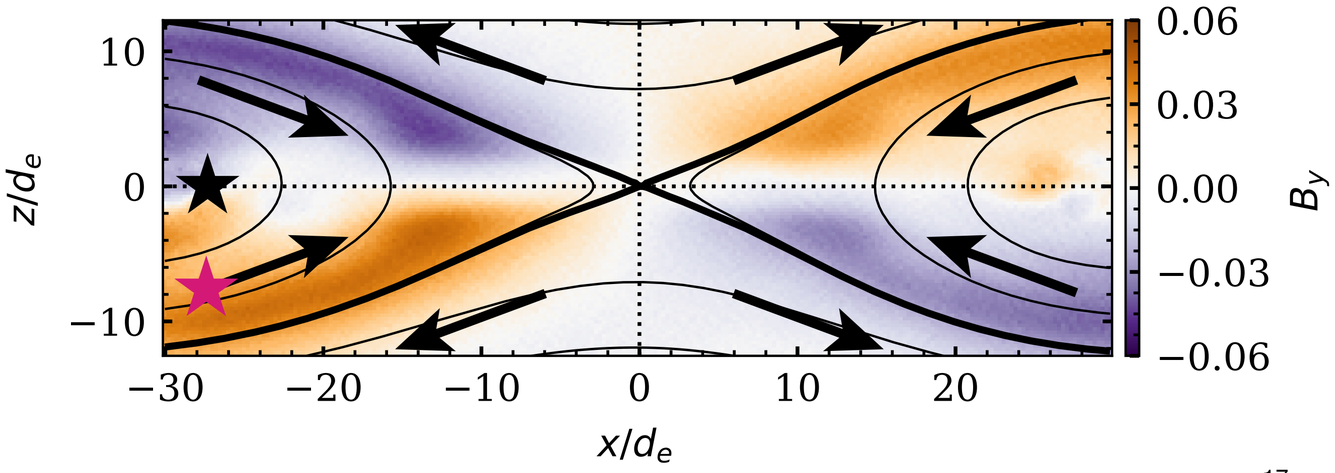

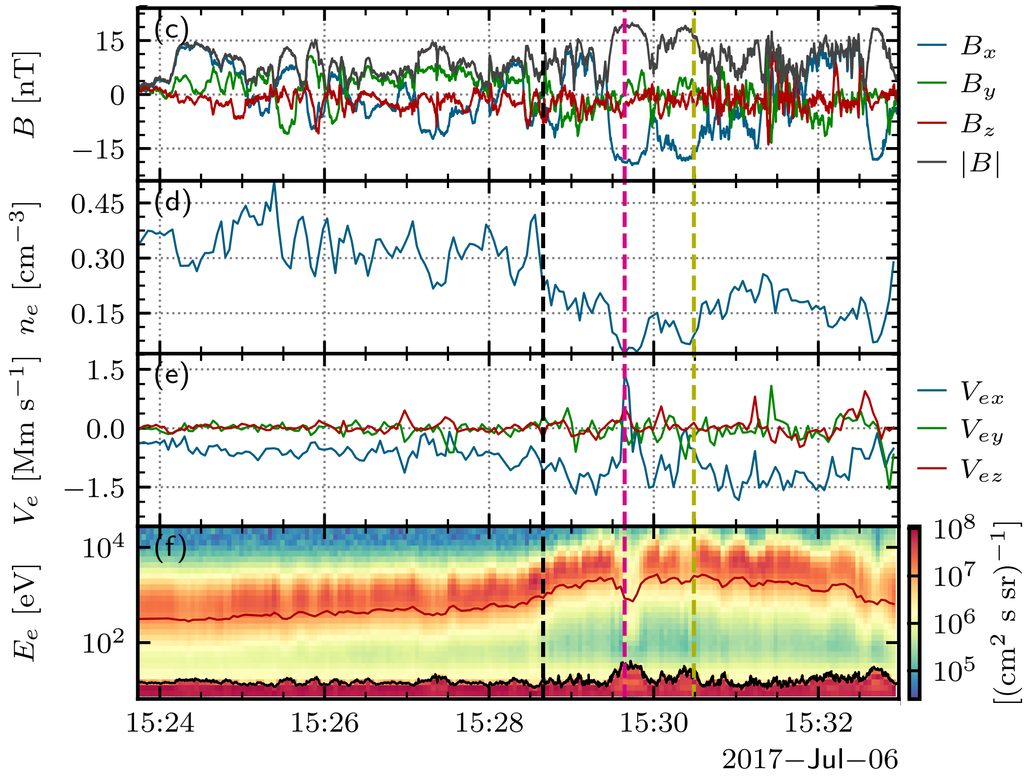

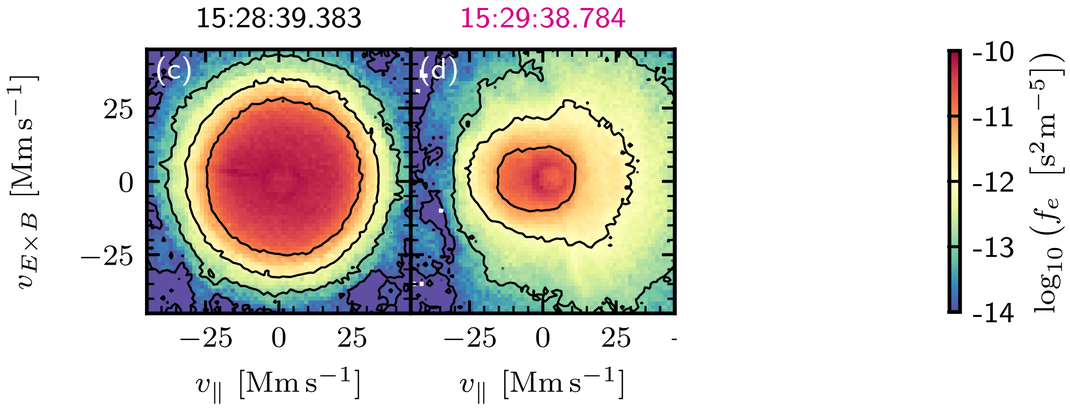

Electron VDFs in the Outflow

[Richard+2025, PRL]

Example

- Flat-top eVDF in the reconnection jet
- Beam + thermalized core at the separatrix flow (producing the Hall current)

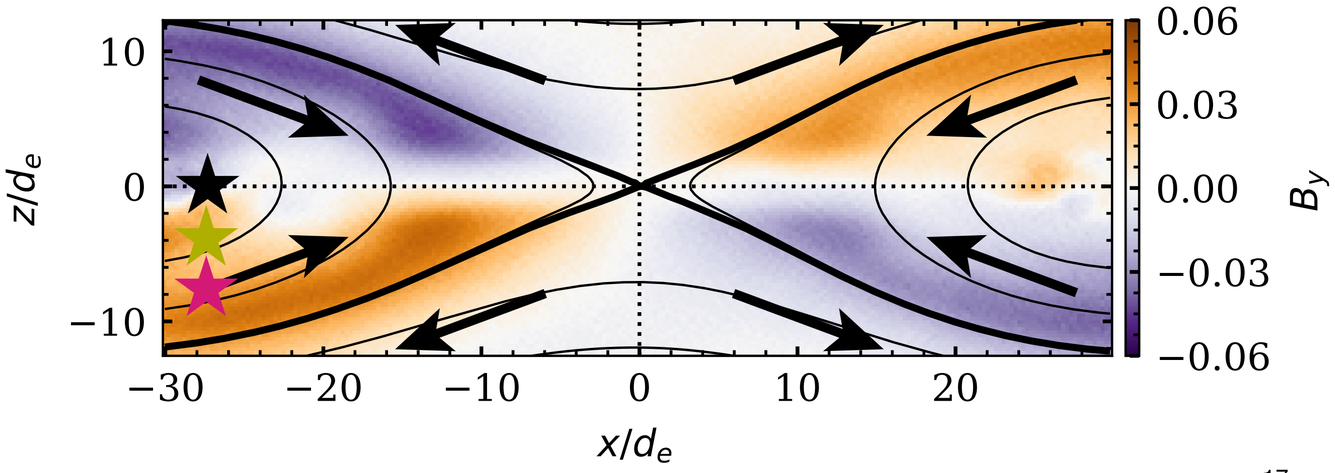

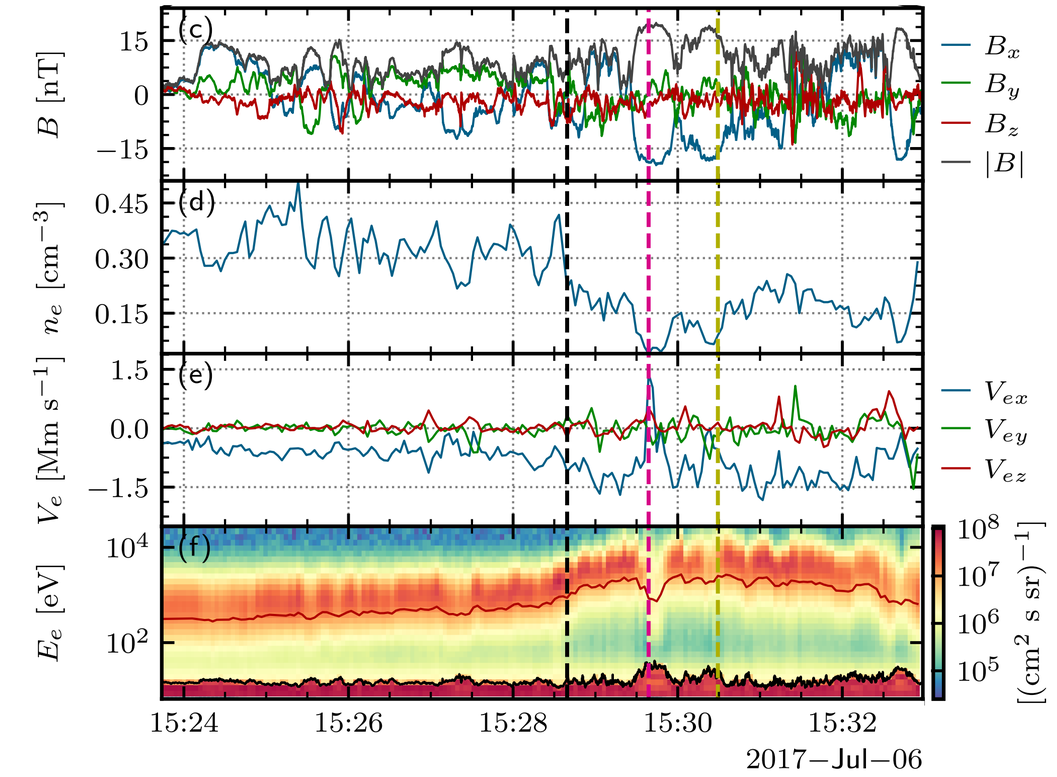

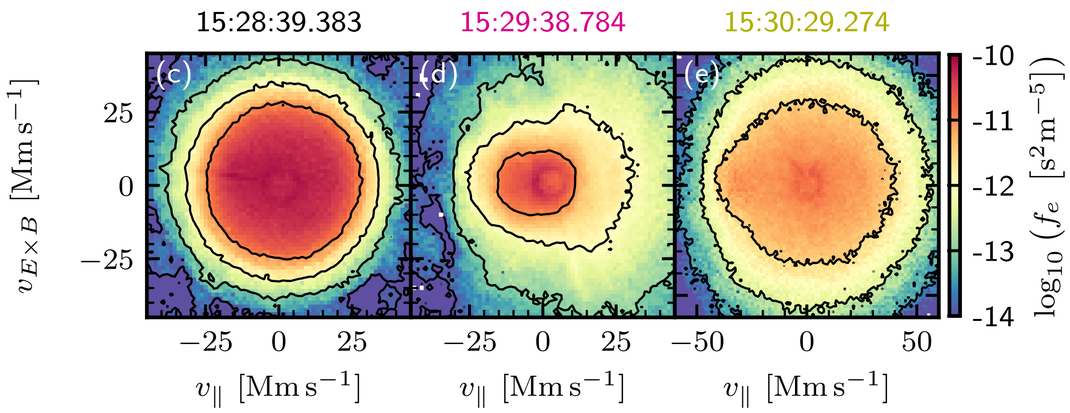

Electron VDFs in the Outflow

[Richard+2025, PRL]

Modeling the electron VDFs

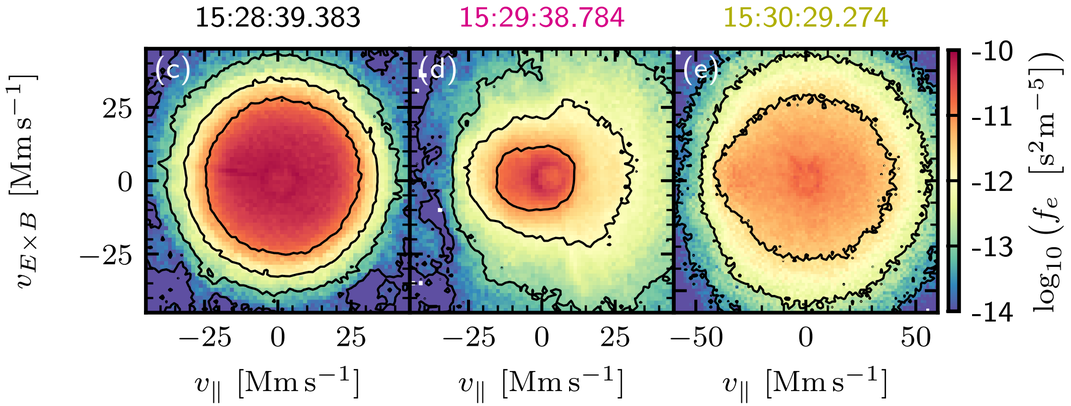

Electron VDFs in the Outflow

[Richard+2025, PRL]

Modeling the electron VDFs

- Model electron VDF (r,q) [Qureshi+2004, PoP] for $v_\perp \simeq 0$

$$f_{(r,q)} = f_0 \left[1 + \left(\frac{v_\parallel^2}{\xi(r,q) v_{te,\parallel}^2} \right)^{r+1} \right]^{-q}$$

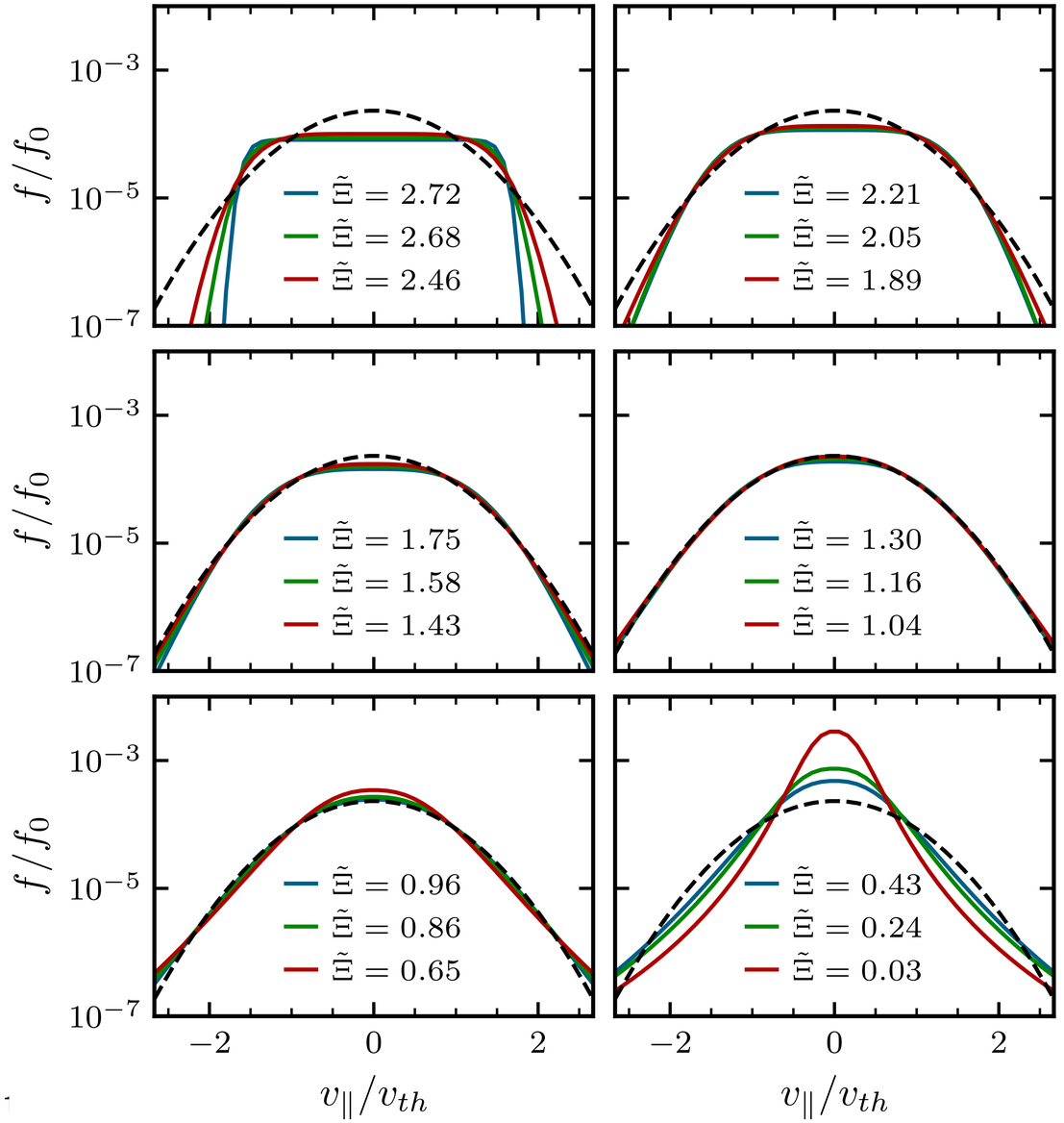

Electron VDFs in the Outflow

[Richard+2025, PRL]

Modeling the electron VDFs

- Model electron VDF (r,q) [Qureshi+2004, PoP] for $v_\perp \simeq 0$

$$f_{(r,q)} = f_0 \left[1 + \left(\frac{v_\parallel^2}{\xi(r,q) v_{te,\parallel}^2} \right)^{r+1} \right]^{-q}$$

- Flatness factor: $\Xi = f(v_{th})/f_0$:

$$\tilde{\Xi} \equiv \frac{\Xi_{(r,q)}}{\Xi_{bM}} = e \left(1 + \frac{1}{\xi^{r+1}} \right)^{-q}$$

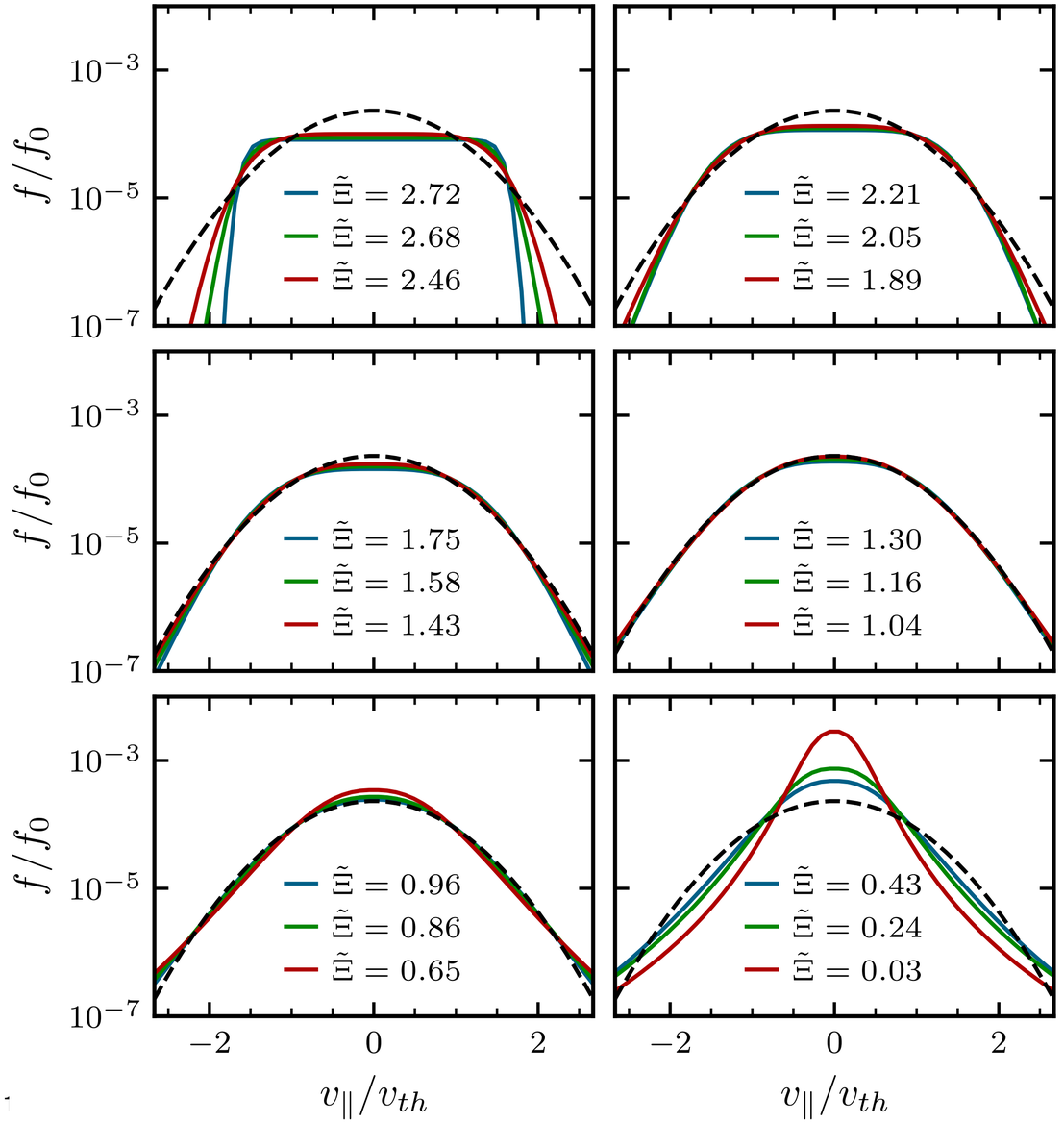

Electron VDFs in the Outflow

[Richard+2025, PRL]

Modeling the electron VDFs

- Model electron VDF (r,q) [Qureshi+2004, PoP] for $v_\perp \simeq 0$

$$f_{(r,q)} = f_0 \left[1 + \left(\frac{v_\parallel^2}{\xi(r,q) v_{te,\parallel}^2} \right)^{r+1} \right]^{-q}$$

- Flatness factor: $\Xi = f(v_{th})/f_0$:

$$\tilde{\Xi} \equiv \frac{\Xi_{(r,q)}}{\Xi_{bM}} = e \left(1 + \frac{1}{\xi^{r+1}} \right)^{-q}$$

- Knee velocity v_Φ corresponding to the acceleration potential $f(v_\Phi)/f_0 = \varepsilon$

$$v_\Phi = \left(\varepsilon^{-1/q} - 1 \right)^{1/2(r+1)} \xi^{1/2} v_{te,\parallel}$$

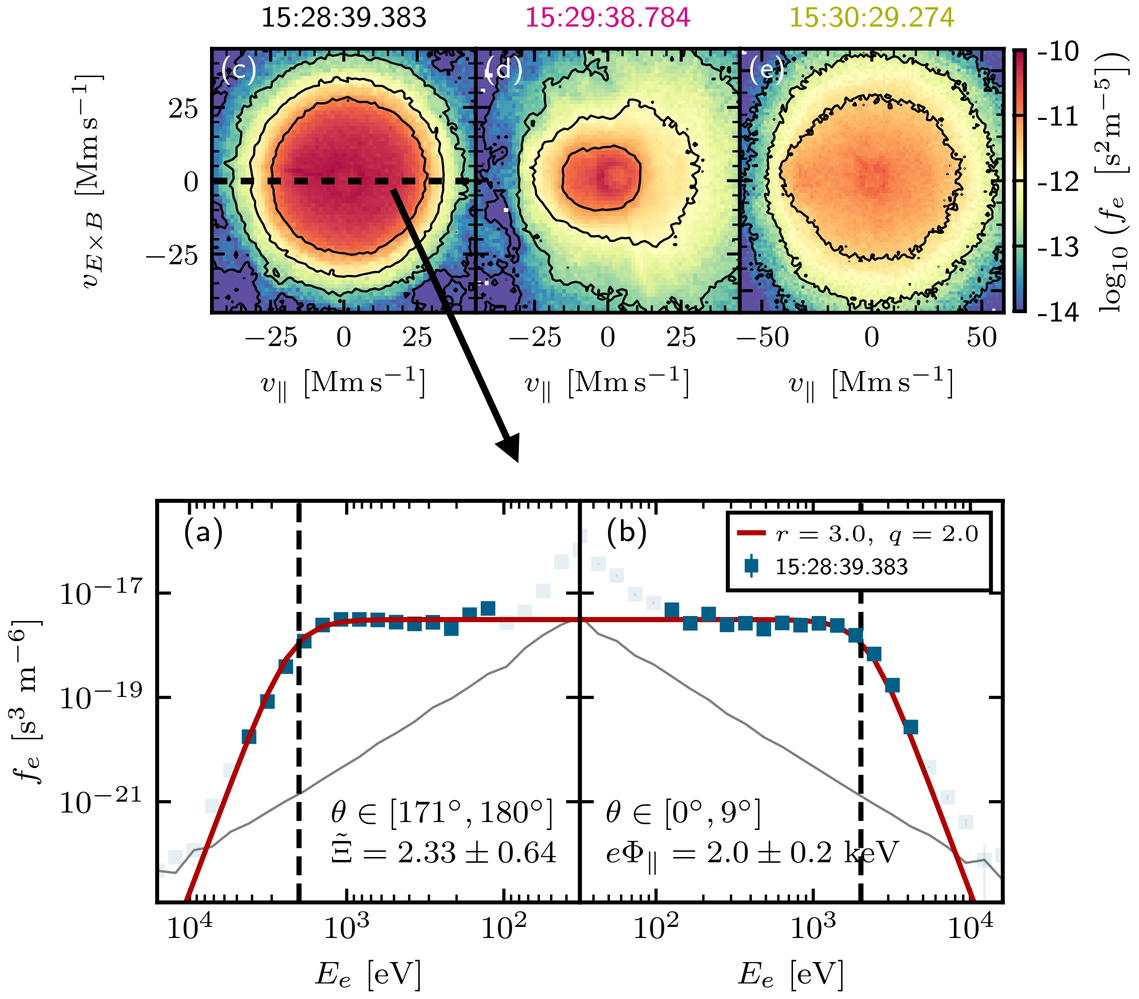

Results

Acceleration potential

[Richard+2025, PRL]

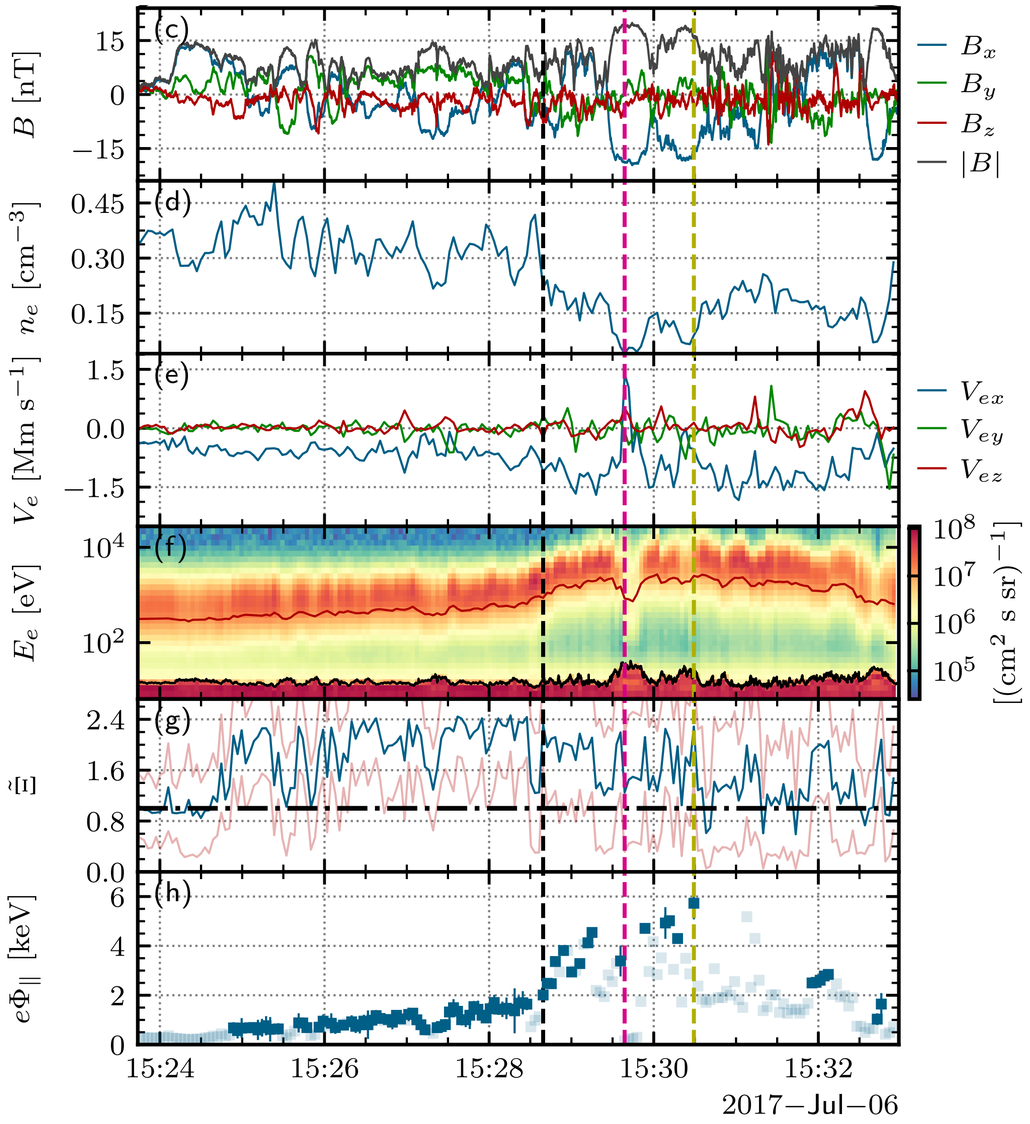

Results

Acceleration potential

- Plasma sheet reconnection followed by lobe reconnection

[Vaivads+2011, AnnGeo]

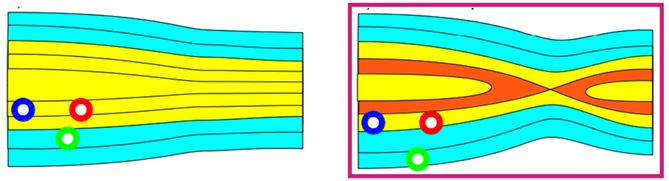

[Richard+2025, PRL]

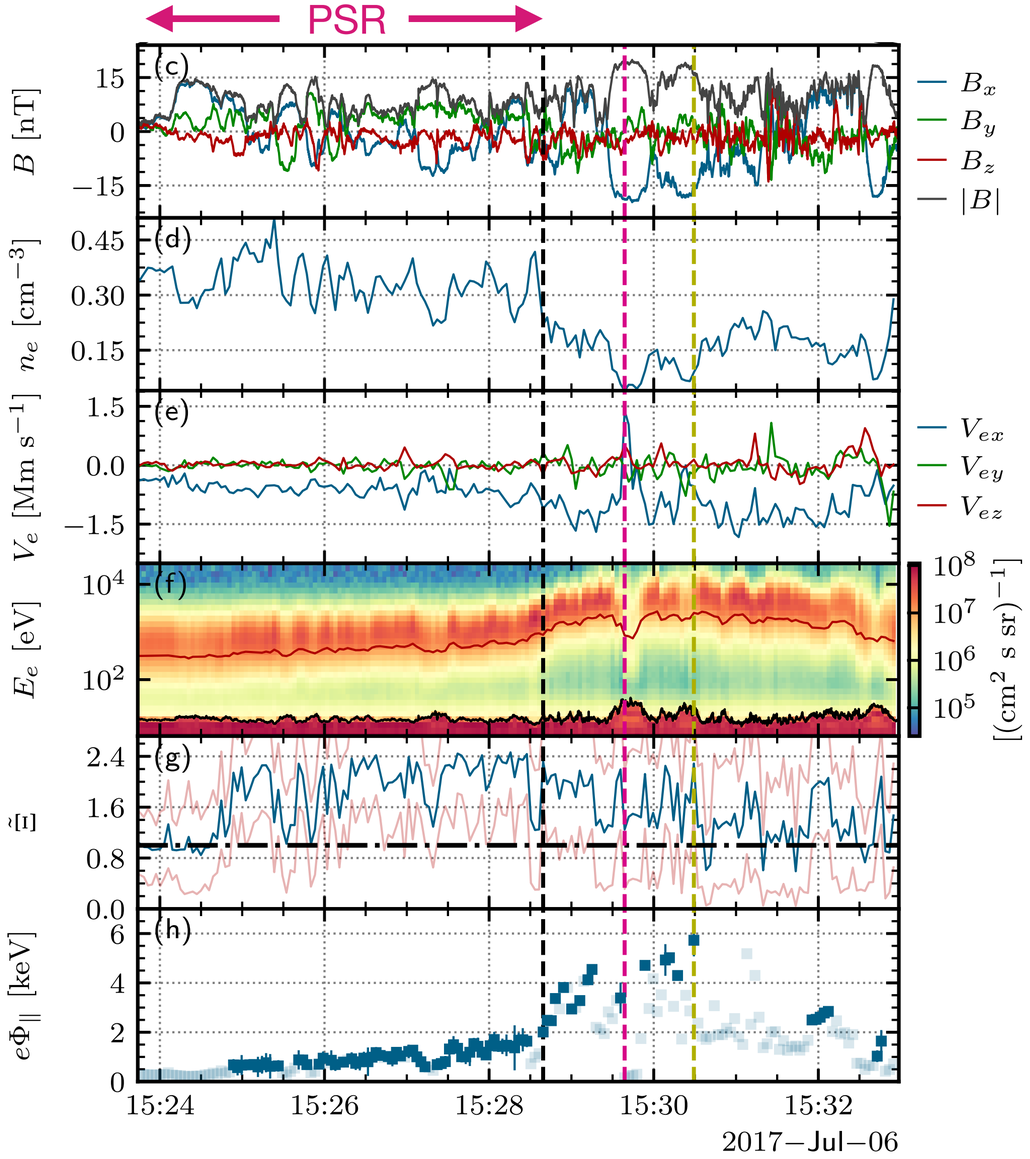

Results

Acceleration potential

- Plasma sheet reconnection followed by lobe reconnection

[Vaivads+2011, AnnGeo]

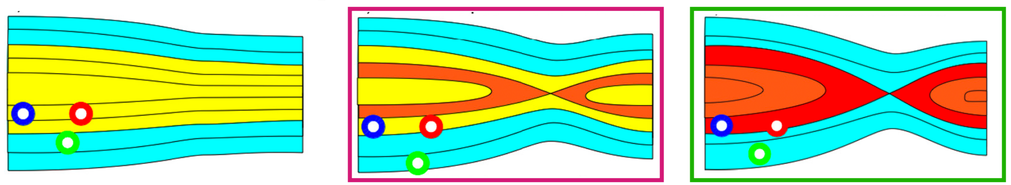

[Richard+2025, PRL]

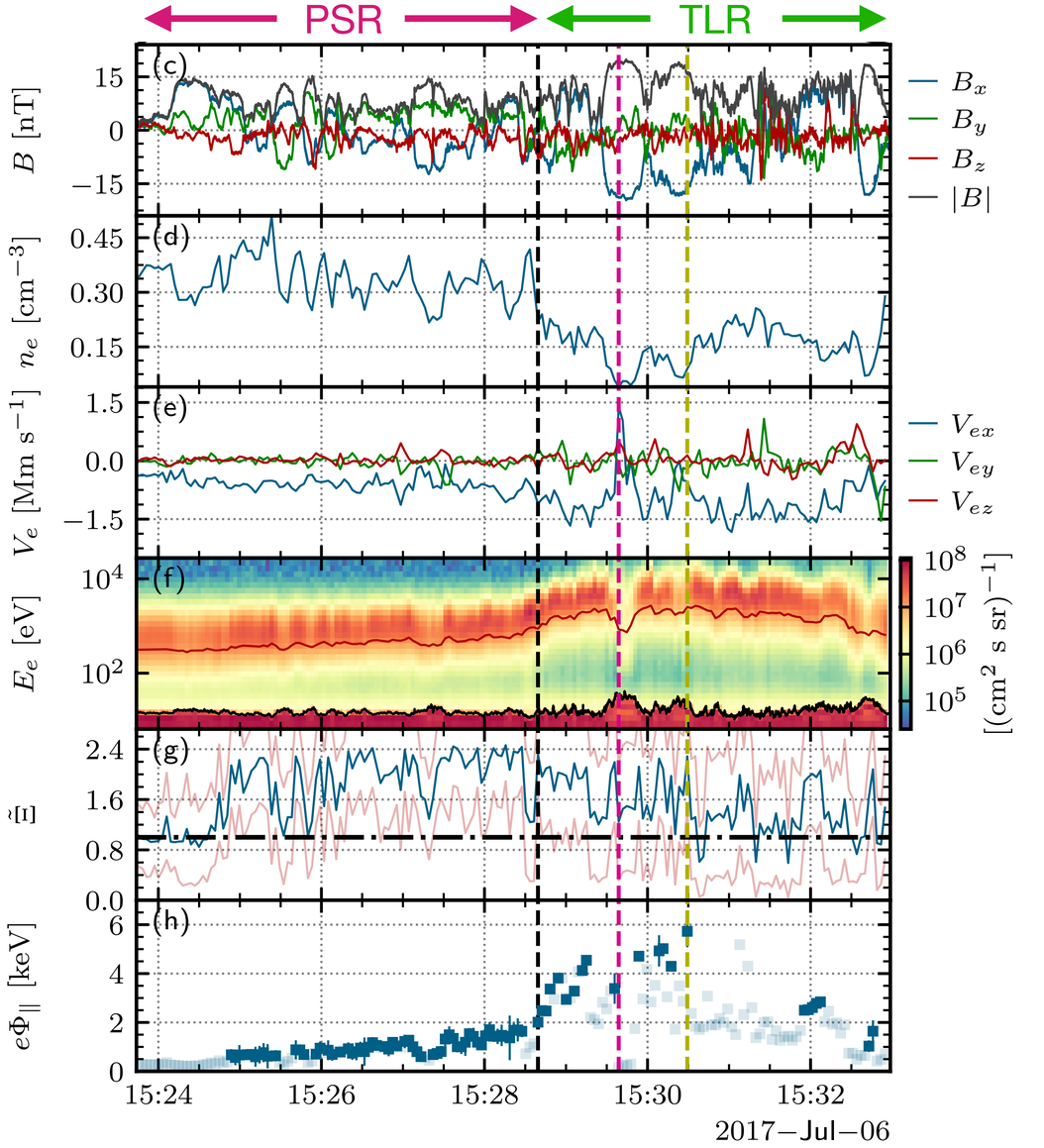

Results

Acceleration potential

- Plasma sheet reconnection followed by lobe reconnection

[Vaivads+2011, AnnGeo]

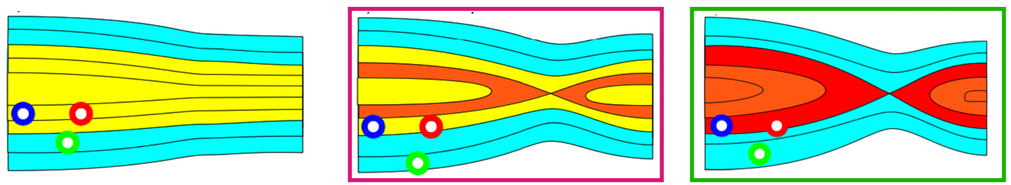

- The increase in acceleration potential is proportional to the increase in inflow Alfvén speed

$$e\Phi_{\parallel}^{TLR}/e\Phi_{\parallel}^{PSR} \sim V_{Ae\infty}^{TLR}/V_{Ae\infty}^{PSR}$$

The acceleration potential increases with the inflow Alfvén speed

[Richard+2025, PRL]

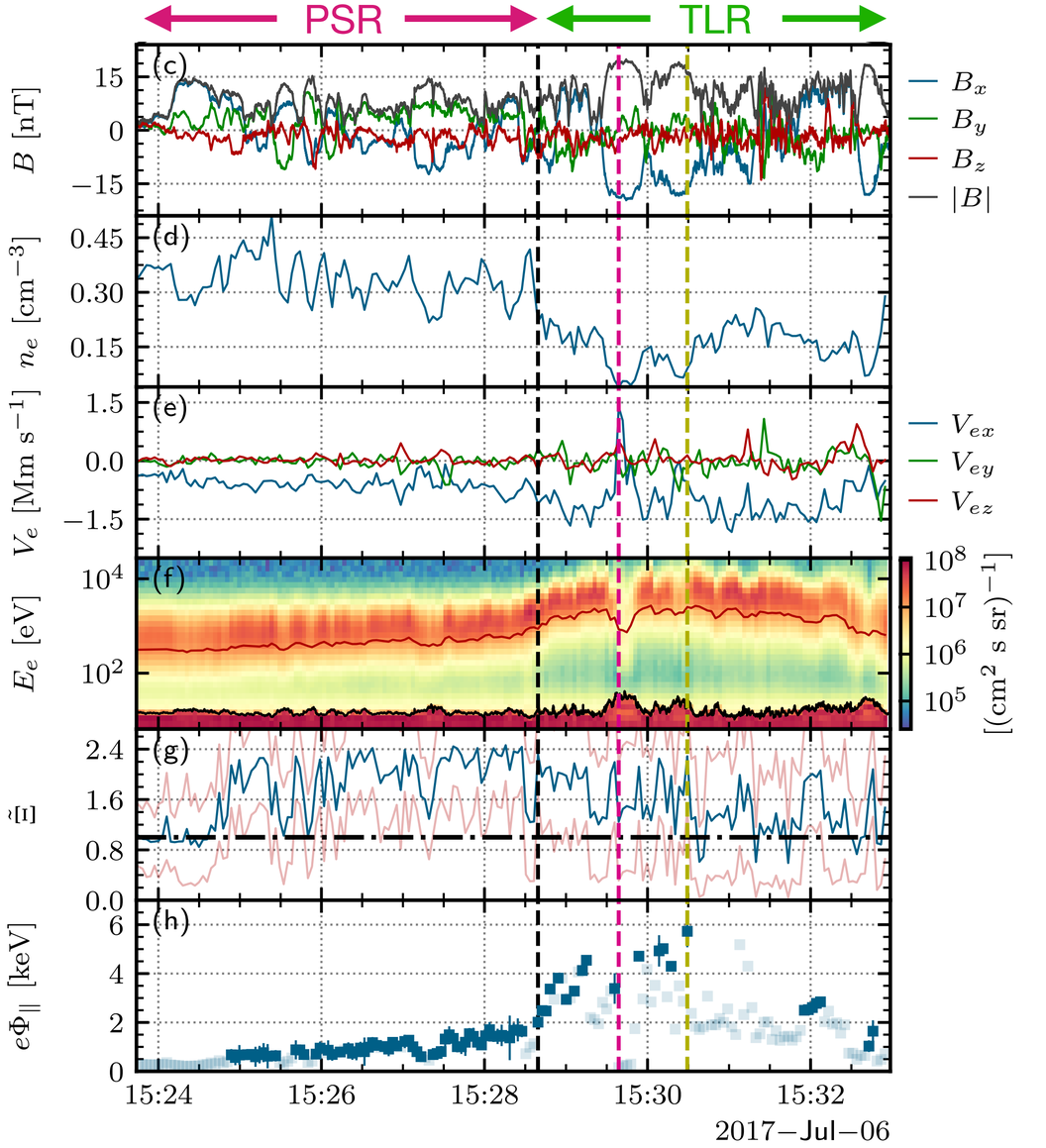

Results

The origin of $E_{\parallel}$

[Richard+2025, PRL]

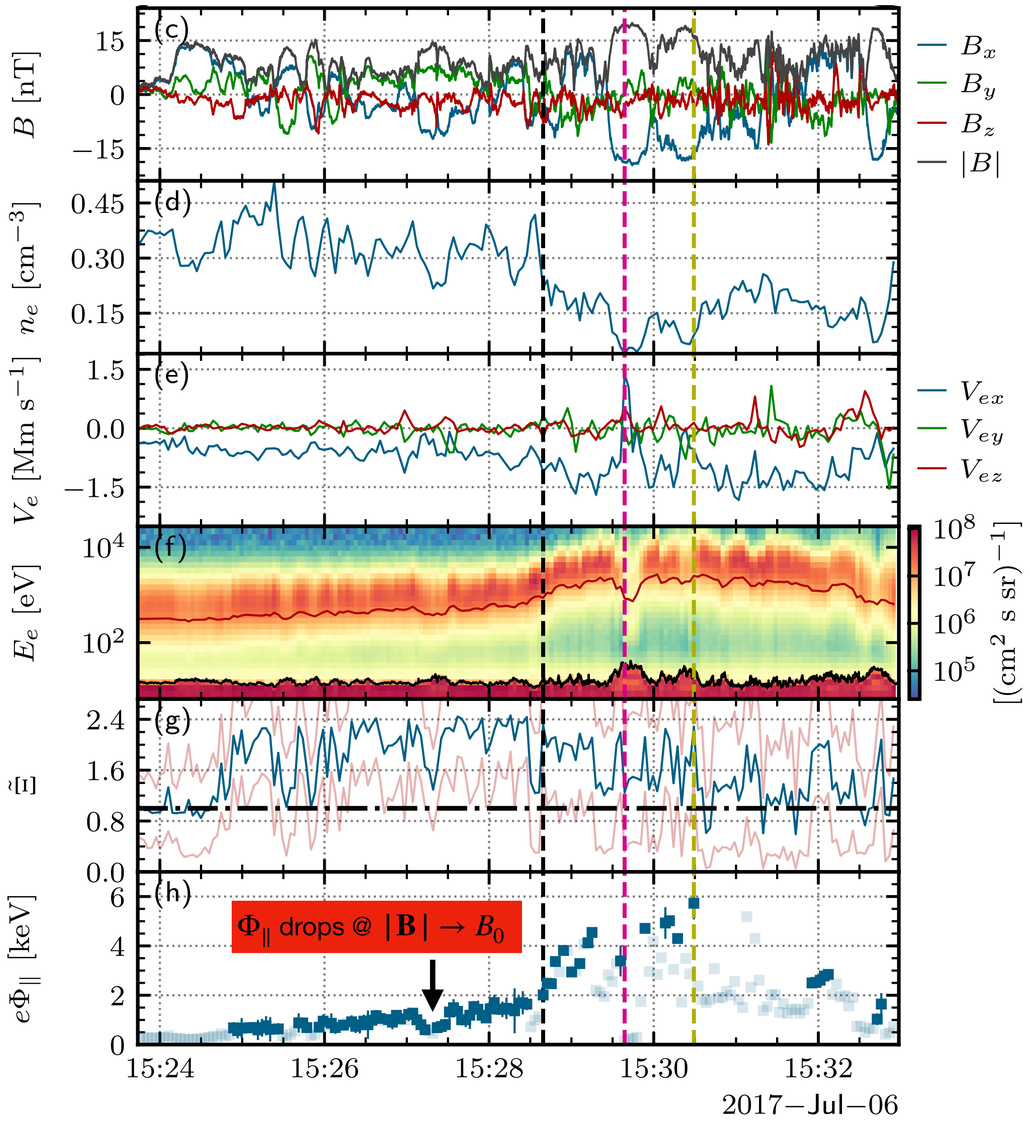

Results

The origin of $E_{\parallel}$

- Steady-state local electron momentum balance along the field line

$$eE_{\parallel} = -\underbrace{\nabla_{\parallel} T_{e\parallel}}_{\Phi_{\parallel T}} - \underbrace{T_{e\parallel} \nabla_{\parallel} \ln n}_{\Phi_{\parallel n}} + \underbrace{(T_{e\parallel} - T_{e\perp}) \nabla_{\parallel} \ln B}_{\Phi_{\parallel B}}$$

[Richard+2025, PRL]

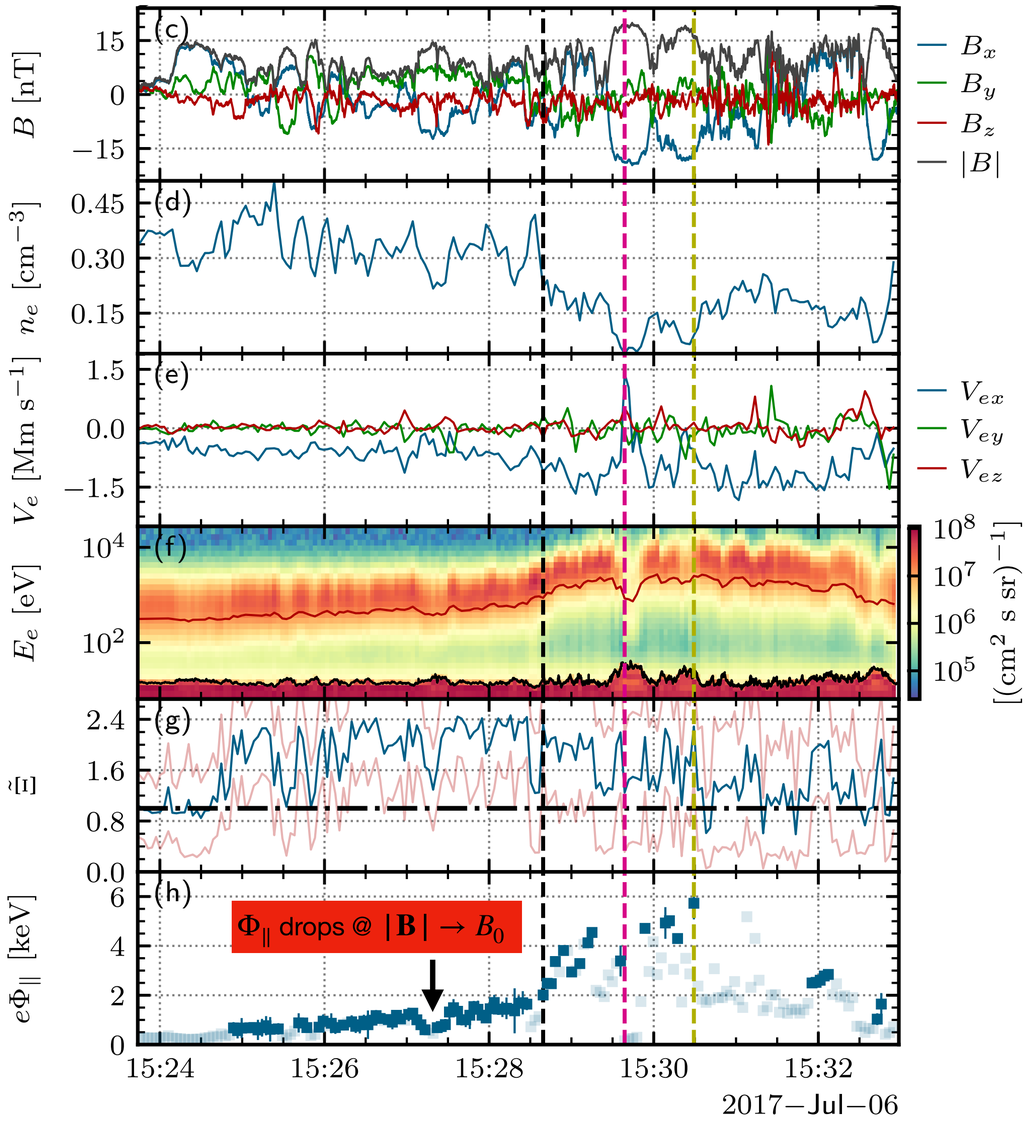

Results

The origin of $E_{\parallel}$

- Steady-state local electron momentum balance along the field line

$$eE_{\parallel} = -\underbrace{\nabla_{\parallel} T_{e\parallel}}_{\Phi_{\parallel T}} - \underbrace{T_{e\parallel} \nabla_{\parallel} \ln n}_{\Phi_{\parallel n}} + \underbrace{(T_{e\parallel} - T_{e\perp}) \nabla_{\parallel} \ln B}_{\Phi_{\parallel B}}$$

- Potential drop (incremental) across the outflow [Haggerty+2015, GRL]

$$e\Delta\Phi_{\parallel} = -\int_b^a E_{\parallel} dl \simeq \left(\frac{e\Delta\Phi_{\parallel T}}{10\ \text{eV}}\right) + \left(\frac{e\Delta\Phi_{\parallel n}}{160\ \text{eV}}\right) + \left(\frac{e\Delta\Phi_{\parallel B}}{50\ \text{eV}}\right)$$

Field-aligned ambipolar electric field is primarily due to electron density gradients

[Richard+2025, PRL]

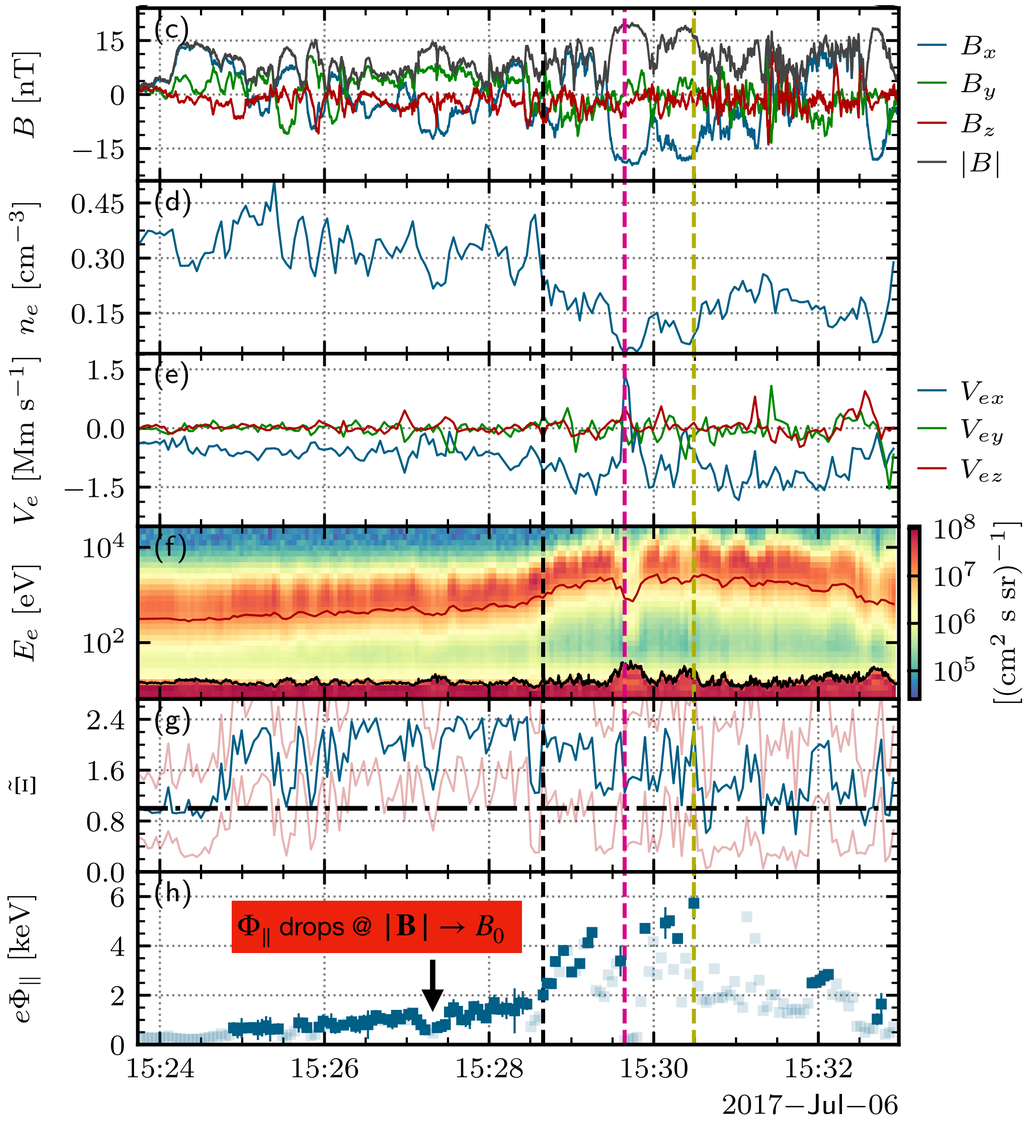

Results

Statistics

[Richard+2025, PRL]

Results

Statistics

[Richard+2025, PRL]

- $e\Phi_{\parallel}$ increases with $T_{e\infty}$ to keep electrons trapped.

[Egedal+2005, PRL]

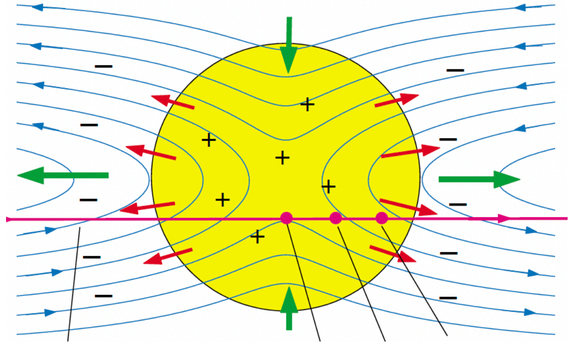

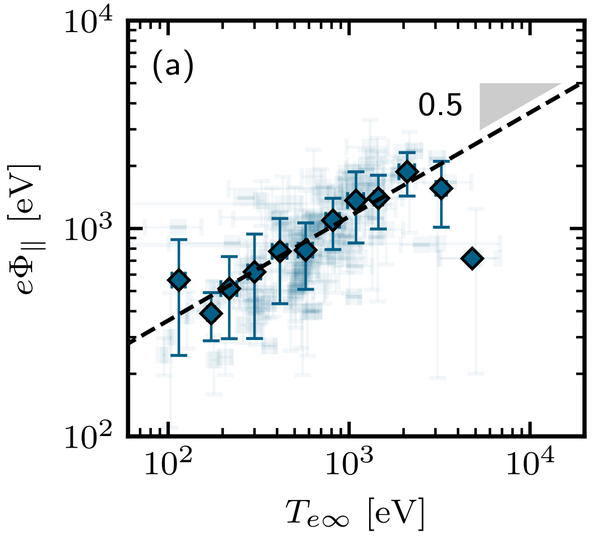

Results

Statistics

- $e\Phi_{\parallel}$ increases with $T_{e\infty}$ to keep electrons trapped.

[Egedal+2005, PRL]

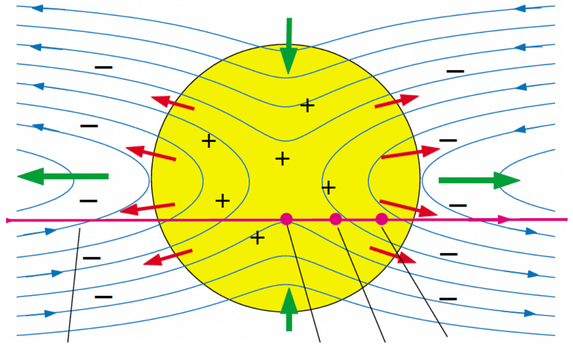

- $e\Phi_{\parallel}$ increases with $V_{Ae\infty}$ to balance the flux tube expansion

[Richard+2025, PRL]

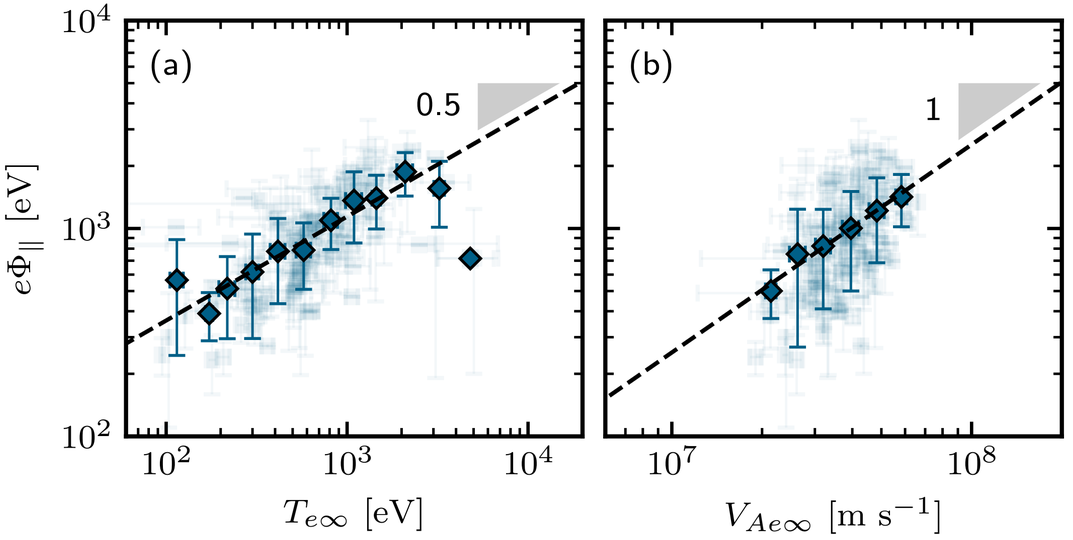

[Egedal+2015, PoP]

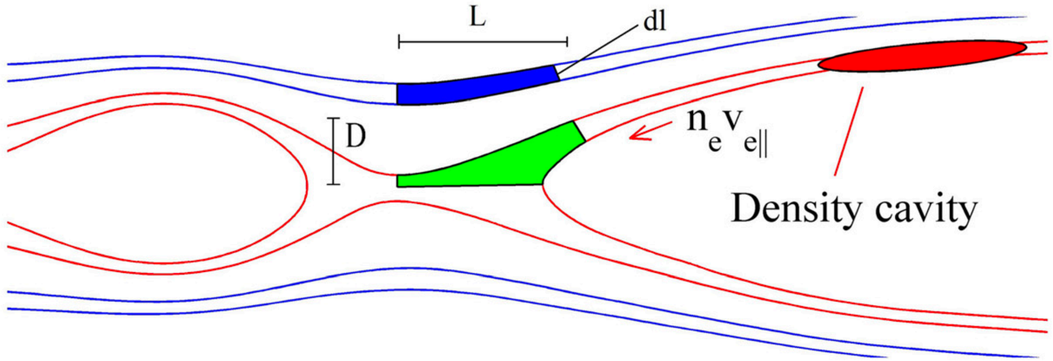

Results

Statistics

[Richard+2025, PRL]

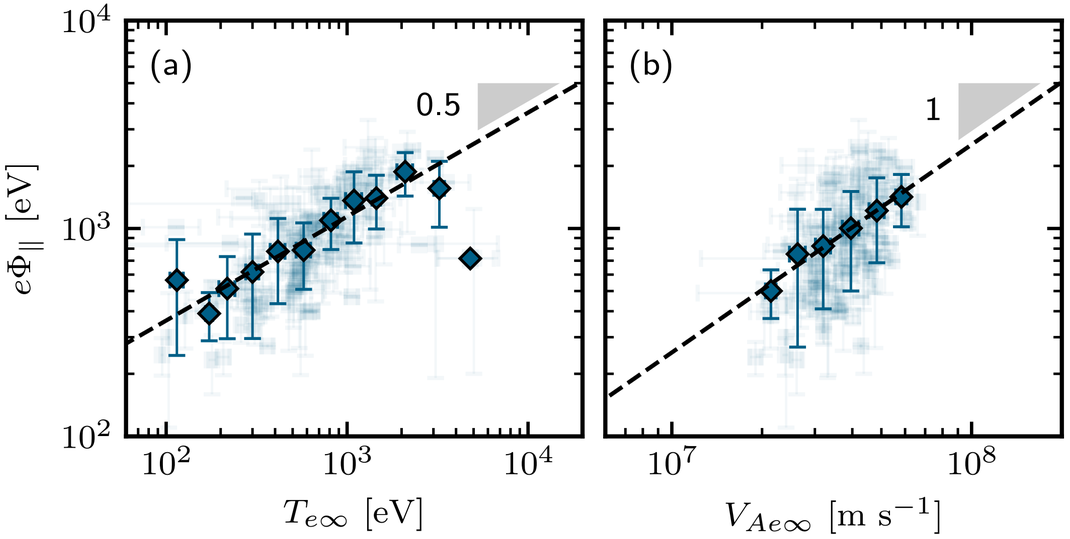

- $e\Phi_{||}$ increases with $T_{e\infty}$ to keep electrons trapped.

[Egedal+2005, PRL]

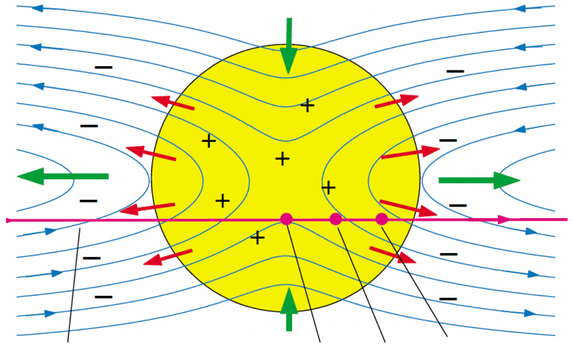

[Egedal+2015, PoP]

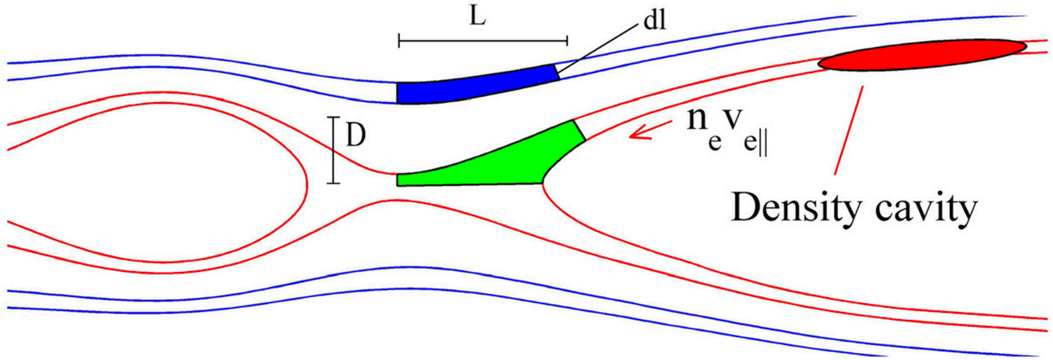

- $e\Phi_{||}$ increases with $V_{Ae\infty}$ to balance the flux tube expansion

$e\Phi_{||}$ increases with $T_{e\infty}$ and $V_{Ae\infty}$ to maintain quasi-neutrality

Results

Role of $E_{\parallel}$ in the energy partition

[Richard+2025, PRL]

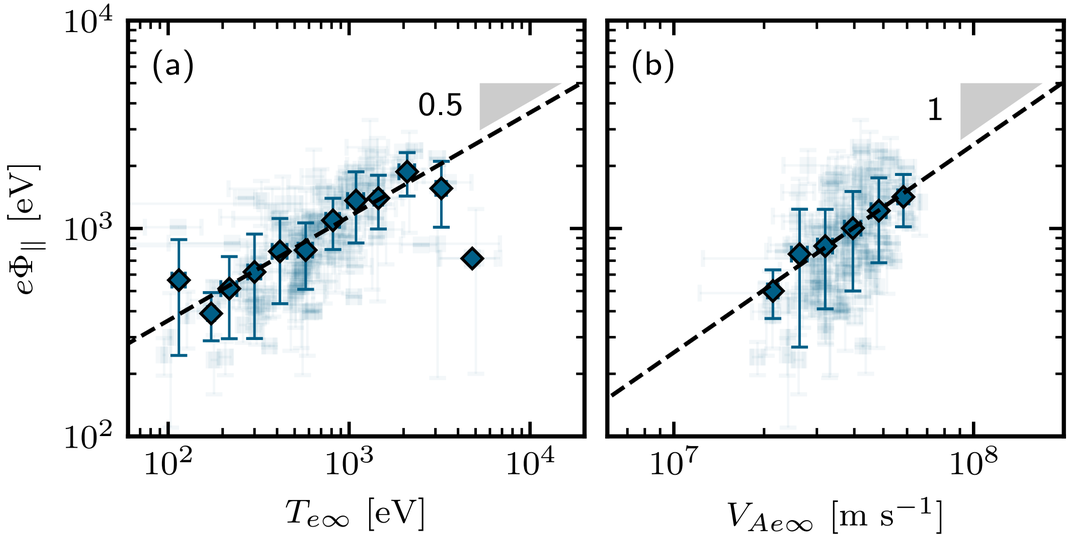

Results

Role of $E_{||}$ in the energy partition

[Richard+2025, PRL]

- The acceleration potential scales as $e\Phi_{||}/T_{e\infty} = \alpha_\Phi \beta_{e\infty}^{-1/2}$

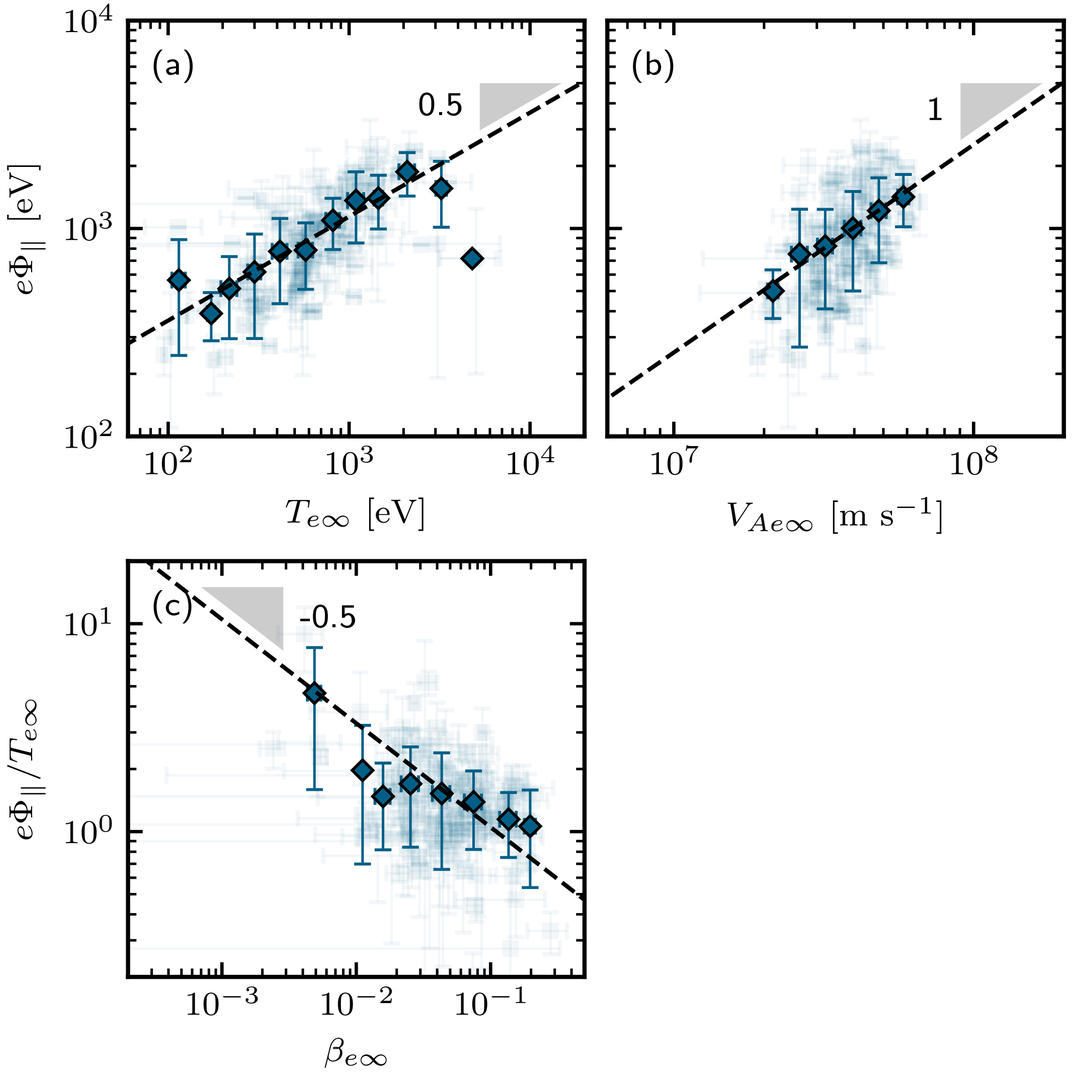

Results

Role of $E_{||}$ in the energy partition

[Richard+2025, PRL]

- The acceleration potential scales as $e\Phi_{||}/T_{e\infty} = \alpha_\Phi \beta_{e\infty}^{-1/2}$
- Electron heating: E_{rec} + $E_{||}$ [Le+2016, PoP, Øieroset+2020, ApJ]

$$\Delta T_e = \alpha_e m_i V_{Ai\infty}^2$$

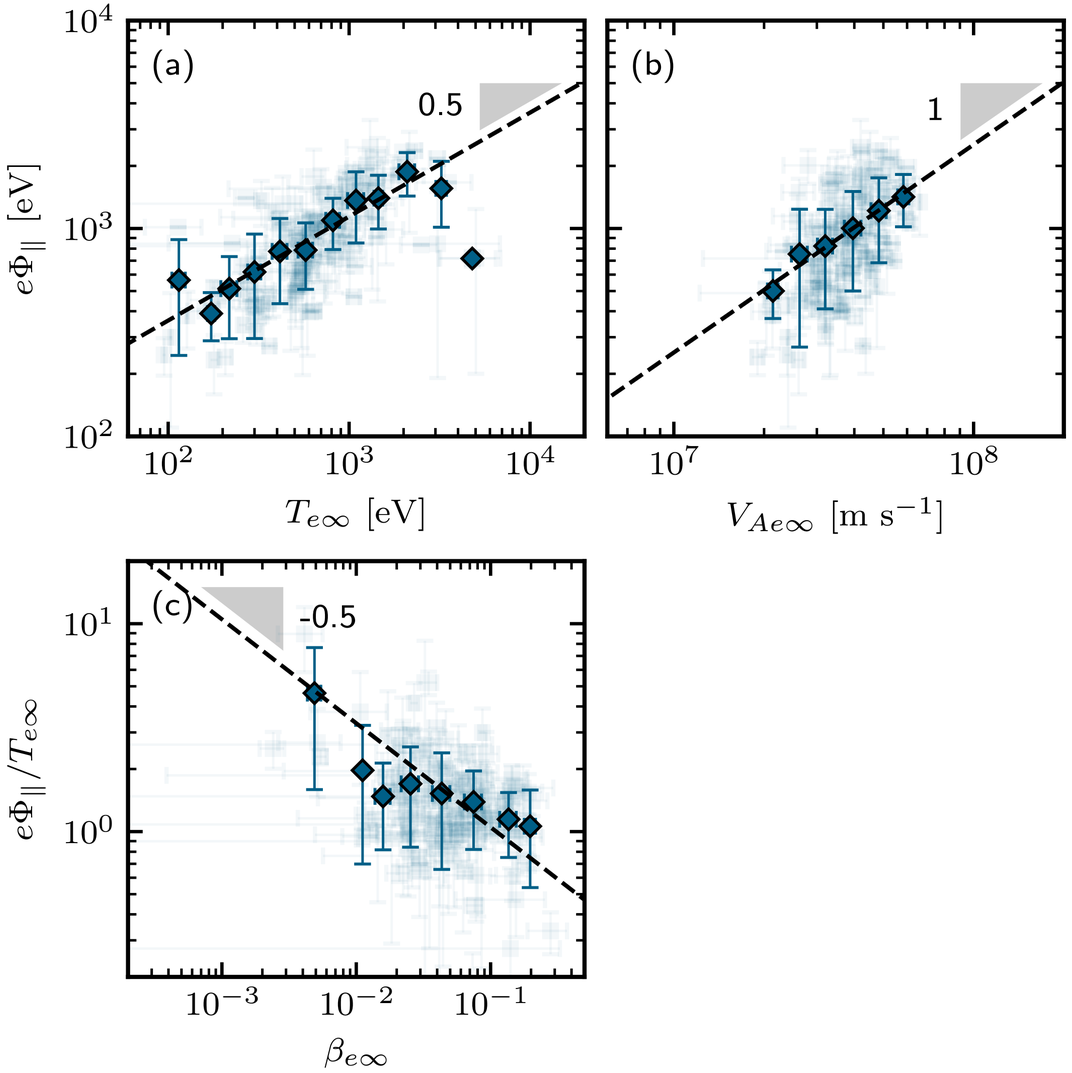

Results

Role of $E_{\parallel}$ in the energy partition

[Richard+2025, PRL]

- The acceleration potential scales as $e\Phi_{\parallel}/T_{e\infty} = \alpha_{\Phi}\beta_{e\infty}^{-1/2}$
- Electron heating: E_{rec} + $E_{\parallel}$ [Le+2016, PoP, Øieroset+2020, ApJ]

$$\Delta T_e = \alpha_e m_i V_{Ai\infty}^2$$

- Ion heating: Pick-up + $E_{\parallel}$ [Drake+2009, JGR, Haggerty+2015, GRL]

$$\Delta T_i = \alpha_{i1} m_i V_{Ai\infty}^2 - 2\alpha_{i2} e\Phi_{\parallel}$$

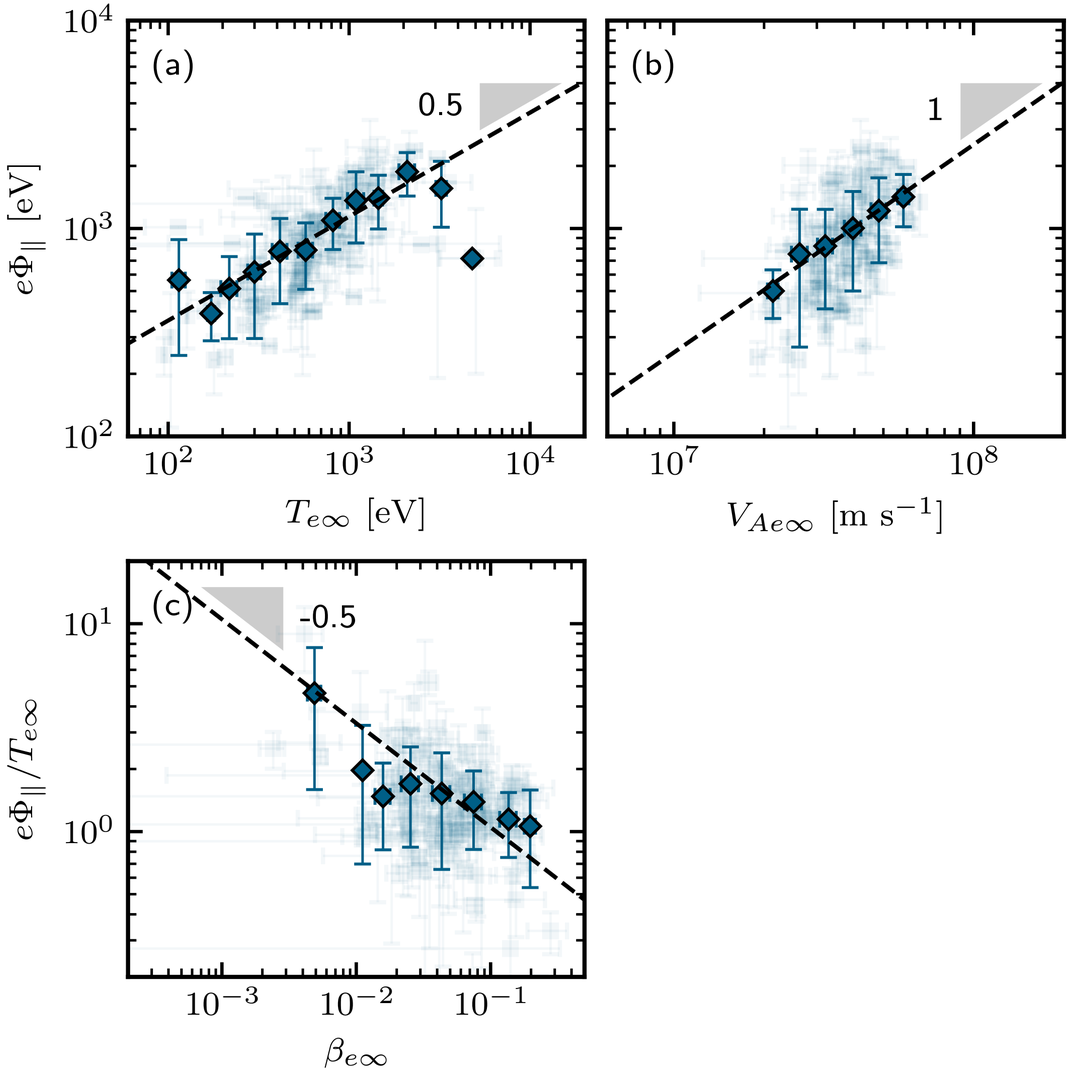

Results

Role of $E_{\parallel}$ in the energy partition

[Richard+2025, PRL]

- The acceleration potential scales as $e\Phi_{\parallel}/T_{e\infty} = \alpha_{\Phi}\beta_{e\infty}^{-1/2}$
- Electron heating: E_{rec} + $E_{\parallel}$ [Le+2016, PoP, Øieroset+2020, ApJ]

$$\Delta T_e = \alpha_e m_i V_{Ai\infty}^2$$

- Ion heating: Pick-up + $E_{\parallel}$ [Drake+2009, JGR, Haggerty+2015, GRL]

$$\Delta T_i = \alpha_{i1} m_i V_{Ai\infty}^2 - 2\alpha_{i2} e\Phi_{\parallel}$$

- Empirical model for the ion-to-electron energy partition

$$\frac{\Delta T_i}{\Delta T_e} = \frac{\alpha_{i1}}{\alpha_e}\left(1 - \frac{\alpha_{i2}\alpha_{\Phi}}{\alpha_{i1}}\sqrt{\beta_{e\infty}}\right)$$

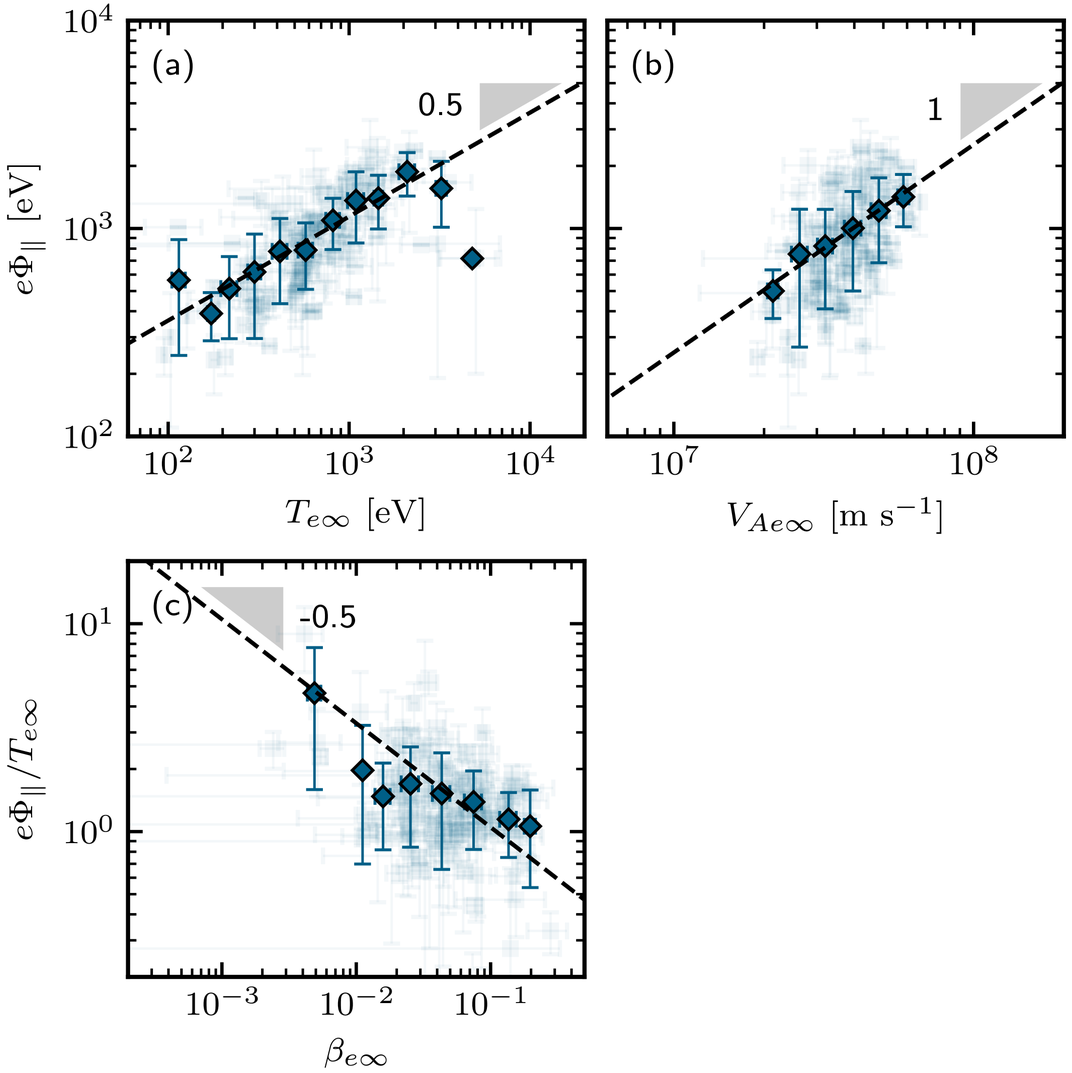

Conclusions

- **Turbulence develops rapidly** in the reconnection jet, **contributing approximately 10% to energy conversion** during magnetic reconnection.

- **Ion VDFs** in the reconnection jet are **efficiently heated** and **maintained near LTE** due to **chaotic interactions in sharply curved magnetic fields.**

- **Electron VDFs** in the reconnection jet are **heated up to 10 times** by **parallel electric fields that develop to maintain quasi-neutrality**.